The Effects of Diatom Oxylipin 2-Trans-4-Trans Decadienal on Gene Expression During Development and Growth of the Tunicate *Ciona intestinalis*

Thesis

The Effects of Diatom Oxylipin 2-trans-4-trans Decadienal on Gene Expression during Development and Growth of the Tunicate *Ciona intestinalis*

A thesis submitted to the Open University of London for the degree of

DOCTOR OF PHILOSOPHY

by

Anna Lettieri

Sponsoring Establishment:

STAZIONE ZOOLOGICA ANTON DOHRN

NAPOLI, ITALY

April 2014

ProQuest LLC.
789 East Eisenhower Parkway
P.O. Box 1346
Ann Arbor, MI 48106 – 1346

This thesis work has been carried out in the laboratory of Dr Adrianna Ianora, at the

Stazione Zoologica Anton Dohrn in Napoli, Italy

Director of studies: Dr. *Adrianna Ianora* (Stazione Zoologica, Napoli, Italy)

Internal Supervisor: Dr. *Margherita Branno* (Stazione Zoologica, Napoli, Italy)

External Supervisor: Prof. *Matthew Bentley* (School of Marine Science and Technology, Newcastle University, England, UK)

A Diego, Tommaso ed Eva

ACKNOWLEDGEMENTS

I would like to thank my director of studies, Dr. Adrianna Ianora, for giving me the opportunity to do this PhD project and for the patient guidance, encouragement and advice she has provided throughout my time as her student.

I would also like to thank my supervisors, Dr. Margherita Branno and Prof. Matthew Bentley, for their scientific and emotional support. I have been extremely lucky to have supervisors who cared so much about my work, and who responded to my questions and queries so promptly.

My special thanks are extended to all the member of the staff of the Functional and Evolutionary Ecology Laboratory and the Cell and Developmental Biology Laboratory at the Stazione Zoologica Anton Dohrn in Napoli who helped me in my supervisor's absence.

Finally, I would like to thank the Stazione Zoologica Anton Dohrn in Napoli, not only for providing the funding which allowed me to undertake this research, but also for giving me the opportunity to attend conferences and meet so many interesting people.

ABSTRACT

Diatoms, a major class of unicellular photosynthetic algae, have traditionally been considered as principal components of planktonic crustacean copepod diets, enhancing their fecundity and development. This idea largely persisted until 1993 when a world-wide group of researchers reported what is now known as the *"diatom-copepod paradox"* (Ban *et al.*, 1997). Although copepods consume diatoms to a large extent, they are not an optimal food for copepod growth, because their consumption leads to longer generation times and increased mortality rates in the offspring (Ianora *et al.*, 2004; Poulet *et al.*, 1994).

The anti-proliferative effect of diatoms on copepod reproduction is caused by the presence of antimitotic compounds, which reduce egg viability in copepods by blocking mitotic divisions during embryogenesis (Poulet *et al.*, 1994). These inhibitory effects are correlated to the production of polyunsaturated aldehydes (PUAs) (Miralto *et al.*, 1999; d'Ippolito *et al.*, 2002a; Ianora *et al.*, 2004), which are produced by diatoms in response to physical damage as occurs during copepod grazing (Pohnert, 2000).

PUAs have been demonstrated to have similar effects on benthic invertebrates such as polychaetes (Caldwell, 2005), sea urchins (Romano *et al.*, 2010) and tunicates (Tosti *et al.*, 2003). In these organisms PUAs induce the disruption of gametogenesis, gamete functionality, fertilization, embryonic mitosis, and larval fitness and competence (reviewed by Caldwell, 2009). The cell targets of these compounds, however, remains largely unknown.

The aim of this thesis was to identify, on a large scale, the genes targeted by the diatom PUA 2-trans-4-trans-decadienal (DD) using the tunicate *Ciona intestinalis*. The

tools, techniques and genomic resources available for *Ciona*, as well as the suitability of *Ciona* embryos for medium-to high-throughput strategies, are key to their employment as model organisms in different fields, including the investigation of toxic agents that could interfere with developmental processes. Here it is demonstrated that DD can induce developmental aberration in *Ciona* larvae in a dose dependent manner. Moreover, through a preliminary analysis of microarray experiments, DD is demonstrated to affect the expression level of genes involved in stress response, developmental processes and cell adhesion.

TABLES OF CONTENTS

PREFACE

This thesis is the result of my PhD conducted from December 2010 to March 2014 in the Functional and Evolutionary Ecology Laboratory at the Stazione Zoologica Anton Dohrn in Napoli, under the supervision of Dr Adrianna Ianora and in collaboration with the Cell and Developmental Biology Laboratory under the supervision of Dr Margherita Branno.

The thesis is organized in six chapters. Chapter 1 introduces the topic of the thesis, through a short overview on the model system, *Ciona intestinalis*, and on the current knowledge about diatom polyunsaturated aldehydes and their effects on marine organisms. Chapter 2 discusses the aim of the thesis, which was to understand the effect of 2-trans-4-trans-decadienal (DD) on *Ciona* development. Chapters 3-4-5, describe the experimental procedures used (decadienal treatments on *Ciona* embryos; microarray analysis and qPCR analysis); each of these three chapters includes a brief introduction, a detailed description of the materials and experimental procedures used, a description of the results obtained and a brief discussion. Chapter 6 discusses and summarizes the results obtained and also discusses future perspectives in this field.

LIST OF FIGURES

LIST OF TABLES

Chapter 1: General introduction

1.1 Diatom oxylipins

Oxylipins constitute a large family of oxidized fatty acids. These bioactive compounds are found abundant in mammals (Kühn *et al.*, 2002; O'Donnell *et al.*, 2009) as well as in non-mammals including plants (Andreou *et al.*, 2009) algae (Guschina and Harwood, 2006), bacteria and fungi (Brodhun *et al.*, 2011). Most oxylipins are bioactive compounds involved in host-microbe communication systems and in defence reactions against pathogens in different organisms. In particular, in eukaryotic micro-organisms they appear to play different roles: metabolism, defence, maturation or differentiation and communication phenomena. (Montanari *et al.*, 2013) In mammals, oxylipins are called eicosanoids, which derive from arachidonic acid and include prostaglandins and leukotrienes and are potent modulators of immune responses and numerous basic host physiologic processes (Funk, 2001). In fungi and fungal-like organisms, oxylipin production is ubiquitous and plays a role in life cycle control, notably in sexual and asexual development (Noverr *et al.*, 2003) for a number of fungal genera including *Aspergillus spp., Alternaria tomato, Septoria fructicola* and *Neurospora* crassa.

In plants, oxylipins stimulate signals implicated in the reinforcement of plant defences against pathogens, provide building units of physical barriers, regulate plant cell death and have a major role in the formation of phytohormones and in senescence (Blée, 2002; Montillet *et al.*, 2002).

Oxylipins have been reported also in diatoms (Miralto *et al.*, 1999; Pohnert, 2000-2002; Fontana *et al.*, 2007) where they have been shown to have multiple functions such as: grazer defense (Ianora *et al.*, 2004, 2011a), allelopathy (Casotti *et al.*, 2005;

Ribalet *et al.*, 2007), cell-to-cell signaling (Vardi *et al.*, 2006), antibacterial activity (Ribalet *et al.*, 2008; Balestra *et al.*, 2011), and bloom termination (Vidoudez and Pohnert 2008; Vidoudez *et al.*, 2011) (Fig. 1.1). Thus, the same secondary metabolites deter different groups of organisms by different modes of action and also act as signal molecules within a diatom population and mediating other plankton interactions.

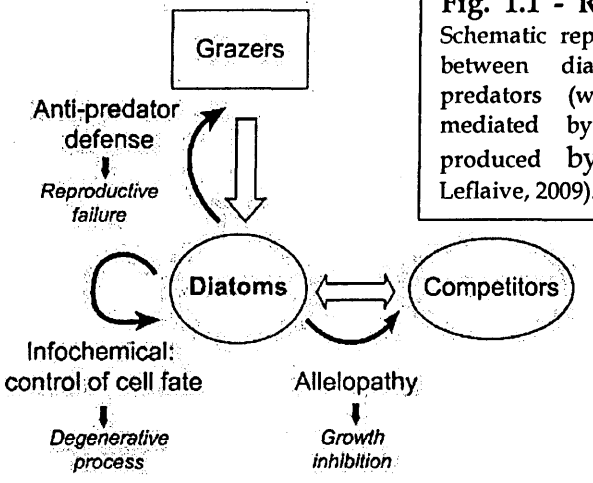

Fig. 1.1 - Role of diatom oxylipins. Schematic representation of the interactions between diatoms and competitors or predators (white arrows) that may be mediated by polyunsaturated aldehydes produced by diatoms (Adapted from Leflaive, 2009).

The first among these molecules to show such characteristics were the polyunsaturated aldehydes (PUAs) 2-trans-4-cis-7-cis-decatrienal; 2-trans-4-trans-7-cis-decatrienal; and 2-trans-4-trans-decadienal, isolated in 1999 by Miralto *et al.* (1999) from three different diatom species: *Thalassosira rotula, Skeletonema marinoi* and *Pseudo-nitzschia delicatissima.* Successively other authors, using different methodologies, have confirmed these findings (Pohnert, 2000-2002; d'Ippolito *et al.*, 2002; Wichard *et al.*, 2005) and have identified a more complete range of PUAs from *S. marinoi* and *T. rotula.*

Diatom oxylipins include short-chain unsaturated aldehydes and hydroxy, keto and epoxyhydroxy fatty acid derivatives (Fontana *et al.*, 2007,) but the most studied are the PUAs (Fig. 1.2). As shown by the examination of 51 freshwater and marine diatom species (71 isolates), PUA production is species and strain dependent (Wichard *et al.*,

2005). Thirty-six per cent of the investigated species release PUAs on wounding in various concentrations (0.01– 9.8 fmol per cell).

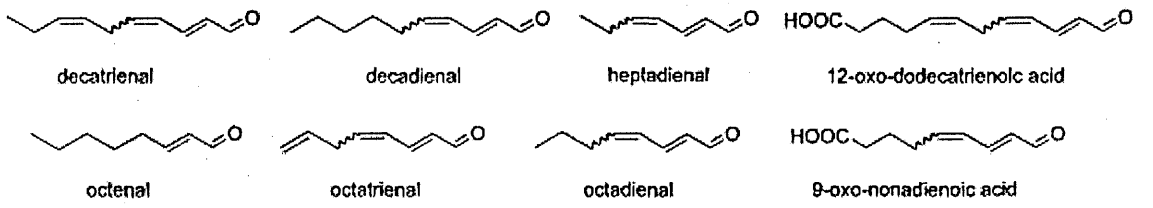

Fig. 1.2 - PUAs structure. The figure showed the structure of the most common α,β,γ,δ-Unsaturated aldehydes from diatoms (Adapted from Pohnert, 2005).

The dominant bioactive PUAs released by diatoms are C10 2E,4E/Z-decadienal (2E,4E/Z-DD) and 2E,4E/Z,7Z-decatrienal (Miralto *et al.* 1999), but also C8 2E,4E/Z-octadienal and 2E,4E/Z-octatrienal and C7 2E,4E/Z-heptadienal (D'Ippolito *et al.*, 2002; Wichard *et al.*, 2005). Diatoms may produce either one PUA or a mixture of several PUAs (Wichard *et al.*, 2005; Fontana *et al.*, 2007).

The mechanism of volatile PUA production has not been described fully. It seems clear that intact diatom cells do not contain free PUAs (Jüttner, 2001). Only on cell damage phospholipids are rapidly cleaved by phospholipases and galactolipases to release free fatty acids (Pohnert, 2002), which are further transformed into PUAs and other metabolites. The main enzymes responsible for the biosynthesis of PUAs were characterized as a phospholipase A2 (PLA2) and LOX-hydroperoxide lyases (Pohnert, 2002). The bioactivity of PUA derivatives is linked to the presence of an α,β- or α,β,γ,δ-unsaturated aldehyde group, which is a structural element typical for lipid peroxidation products. Molecules bearing this aldehyde group are potent Michael

acceptors (Vollenweider *et al.*, 2000), which can form covalent adducts with nucleophiles and may thus be toxic through interference with many cellular processes. Moreover, it has been demonstrated that the toxicity of these metabolites for sea urchins increases with increasing chain length from C7 to C10 (Adolph *et al.*, 2003).

1.1.1 Effects of diatom oxilipins on marine organisms

Diatoms have traditionally been considered as principal components of planktonic copepod diets, enhancing copepod fecundity and supporting major fisheries (Legendre, 1990). But a world-wide group of researchers reported that, although copepods do consume diatoms to a large extent, their consumption leads to elongated generation times and increased mortality rates in the offspring of their grazers (Poulet *et al.*, 1994; Ban et al. 1997; Ianora *et al.*, 2004). The discovery that diatoms produced PUAs (Miralto *et al.*, 1999) with antiproliferative effects on grazers gave impetus to research that led to study the effects of these compounds not only on copepods but also in other marine organisms. To date oxylipins, and PUAs in particular, have been demonstrated to have similar effects on benthic invertebrates such as polychaetes (Caldwell, 2005), sea urchins (Romano *et al.*, 2010) and tunicates (Tosti *et al.*, 2003). Effects of these bioactive compounds derived from diatoms include the arrest of embryogenesis, induction of teratogenic effects in larvae and inhibition of fertilization success. In particular, 2-trans,4-trans-decadienal (DD) alters actin filaments, tubulin polymerization, DNA replication and mitochondrial migration after contraction, leading to a disturbance in cleavage formation. However, DD also induces larval teratogeny at low concentrations, possibly due to actin perturbation.

Although DD effects are well known and well characterized, the majority of these studies have been focused on the impact of these compounds (in particular of 2-

trans,4-trans-decadienal) on organism physiology and though their biological activity was observed in all cases, their inhibitory mechanism still remains unknown (Adolph *et al.*, 2004). So far, despite the enormous amount of experiments showing that diatom oxylipins negatively impact invertebrate reproduction and development, information on the molecular mechanisms and the associated genes underlying the effects of the oxylipins on the development of marine organisms is lacking.

Just recently, a line of research to clarify the molecular mechanisms affected by diatom oxylipins has been developed at the Stazione Zoologica. Several works on different organisms, such as copepods (Lauritano *et al.*, 2011a-b, 2012a-b; Carotenuto *et al.*, 2014) and sea urchins (Romano *et al.*, 2011; Marrone *et al.*, 2012), have studied the effects of oxylipins on the expression levels of genes involved in stress responses and developmental processes.

1.2 Stress response

Most biochemical processes inside an organism try to maintain an equilibrium state. The ability of the body or a cell to seek and maintain a condition of equilibrium or stability within its internal environment is known as homeostasis.

At the cellular level all organisms respond to a large variety of unfavorable (stress) conditions, which are categorized under three major headings – environmental, pathophysiological, and intracellular stressors that can continuously disrupt homeostasis. Organisms may react to these stressors by activating a series of cellular defense systems that can be summarized as "first and second lines of defense" (Lauritano *et al.*, 2011). The first is a multixenobiotic resistance system (MXR), also

known as multidrug resistance system (Sarkadi *et al.*, 2006). MXRs have been detected in a plethora of marine organisms including sponges, mussels, oysters, crabs, worms, sea stars, clams and fishes (Lauritano *et al.*, 2012b). The "second line of defense", via metabolic enzymes, essentially consists in two phases, catalyzed by Phase I and Phase II enzymes, the purpose of which is to facilitate elimination of compounds from the body (Kozlowsky-Suzuki *et al.*, 2009). Phase I reactions can involve oxidation, reduction, hydrolysis, hydration and dehalogenation of these compounds. The most common reaction is to oxidize them by converting a C-H bond to a C-OH, which is the reaction site for successive possible detoxification reactions. Phase I enzymes are mainly the cytochrome P450 (CYP450) supergene enzyme family that generally constitute the first enzymatic defense against foreign compounds. Phase II reactions generally follow those of Phase I and consist in conjugation reactions that render the substrate water soluble thereby facilitating elimination from the cell. The most widely conserved stress response pathways are the heat shock protein 70 (HSP70) chaperone system and GSH homeostasis system.

1.2.1 Heat shock proteins

The environmental stress response in all organisms as diverse as pro- and eukaryotes is generally coupled with a remarkable change in gene expression patterns and an enhanced synthesis of several 'stress proteins' (Schlesinger *et al.*, 1982). Because they were first described in *Drosophila melanogaster* larvae that were accidentally exposed to elevated temperatures (Ritossa, 1962), these stress-related proteins were called heat-shock proteins (Hsps).

Extensive research on Hsps revealed also a constitutive expression of some members of these proteins, suggesting that they are also essential in maintaining the

cellular functions under normal physiological conditions. These members are therefore designated as heat-shock cognate proteins (Hscs). Furthermore, Hsps respond not only to increased temperatures, but also chemicals, heavy metals, UV light, hypoxia and other stressors can induce their synthesis (Krenech *et al.*, 2013).

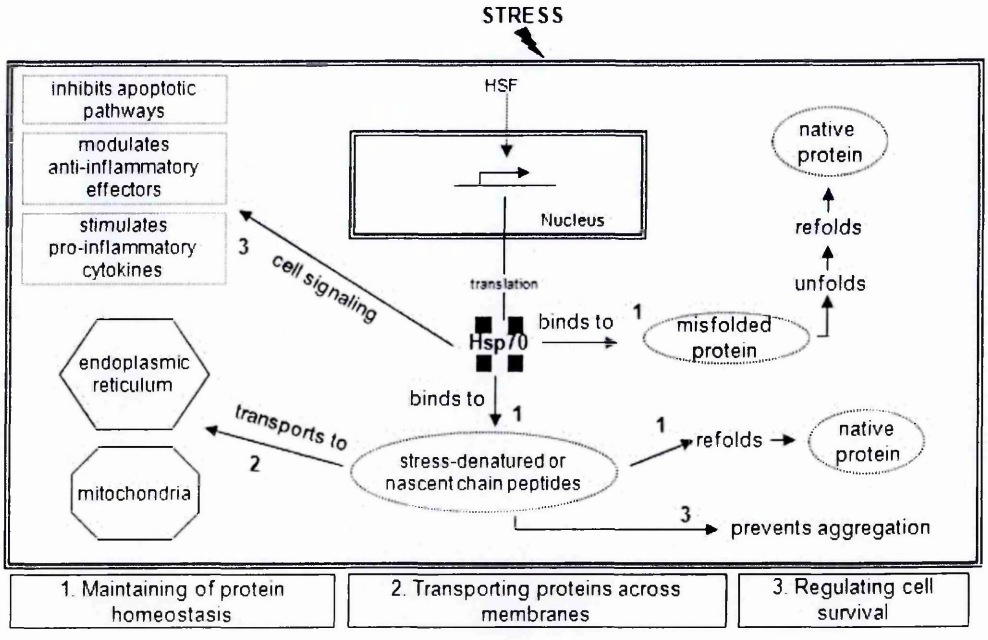

Fig. 1.3 - Multiple actions of 70-kDa heat shock protein. This diagram shows the multiple roles of HSP70 under stress condition (Adapted from Dörthe and Katschinski, 2004).

Under normal (nonstressful) conditions, molecular chaperones assist in the routine folding and compartmentalization of newly synthesized proteins and they also take part in a variety of other cellular functions. During thermal or other forms of stress, heat-induced HSPs bind to denatured proteins, thereby preventing their aggregation and aiding in their refolding into native, functional states following restoration of ambient temperature (Dörthe and Katschinski, 2004). HSPs have been classified in eukaryotic cells by their molecular weight. To date, there are six identified HSP families (HSP100, HSP90, HSP70, HSP60, HSP40, and the small HSPs).

The best studied family of heat-shock proteins are known as the stress-70 family and are named in relation to their molecular weight (70 kDa). This family comprises of three main isoforms (Morris *et al.*, 2013):

1) Solely constitutive: present during normal cell functioning, amongst other roles, they carry out folding of nascent polypeptides under normal cellular conditions (known as heat-shock cognates, e.g. HSC70).

2) Solely inducible: up-regulated in cells in response to stressful stimuli.

3) Constitutive and inducible: expressed during normal cell functioning and also up-regulated in response to stressful stimuli.

Heat-shock proteins, and in particular the HSP70 family, have been suggested by many in the past two decades as a good universal biomarker for stress, and superficially, it is easy to see why. Effective stress biomarkers need to meet certain criteria, they must be: quantifiable, universal within the study group, sublethal, and reliable for interpretation (Morris *et al.*, 2013). HSP70 family proteins are ubiquitous and highly conserved in nearly all organisms, making the genes encoding them easy to isolate and identify within a genome. They are responsive to a large variety of stresses.

Laboratory and field studies have shown the potential of Hsp70 as a biomarker, especially in sentinel species (Pyza *et al.*, 1997). Induction of Hsp70 in response to exposure to heavy metals and endocrine disrupting chemicals (EDCs) has been reported in some invertebrates (Pyza *et al.*, 1997). In some detailed studies, induced levels of Hsp70 were reported in samples collected from contaminated sites (Yoshimi *et al.*, 2002; Kohler *et al.*, 2007). In mollusks, the Hsp70 biomarker has shown a good correlation with the level of pollution (Wepener *et al.*, 2005). The components of the

HSP70 chaperone system were found also in the tunicate *Ciona intestinalis* (Wada *et al.*, 2006).

1.2.2 Glutathione

Glutathione (GSH; L-c-glutamyl-L-cysteinylglycine) is the principal non-protein thiol involved in antioxidant cellular defence. It is a tripeptide composed of cysteine, glutamic acid, and glycine and its active group is represented by the thiol (-SH) of cysteine residue. In cells, GSH can be free or bound to proteins. Free GSH is present mainly in its reduced form, which can be converted to the oxidized form during oxidative stress, and can be reverted to the reduced form by the action of the enzyme GSH reductase (Fig. 1.4b). The redox status depends on the relative amounts of the reduced and oxidized forms of glutathione (GSH/GSSG) (Pastore *et al.*, 2012). In normal conditions, the reduced GSH is predominant over the oxidized form. In stress condition oxidized GSSG is predominant.

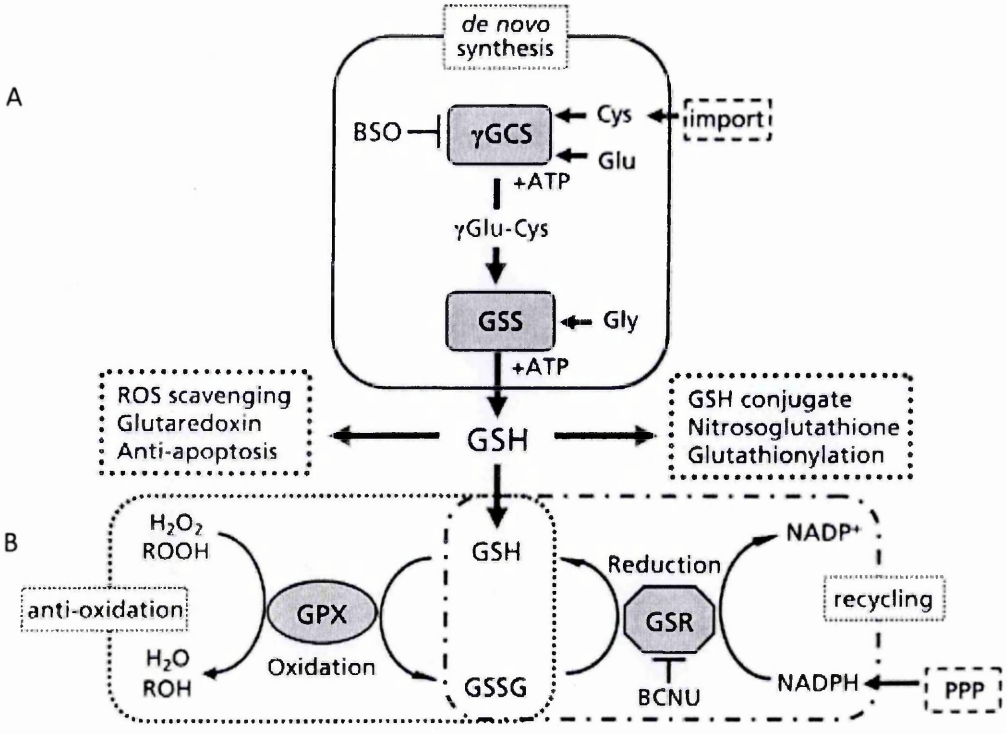

Fig. 1.4 - Roles and metabolism of glutathione. A. γ-GCS and GSS coordinately catalyze *de novo* synthesis of GSH from three amino acids: Cys, Glu, and Gly. B. GPX reduces various peroxides, including hydrogen peroxide, by electrons from GSH. The resultant GSSG is reduced back to GSH by GSR via the donation of electrons from NADPH supplied from the pentose phosphate pathway (PPP). GSH not only supplies electrons to peroxides, but also plays multiple roles in cells. (Adapted from Fujii *et al.*, 2011).

It is important to note that shifting the GSH/GSSG redox toward the oxidizing state activates several signaling pathways, including apoptosis signal-regulated kinase 1, and mitogen- activated protein kinase, (Lu, 2009) which reduce cell proliferation and increase apoptosis. GSH displays remarkable metabolic and regulatory versatility (Fig.1.5). The synthesis of GSH from glutamate, cysteine, and glycine is catalyzed sequentially by two cytosolic enzymes (Fig. 1.4A). The first enzyme is named glutamate-cysteine ligase (GCL), formerly γ-glutamylcysteine synthetase (GCS), and is rate-limiting (Dickinson, 2002). GCS is an heterodimer, which can be dissociated into a

modulatory, or light subunit (GCLM) and a catalytic, or heavy, subunit (GCLC). The second enzyme is glutathione synthetase (GS); this enzyme functions as a homodimer of 118 kDa and is responsible for the addiction of glycine to γ-glutamylcysteine created by CGL to form GSH (Dickinson, 2002).

Fig. 1.5 - GSH functions. Glutathione plays numerous functions, but mainly it participates in the regulation of the cellular redox state (oxidation-reduction reactions). The state of glutathione is modulated by oxidants, nutritional factors and other factors such as defence responses to pathogens. (Adapted from Pedro Díaz-Vivancos 2013- (http://antioxidantsgroup.wordpress.com/2013/07/04/antioxidant-defense-mechanisms-i-non-enzymatic-mechanisms/).

Glutathione plays a major role in cell proliferation and death, DNA synthesis and repair, regulation of protein synthesis, prostaglandin synthesis, amino acid transport and enzyme activation, maintains essential thiol status, regulates immune functions, and plays a role in spermatogenesis and sperm maturation (Droege, 2002). The mechanism of detoxification involving GSH is believed to proceed through two distinct pathways. First, GSH effectively scavenges free radicals and other reactive

oxygen species (hydroxyl radical, lipid peroxyl radical, peroxynitrite, and H_2O_2) directly and indirectly through enzymatic reactions. In such reactions, GSH is oxidized to form GSSG, which is then reduced to GSH by the NADPH-dependent glutathione reductase. In addition, glutathione peroxidase catalyzes the GSH-dependent reduction of H_2O_2 and other peroxides (Winterbourn, 2008). Second, GSH reacts with various electrophiles, physiological metabolites (e.g., estrogen, melanins, prostaglandins, and leukotrienes), and xenobiotics (e.g., bromobenzene and acetaminophen) to form mercapturates (Pastore *et al.*, 2012). These reactions are initiated by glutathione-S-transferase (a family of Phase II detoxification enzymes).

1.3 *Ciona intestinalis*

1.3.1 The organism

Ciona intestinalis belongs to the Tunicate (or Urochordate) *subphylum* that, together with Cephalochordate (amphioxus) and Vertebrate *subphyla*, constitute the Chordate *phylum*.

The Tunicate *subphylum* is constituted by diverse groups of animals all having in common the cellulose-containing tunic that covers their body (Nakashima *et al.*, 2004) and from that Tunicate name is derived. They are traditionally divided into three classes: ascidians (sea squirts), thaliaceans (salps) and appendicularians (larvaceans).

Ciona intestinalis belongs to the ascidians, which are, in the first part of their life, planktonic swimming larvae (figure 1.6 A). After substrate settlement, larvae undergo a process of metamorphosis, becoming adult sessile filter feeder animals (figure 1.6 B). The adult form of ascidians could hardly justify their close phylogenetic relationship with vertebrates, since none of the distinctive features of the chordate body plan is

clearly present. It is indeed in the larval stage that the basic landmarks of the phylum, such as the notochord, the dorsal hollow nerve cord and segmented muscles (Holland *et al.*, 2004), are recognizable (figure 1.6 A, on the right).

Ciona larvae possess an extremely simplified structure. They develop very quickly (within 24 hours after fertilization, at 18°C) following a well-known developmental plan.

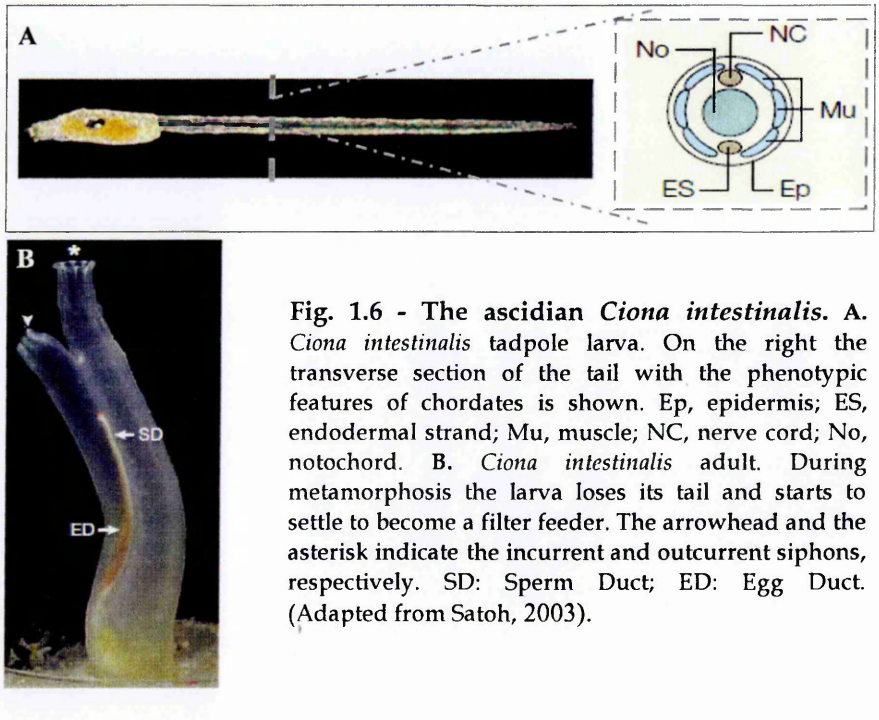

Fig. 1.6 - The ascidian *Ciona intestinalis*. **A.** *Ciona intestinalis* tadpole larva. On the right the transverse section of the tail with the phenotypic features of chordates is shown. Ep, epidermis; ES, endodermal strand; Mu, muscle; NC, nerve cord; No, notochord. **B.** *Ciona intestinalis* adult. During metamorphosis the larva loses its tail and starts to settle to become a filter feeder. The arrowhead and the asterisk indicate the incurrent and outcurrent siphons, respectively. SD: Sperm Duct; ED: Egg Duct. (Adapted from Satoh, 2003).

1.3.2 The model system

After being used for over a century as a model for embryological studies, ascidians, such as *Ciona intestinalis*, have become, in the past decade, an increasingly popular organism to investigate the molecular mechanisms underlying cell-fate specification during chordate development. *Ciona* embryos indeed permit detailed visualization of gene expression by whole-mount in situ hybridization (Satoh,

2001).The clonal restriction of larval tissues occurs early within the 64-110 cell stage, and the lineage leading to the formation of larval tissues has been depicted almost completely (Nishida, 1987). The *C. intestinalis* genome is ~155 Mb in size, approximately one twentieth the size of the human genome (Dehal *et al.*, 2002). Of these, ~117 Mb are composed of non repetitive, euchromatic sequence, coding for ~16,000 genes, approximately half the number present in the human genome. An annotated assembly of the genome is freely available through the JGI's Web site (http://genome.jgi-psf. org/ciona/), providing a resource that greatly accelerates the identification of homologs of genes previously studied in other organisms. In addition to the sequencing of the genome, a large-scale expressed sequence tag (EST) project has been carried out, resulting in the characterization of ~18,000 independent cDNA clones, estimated to represent ~85% of the *C. intestinalis* transcripts (Satou *et al.*, 2002; Satoh *et al.*, 2003). The results of this EST survey are available through the Kyoto University Web (http://ghost.zool.kyoto.ac.jp/index1.html) and in most cases cDNA clones are linked to their best hit in the *C. intestinalis* genome assembly. For several cDNA clones, in particular for those encoding transcription factors, expression data from *in situ* hybridizations are also available (Satoh *et al.*, 2003; Imai *et al.*, 2004). The small size of the *C. intestinalis* genome provides a distinct advantage for understanding genome organization and gene function.

1.3.3 Embryogenesis

Classically, ascidians embryogenesis has been considered a typical example of mosaic development, in which embryonic territories are specified from the zygotic stage throughout ooplasmic segregation of maternal determinants (Conklin, 1905a and Conklin 1905b). Blastomeres dissociated from an early cleavage stage, until the 110-cell

stage, show that the differentiation of epidermis, muscle and endoderm is autonomous without the involvement of any cell-cell signalling. In contrast, some ascidian territories, such as notochord, brain and pigment cells, failed to differentiate when embryonic cells were dissociated suggesting that the development of those tissues is non-autonomous and requires cell interactions (Nishida, 1997).

Ascidian embryonic development is very simple, fast and easy to follow. Soon after fertilization an invariant and bilaterally symmetrical cleavage program starts; the developmental stages of early ascidian embryos are named according to the number of cells, like 8-, 16-, 32-, 64-, 110-cell stages (Fig. 1.7 A, B; Satoh, 2003) and each blastomere is distinguishable with a specific and predictable lineage (Conklin, 1905c). The 8-cell stage embryo consists of the founder cells of four lineages, with the cells of the vegetal pole indicated by capital letters (A4.1 and B4.1) and animal cells named with small letters (a4.2 and b4.2; Fig. 1.7 A; Conklin, 1905c). The embryo continues to cleave in a bilaterally symmetrical manner and thus each blastomere name refers to a pair.

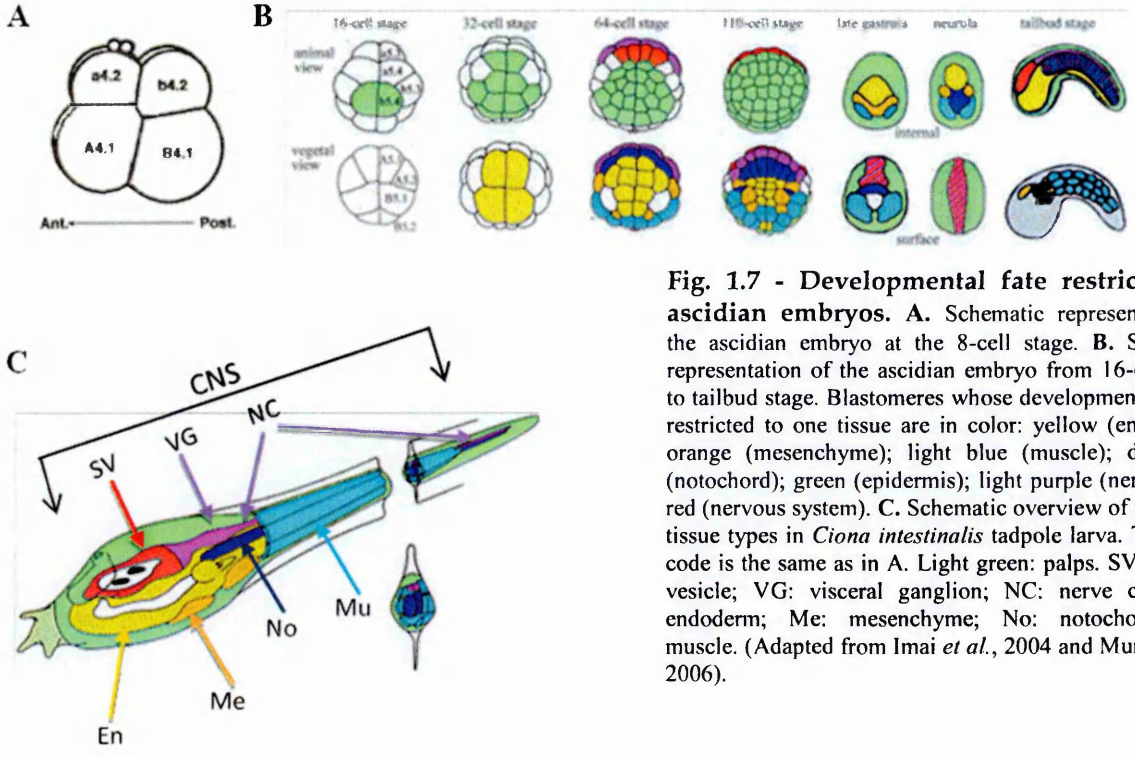

Fig. 1.7 - Developmental fate restriction in ascidian embryos. A. Schematic representation of the ascidian embryo at the 8-cell stage. **B.** Schematic representation of the ascidian embryo from 16-cell stage to tailbud stage. Blastomeres whose developmental fate is restricted to one tissue are in color: yellow (endoderm); orange (mesenchyme); light blue (muscle); dark blue (notochord); green (epidermis); light purple (nerve cord); red (nervous system). **C.** Schematic overview of the major tissue types in *Ciona intestinalis* tadpole larva. The color code is the same as in A. Light green: palps. SV: sensory vesicle; VG: visceral ganglion; NC: nerve cord; En: endoderm; Me: mesenchyme; No: notochord; Mu: muscle. (Adapted from Imai *et al.*, 2004 and Munro *et al.*, 2006).

In contrast to the blastomeres of vertebrates, those of most ascidians are fate restricted early during development, from the beginning of gastrulation, shortly before the 110-cell stage (Munro *et al.*, 2006). At the tailbud stage the main tissues and organs that constitute the future larva begin to be differentiated (Fig. 1.2 B; Satou *et al.*, 2001).

As previously mentioned, *Ciona* larvae develop in a relatively short time, within 24 hours after fertilization.The formation of the tadpole larva involves all the morphogenetic movements responsible for the shaping of vertebrate embryos (*e.g.* convergent extension, invagination, cell migration, oriented cell divisions), occurring within a small number of cells. Interestingly, cleavage patterns, cell lineages and the final body plan are remarkably conserved between distantly related ascidian genera, such as *Ciona* and *Halocynthia*, which diverged several hundred years ago (Hudson and Yasuo, 2008; Lemaire, 2009). Since the overall ontogeny of these organisms is very

similar, cell lineage data obtained in one species can often be considered valid for another.

Ciona larvae are made of only ~2600 cells, organized into a small number of organs that include the epidermis, the central nervous system (CNS), the endoderm and mesenchyme in the trunk, the notochord and muscle in the tail (Fig. 1.2 C; Katz, 1983). At the rostral end the larvae bear palps (Fig. 1.2 C, light green), adhesive structures which allow attachment to a suitable substrate to begin metamorphosis, usually within a few hours after hatching. It takes 2 or 3 months for the juvenile to become an adult with reproductive capability, depending on the temperature of the environment (Marikawa *et al.*, 1994).

1.3.4 Body axis specification

The polarization of oocytes, eggs and embryos arises from a rupture of symmetry caused by localized signaling resulting in redistributions of organelles and/or macromolecular complexes along axes (Sardet *et al.*, 2005).

Mature ascidian oocytes are arrested in metaphase of meiosis I (Met I) and display a pronounced animal-vegetal (a-v) polarity. The primary a-v axis of mature oocytes of the solitary ascidian *Ciona intestinalis* is characterized by the presence of a meiotic spindle situated at the animal pole and the polarized distribution of two concentric peripheral domains: a subcortical domain rich in mitochondria (called myoplasm) and a cortical domain rich in endoplasmic reticulum associated with some maternal postplasmic/PEM RNAs (cER/mRNA domain). Additional differences along the a-v axis include differences in the distribution of microfilaments and microtubules which are respectively enriched and conspicuously absent from the subcortical

myoplasm domain (Sardet *et al.*, 2005). This polarization occurs during meiotic maturation, after the meiotic spindle and chromosomes have moved in the cortex defining the animal pole; these events are actin-dependent (Prodron *et al.*, 2006). This primary axis plays important roles at the time of fertilization and embryonic development since in some ascidians there is evidence that sperm enters preferentially in the animal hemisphere and the fertilization-triggered contraction always propagates in a general a-v direction (Nishida, 2005). The a-v axis together with the site of sperm entry defines polarized cues which direct a series of cortical and cytoplasmic reorganizations leading to the acquisition of d-v and a-p axes of the embryo (Prodon *et al.*, 2005).

At fertilization, the sperm enters the egg in its animal hemisphere, marked by the polar bodies. This triggers two successive phases of cytoplasmic rearrangements, also called ooplasmic segregations (Sardet *et al.*, 2007). Reorganizations occur in two major phases. Shortly after fertilization (0–5 min in *Ciona*), the first phase is actin-dependent and concentrates cortical maternal determinants for the vegetal-most fate, endoderm, and for gastrulation at the vegetal pole of the embryo (Nishida, 2005). The second phase of reorganization (25–45 min in *Ciona*) brings maternal axial determinants components along the microtubules toward the future posterior pole and is relevant to specification of the a-p axis (Nishida, 2005).

An important consequence of the reorganizations of the first cell cycle is to position maternal determinants. These developmental determinants must be properly localized to ensure their distribution into the appropriate lineage to pattern the embryo (Nishida, 1997, 2005).

The animal body plan is determined by a series of complex genetic cascades or gene regulatory networks (Yamada *et al.*, 2005). The first cue for activation of the gene networks is transcripts and/or proteins that are provided maternally supplied information, which subsequently triggers the zygotic program. This transition has been called the maternal-to-zygotic transition (MZT) (Tadros and Lipshitz, 2009). The MZT often coincides with the mid-blastula transition (MBT) when cell divisions become asynchronous and cell cycles become longer. In embryos of the ascidian *Ciona intestinalis* cell division becomes asynchronous and the duration of cell cycles becomes longer after the16-cell stage. This suggests that the MZT begins between the 8- and 16-cell stages in the ascidian embryo (Matsuoka *et al.*, 2013).

1.3.5 Tail elongation

Axial elongation is a key morphogenetic process that serves to shape developing organisms. Tail extension in the ascidian larva represents a striking example of this process.

The tail contains a notochord flanked dorsally by the nerve cord, ventrally by the endodermal strand, and bilaterally by three rows of muscle cells. Elongation of the embryonic a-p axis is one of the mechanical functions of the notochord. Analysis of the *Ciona* notochord mutant *aim* (Jiang, *et al.*, 2005) demonstrates the requirement of the notochord for ascidian embryo elongation. It is not known if the notochord is the only driving force for tail elongation, although the phenotype of another mutant, Chongmague, suggests that the posterior tail epidermis can elongate to a certain extent even when notochord elongation is disrupted (Nakatani *et al.*, 1999).

Notochord formation

Ascidian notochord cells originate from a monolayer of 40 post mitotic mesoderm cells, called the notochord plate. Notochord formation in ascidian embryos is shown schematically in figure 1.8. The ascidian notochord arises from two distinct lineages: a primary lineage which derives from anterior blastomeres A7.3 and A7.7 (and their bilateral partners) producing the anterior 32 cells, and a secondary lineage which derives from the posterior blastomere B8.6 (and its bilateral partner) producing posterior 8 cells (Nishida, 1987).

As development progresses, the maternally supplied β-catenin translocates from the cytoplasm to the nucleus in the vegetal blastomeres. In the A-line lineage, β-catenin directly activates FoxD, which, in turn, activates ZicL (at present, it is not clear whether FoxD activates ZicL directly, or indirectly through an induction signal). ZicL, together with other transcription factors, might activate Ci-Bra. In the B-line, FoxD activates Notch, which, in turn, activates Ci-Bra. The activation of Ci-Bra leads to the activation of its downstream targets, which are the notochord structural genes. Specification of the notochord requires an inductive signal from the endoderm, which has been identified as fibroblast growth factor (FGF) (Kim *et al.*, 2000; Minokawa *et al.*, 2001). In the primary lineage this induction occurs at the 32-cell stage and notochord precursors acquire developmental autonomy at the 64-cell stage. The secondary lineage differentiates slightly later and becomes restricted to notochord fate at the 110-cell stage.

FGF is expressed in A5.1,A5.2 and B5.1 at the 16-cell stage; A6.1,A6.2,A6.3,A6.4 and B6.1 at the 32-cell stage; and A7.4,A7.8 (both nerve-cord lineage) and B7.4 (muscle lineage) at the 64-cell stage. The genetic cascade of FGF seems independent of the FoxD

cascade, and FGF has an essential role in mesenchyme induction and a partial role in A-line notochord induction.

At the 110-cell stage, coinciding with the onset of gastrulation, all cells undergo two more divisions along the anterior-posterior (a-p) axis of the embryo which occur in the ensuing 75 minutes, by which the 40 notochord cells are generated. At the end of the final two mitoses, the cells of the developing notochord form a monolayer epithelium with the basal side coming in contact with the neural plate on the dorsal side (Munro and Odell, 2002).

At gastrulation, the ascidian notochord follows a morphogenetic program that includes convergent and extension (C/E) followed by anterior-posterior (a-p) elongation (Satoh, 1994; Munro and Odell, 2002): the right and left progenitor cells of cubical shape converge towards the midline of the vegetal side of the embryo (in ascidian embryos, morphogenesis takes place on the vegetal side Fig. 1.9). The cells then undergo intercalation to organize into a column of 40 stacked cells and extend anteroposteriorly. Then intracellular vacuoles or extracellular vacuoles are produced, which increase the cell or notochord volume to elongate the tail. The notochord cells exhibit polarity first in the m-l axis during convergence and subsequently in the a-p axis during extension and elongation. During these cell movements and/or subcellular changes, the mid axis of the embryo is established (Jiang and Smith, 2007). The convergence and extension processes are associated to at least three molecular mechanisms: actin-based protrusive extension; actomyosin-based cortical contractility and integrin or cadherin-based cell adhesion.

Previous studies have demonstrated that, during ascidian tail morphogenesis, notochord and muscle differentiation are crucial (Di Gregorio *et al.*, 2002). Moreover,

extension of the notochord is required for organization of the muscle cells. If the notochord does not extend properly in the embryos, the tails of these tadpoles are malformed and often kinked (Di Gregorio *et al.*, 2002). The same paper also indicated that signals from the notochord are required to organize both muscles and endodermal strand (Di Gregorio *et al.*, 2002).

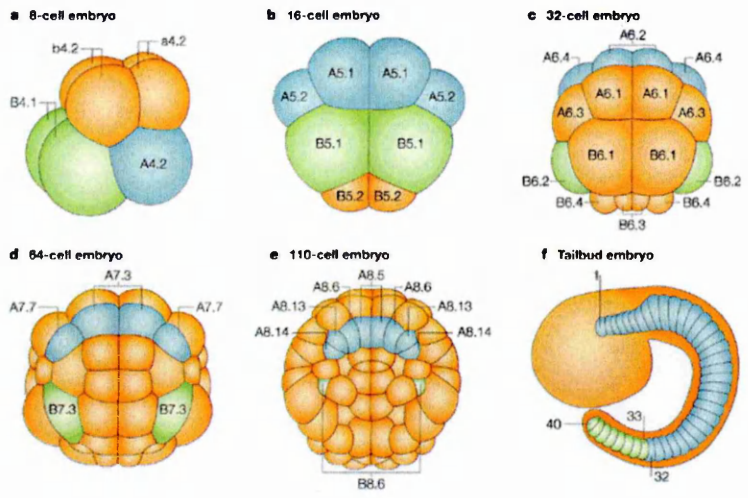

Fig 1.8 - Notochord formation in ascidian embryos. The lineages of notochord cells are denoted by the capital letters A and B.Blastomeres are named according to Conklin's nomenclature. The lineage of the 40 notochord cells is completely derived from 32 A-line and 8 B-line blastomeres (panel f). The A-line notochord potential (shown in blue) is inherited by A5.1 and A5.2 in the 16-cell embryo (panel b), by A6.2 and A6.4 in the 32-cell embryo (panel c) and by A7.3 and A7.7 in the 64-cell embryo (panel d). A7.3 and A7.7 become restricted to give rise to the notochord, and divide three times to form 32 notochord cells at the anterior and middle part of the tail (panels e and f). Also,B5.1 of the 16-cell embryo (panel b), B6.2 of the 32-cell embryo (panel c), B7.3 of the 64-cell embryo (panel d) and B8.6 of the 110-cell embryo (panel e) are the presumptive B-line notochord cells (shown in green).The B8.6 pair become restricted to the notochord, giving rise to 8 notochord cells in the posterior part of the tail after two divisions (panel f). Therefore, every notochord cell has a history of nine divisions between the zygote stage and the ultimate differentiation. (Adapted from Satoh, 2003)

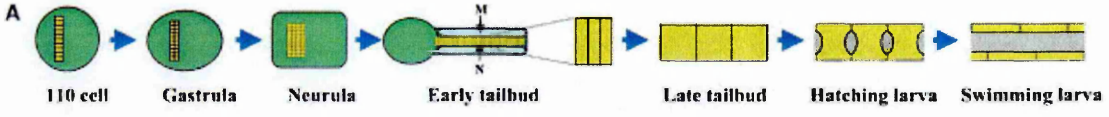

Fig 1.9 - Ascidian notochord development from the onset of gastrulation to the completion of convergent extension. During gastrulation, convergence/ extention (c/e) converts a four by ten sheet of developing notochord cells into a column of 40 stacked cells. Following c/e, notochord development continues as individual cells elongate in the a-p axis, in part by secreting extracellular matrix into the spaces between neighboring cells. Finally, these spaces fuse to form locus a tube that runs the length of the larval tail. (Adapted from Jiang 2005)

Chapter 2 - Aim of the thesis

The aim of this thesis was to better understand the molecular mechanisms underlining the toxicity of 2-trans,4-trans-decadienal (DD), the most widely studied diatom oxylipin, using the tunicate *Ciona intestinalis* as a model organism.

Ciona, in addition to providing a simple experimental system for the investigation of molecular mechanisms during development, offers a number of genomic and post-genomic tools suitable for molecular biology studies. So, *Ciona* seem to be a very useful choice to our purpose.

Since the goal of this thesis is to study the possible effects of the DD on development, the following experimental design was chosen: *ciona* embryos will be treated with decadienal at increasing concentrations and allowed to develop up to hatching. After hatching, two parameter will be observed: the hatching success (meant as percentage of hatched larvae) and the presence of aberrations on hatched larvae. Then, to analyze the DD effects at molecular level, RNA from treated embryos will be used in two different approach: microarray and quantitative Real-time PCR.

Previous studies have tried to explain the effects of diatom oxylipins on different organisms (such as copepods and sea urchin) using quantitative Real-time PCR, focusing on a small number of genes. Here, I utilized a more general approach, the chip microarray that allowed for the study of thousands of genes simultaneously. Since, the effects of diatom oxylipins are not yet clarified, a more general approach results more useful in this case.

This approach provides a broad view on which genes are affected by exposure to DD. Once the pathways affected by DD were discovered, the most interesting or the most affected pathways could be studied in greater detail.

The ultimate goal was to better understand the toxic effects of DD on *Ciona* development, and to use this information to explain DD effects on other marine organisms. Moreover, the results of this work will be useful also to create a molecular toolbox for ecotoxicological studies.

Chapter 3: Decadienal (DD) treatments on *Ciona intestinalis* eggs and embryos

3.1 Introduction

Diatoms are a major class of unicellular algae that have traditionally been considered to be essential in sustaining the marine food chain. This paradigm was challenged over a decade ago with the discovery that they produce polyunsaturated aldehydes (PUAs) that induce abortions and teratogenesis in grazing predators (Miralto *et al.*, 1999). By definition, teratogens are substances that induce structural malformations in the offspring of organisms exposed to them during gestation. The structural malformations that can occur include fetal growth retardation, embryo and fetal mortality, and functional impairment due to malformed limbs or organs (Ianora *et al.*, 2006). In fact, PUAs and, in particular, 2-trans-4-trans-decadienal (referred to as decadienal-DD in the present work) were shown to decrease hatching success and to induce strong developmental aberrations in different marine organisms (Tosti *et al.*, 2003).

The aberrant phenotypes observed range from malformed or a reduced number of feeding or swimming appendages in copepods (Ianora *et al.*, 2004), shortening of the apical spicules and arms (Romano *et al.*, 2010) and stunted and asymmetrical larval arms (Caldwell, 2009) in sea urchins, incomplete ciliary band formation in polychaete larvae (Caldwell, 2009) to aberrations on sensory organ pigmentation and stunted elongation of the tail in ascidians (Tosti *et al.*, 2003). All these authors showed that the degree and frequency of asymmetrical (teratogenic) development increased with increasing PUA concentrations, and there was a clear stage-specific effect, with earlier

larval stages being the most affected (Ianora *et al.*, 2010). The concentrations of DD inducing teratogenesis ranges from 0.05 to 30 μg mL^{-1}, depending on the organism and experimental conditions. More specifically, in the sea urchin *Paracentrotus lividus* DD concentrations inducing teratogenesis range between 0.2-0.8 μg mL^{-1} (1.3-5.26 μM) with the lethal dose being 1 μg mL^{-1} (6.58 μM Romano *et al.*, 2010). In this range of concentrations, the authors observed an increase in the number of abnormal sea urchin plutei and delayed development. Moreover, hatched larvae showed several degrees of malformations, which became more severe as DD concentrations increased (Romano *et al.*, 2010). In the sea urchin *Psammechinus miliaris* DD concentrations ranged from 0.1-0.5-1 μg mL^{-1} (0.66-3.29-6.58 μM) (Caldwell *et al.*, 2005), that are in the same range of DD concentrations as in *P. lividus*. Polychaetes are even more sensitive to DD. In fact, in these organisms DD induced morphological malformations at concentrations of 0.01-0.05 μg ml^{-1} (0.066-0.0329 μM, -Caldwell *et al.*, 2005). In the tunicate *Ciona intestinalis*, Tosti *et al.* (2003) observed developmental aberrations at DD concentrations of 0.2 μg mL^{-1} (1.32 μM). Planktonic copepods showed malformations at DD concentrations of 1 μg mL^{-1} (6.58 μM-Ianora *et al.*, 2010), that are much higher than those tested in the other organisms described above. These findings indicate that benthic organisms may be more sensitive to these metabolites compared to copepods. There is also another planktonic crustacean, *Daphnia pulicaria*, that has shown a high resistance to DD treatment; higher than copepods. In fact, when treated with DD concentration ranging from 0.5 to 3.0 μg mL^{-1}, this organisms showed a significant impairment of development (40% shed the first membrane) at a DD concentration of 2.5 μg mL^{-1}, (Carotenuto *et al.*, 2005).

The specific effects of diatom- PUAs have been studied extensively in field and *in vitro* experiments. Regarding *in vitro* studies, two types of experiments have been

classically performed: feeding experiments in which grazers are fed with PUA-producing diatoms (Miralto *et al.*, 1999; Carotenuto *et al.*, 2002; Ianora *et al.*, 2004), and incubation tests in which individuals are exposed to pure compounds directly (Adolph *et al.*, 2004; Caldwell *et al.*, 2004; Romano *et al.*, 2010) or PUAs are mediated by carriers, such as giant aldehyde-encapsulating liposomes (Buttino *et al.*, 2008).

In my thesis, *in vitro* experiments (incubation tests) were performed on the tunicate *Ciona intestinalis* testing the PUA 2-trans, 4-trans decadienal (DD) as a model aldehyde because this PUA is the most comprehensively studied, is commercially available, inexpensive and sufficiently stable to allow for a range of laboratory bioassays to be conducted (Caldwell, 2009). Tests were performed on *Ciona intestinalis* because ascidian embryogenesis is comparatively simple and well documented; it is characterized by a stereotyped development that is based on invariant early cell lineages and remarkably small cell numbers. Moreover, a very large number of synchronous developing embryos can be obtained that, thanks to their relatively large size (100 μm), can be easily manipulated. These unique features make it an appropriate experimental system in developmental biology and an ideal animal to study the effects of PUAs on embryonic development.

3.2 Materials and Methods

3.2.1 Collection of Animals and Harvesting of Gametes

Ciona intestinalis were collected from Villaggio Coppola (Naples, Italy), from January to May, and maintained in tanks with constantly flowing seawater for seven

days under constant light to accumulate gametes. Eggs and sperm were obtained surgically from the gonoducts. Eggs were fertilized by mixing with sperm from other individuals for 15 min in filtered sea water at room temperatures, in 1.5 mL Eppendorf conical tubes.

3.2.2 Decadienal solutions

2-trans-4-trans-decadienal (DD) was purchased from Acros Organics (part of Thermo Fischer Scientific, Geel, Belgium). A stock solution of 6mg mL^{-1} was prepared by dissolving 4.1μL DD in 500 μL DMSO. Work solution of 0.6mg mL^{-1} was obtained by diluting appropriate volumes of stock solution in DMSO. DMSO had no effect on *C. intestinalis* up to 1% DMSO in filtered seawater (DMSO showed toxicity on the embryonic development of *Ciona intestinalis* only at concentrations above 6.4 mL L^{-1}- Bellas, 2005). Treatment solutions were prepared adding appropriate volumes of working solution to filtered seawater.

3.2.3 Experimental set up

In these experiments, the same number of eggs per well was used. This is an important experimental condition because the effect of DD depends on the egg density used in each test. This was observed in sea urchins by at least two independent studies (Hansen *et al.*, 2004 and Romano *et al.*, 2010). These authors observed that the dose required for a complete block of cell division depended on the egg concentration, and this was ascribed to the interactions between PUAs and nucleophilic sites on both the egg surface or in the cytosol (Hansen *et al.*, 2004). The number of eggs per well was chosen according to Bellas *et al* (2003), who argued that experimental design of toxicity tests with marine invertebrate gametes, embryos or larvae should consider the number

of gametes, embryos or larvae to be observed in each experimental vial, and the number of replicates needed in each treatment. According to their results, they recommend five replicates per treatment and observing 100 individuals per replicate at least (Bellas *et al.*, 2003). Each experiment was conducted, therefore, in 5 replicates and with at least 100 individuals. The statistical analysis was performed on ten different experiments. An experiment was considered valid for statistical analysis when <50% control larvae were morphologically abnormal (Bellas *et al.*, 2003). Higher percentages of background larval abnormalities indicate poor quality of the biological material and have a limited validity, because toxicity may be overestimated and there could be an unpredictable interaction between the factor that causes the abnormalities and the toxicant under study. *C. intestinalis* embryo-larval tests with control abnormalities higher than 50% were therefore not considered in the analysis, as suggested by Bellas. The same author recommended a density of sperm of 10^6 mL^{-1} to fertilize eggs. These authors found that concentrations below 10^6 sperm ml^{-1} caused a fertilization rate of 20% (Bellas *et al.*, 2003).

I chose to treat both newly-fertilized and 32-cell stage embryos in order to discriminate DD effects on maternal and zygotic transcripts, considering that in embryos of the ascidian *C. intestinalis*, zygotic gene expression starts between the 8- and 16- cell stages (Matsuoka *et al.*, 2013). To date, the earliest zygotic expression in ascidians has been observed in the eight-cell stage. Expression of various genes starts at the 32-cell stage, corresponding to the mid-blastula stage in ascidians (Nishida *et al.*, 2005).

3.2.4 Pre-treatments

Eggs and sperm were treated with DD before fertilization in two different experiments. In the first experiment, eggs were collected from the gonoduct; approximately five hundred eggs (500 embryos for each DD concentration tested and 500 for the control) were placed into 60 mm cell culture dishes containing increasing DD concentrations, ranging from 0.2 to 0.6 μg mL^{-1} in filtered seawater. After 10 minutes, eggs were transferred to new 60 mm cell culture dishes containing only filtered seawater and were fertilized. For fertilization, not treated spermatozoa were added at a final concentration of 10^6 to cells the 60 mm cell culture dishes containing the pretreated eggs mL^{-1} (Tab.I.1). In the second experiment, sperm were treated with increasing DD concentrations ranging from 0.5 to 2 μg mL^{-1} which were then used to fertilize virgin not treated oocytes. In this case, spermatozoa were collected directly from the gonoduct, placed in 2 mL Eppendorf conical tubes containing DD solutions, and kept in these solutions for 10 minutes. An appropriate volume of treated sperm solution was added to egg solutions to fertilize the eggs in 60 mm cell culture dishes (Tab.III.1). The DD concentrations used to treat the sperms are higher than those used to treat the eggs and they were experimentally selected after preliminary tests. All the DD concentrations used in these experiments were experimentally selected.

Pre-treatment	Stage	DD concentrations	Time of treatment	Number of experiments
	Egg	0.20-0.40-0.60 µg mL^{-1}	10 minutes	15
	Sperm	0.50-1.0-2.0 µg mL^{-1}	10 minutes	15

Tab. III.1 - Description of the pre-treatment experiment conditions. In this table, the conditions of the pretreatment experiments are summarized. Stage column: the stage treated with the DD. DD concentrations column: DD concentrations used during the treatments. Time of treatment column: length of the treatment. Number of the experiments column: total number of the experiments conducted.

3.2.5 Treatments

Soon after fertilization, approximately five hundred embryos (for each DD concentrations used) were transferred to 60 mm cell culture dishes containing increasing DD concentrations (Tab.III.2). Another five hundred embryos from the same fertilization event were transferred to other 60 mm cell culture dishes containing only sea water and used as a control (for the fertilized eggs treatment). From the same fertilization events, five hundred embryos (for each DD concentrations used) were transferred to 60 mm cell culture dishes containing only sea water and were allowed to develop to the 32-cell stage (about 9 h), After 9 h they transferred in to 60 mm cell culture dishes containing increasing DD concentrations (Tab.III.2). A group of 32-cell stage embryos (five hundred) was transferred in a cell culture dishes containing only sea water and used as a control (for the 32-cell stage treatment). After DD treatment embryos were incubated to hatching at 21°C. During the development, to evaluate a possible delay of the hatching, embryos were observed under light microscope every thirty minutes up to hatching.

DD treatment	Stage	DD concentrations	Number of embryos	Number of experiments
	Fertilized eggs	0.30-0.35-0.4-0.45-0.50 µg mL^{-1}	500 for each DD concentrations + CTRL	15
	32-cell stage embryos	0.30-0.35-0.4-0.45-0.50 µg mL^{-1}	500 for each DD concentrations + CTRL	15

Tab. III.2 – Description of the treatment experiment conditions. In this table, the conditions of the treatment experiments are summarized. Stage column: the stage treated with the DD. DD concentrations column: DD concentrations used during the treatments. Time of treatment column: length of the treatment. Number of the experiments column: total number of the experiments conducted.

3.2.6 Recovery experiments

Recovery experiments were also conducted. Eggs were collected from one individual, fertilized with sperm from a different individual, divided in three batches and treated with the same DD concentrations (ranging from 0.3- 0.50 µg mL^{-1}). All three batches were incubated at 21°C. The first batch was incubated up to hatching; the second batch was incubated up to the 8-16 cell stage, rinsed twice for five minutes in fresh seawater and incubated at 21°C up to hatching; the third batch was incubated up to the 32-cell stage, rinsed twice for five minutes in fresh seawater and incubated at 21°C up to hatching (Fig.3.1) A wash step was introduced after treatment on 32-cell stage embryos as well. In this case, eggs were collected from one individual, fertilized with sperm from a different individual, divided in two batches and allowed to develop up to the 32-cell stage and then treated with the same DD concentrations (ranging from 0.30- 0.50 µg mL^{-1}). Both batches were incubated at 21°C. The first batch was incubated up to hatching; the second batch was incubated for two hours (until gastrula stage), rinsed twice for five minutes in fresh seawater and incubated at 21°C up to hatching (Fig. 3.2).

Recovery experiments	Stage	DD concentrations	Number of embryos	Number of experiments
	Fertilized eggs	0.30-0.35-0.4-0.45-0.50 µg mL^{-1}	500 for each DD concentrations + CTRL	15
	32-cell stage embryos	0.30-0.35-0.4-0.45-0.50 µg mL^{-1}	500 for each DD concentrations + CTRL	15

Tab. III.3 - Description of the recovery experiment conditions. In this table, the conditions of the recovery experiments are summarized. Stage column: the stage treated with the DD. DD concentrations column: DD concentrations used during the treatments. Time of treatment column: length of the treatment. Number of the experiments column: total number of the experiments conducted.

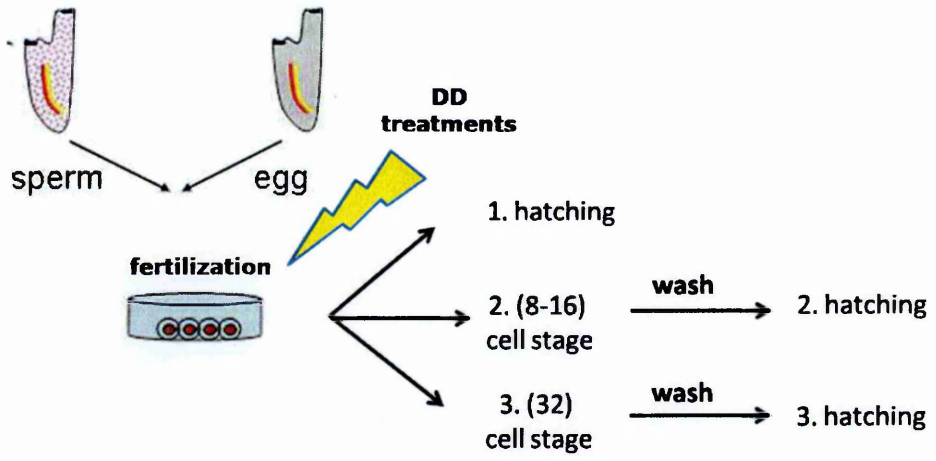

Fig. 3.1 - Schematic representation of the recovery experiments on fertilized eggs. This picture offers a schematic view of recovery experiments on fertilized eggs.

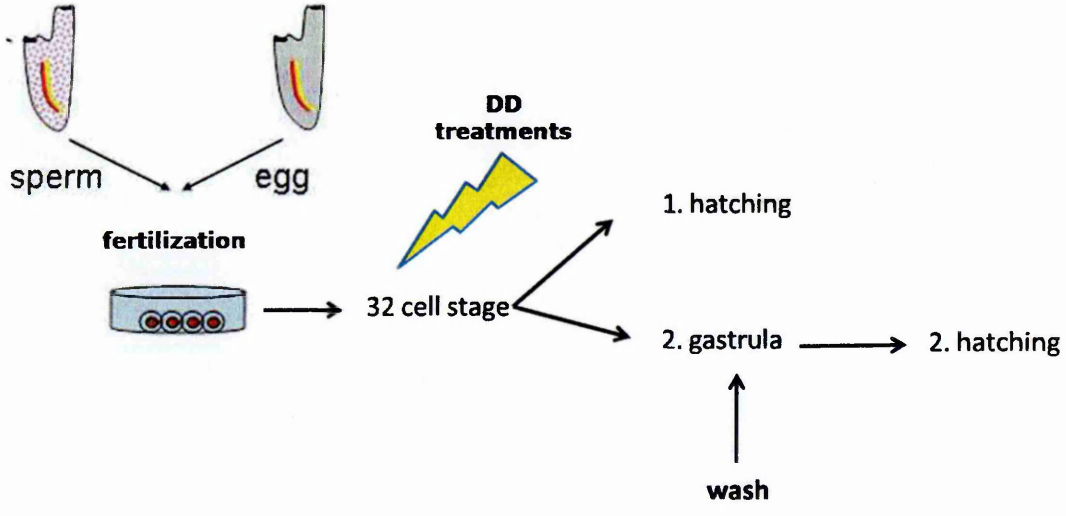

Fig. 3.2 - Schematic representation of the recovery experiments on 32-cell stage embryos. This picture offers a schematic view of recovery experiments on 32-cell stage embryos.

3.2.7 Statistical analysis

Statistical comparisons between treatments and the corresponding control were carried out using a one-way ANOVA test. A value of $p< 0.05$ was considered statistically significant. To conduct this statistical analysis ten different experiments were considered.

3.3 Results

3.3.1 Pre-treatments

The treatment of virgin oocytes with increasing DD concentration resulted in a little delay in development. This retardation was not accurately calculated. The pretreatments of the eggs before the fertilization had no effect on the hatching success and on the larval phenotype. In the case of DD treatment of the sperm before the fertilization, none effect was observed at all.

3.3.2 Treatments

DD effect on hatching success and on larval phenotype

When 32-cell stage embryos were incubated with DD concentrations ranging from 0.30 μg mL^{-1} to 0.50 μg mL^{-1}, a decreasing number of hatched larvae were observed (Fig 3.3). This effect was dose-dependent. Moreover, at these DD concentrations, an increased number of abnormal hatched larvae were observed (Fig. 3.5). At the lowest DD concentrations tested (0.3 μg ml^{-1}) larvae had a mild abnormal phenotype (Fig. 3.7 G); at higher DD concentrations (ranging from 0.35- 0.40 μg mL^{-1}) the abnormal phenotype became more severe (Fig. 3.7 H-I). Aberrations occurred

mainly on the larval tail; at 0.30 μg mL^{-1} tails resulted shorter than the control. Moreover, in control tail cells were well intercalated and well vacuolated; in fact, in the control tail a central lumen was clearly visible between adjacent notochord cells compared to the abnormal tail; at higher DD concentrations (0.35-0.40 μg mL^{-1}) aberrant phenotypes become more severe: the tail was even shorter and was kinked and disorganized; while the trunk seemed quite normal. The observed phenotype was worse at DD concentrations of 0.45 μg mL^{-1} (Fig. 3.7 L), where larvae were completely disorganized and failed to hatch. At the highest concentration tested (0.50 μg mL^{-1}) no development was observed.

After treatment also on newly fertilized eggs (with the same DD concentrations 0.30 μg mL^{-1} - 0.50 μg mL^{-1}) a decreasing number of hatched larvae was observed (Fig. 3.4). In this case larvae were normal at DD concentrations up to 0.30 μg mL^{-1}, whereas abnormal larvae were obtained at DD concentrations ranging from 0.35-0.45 μg mL^{-1} (Fig. 3.6). It is interesting to note that aberrations still occurred on the tail of these abnormal larvae (Fig. 3.7 A-E). Moreover, at 0.35 μg mL^{-1} abnormal larvae showed a severe phenotype.

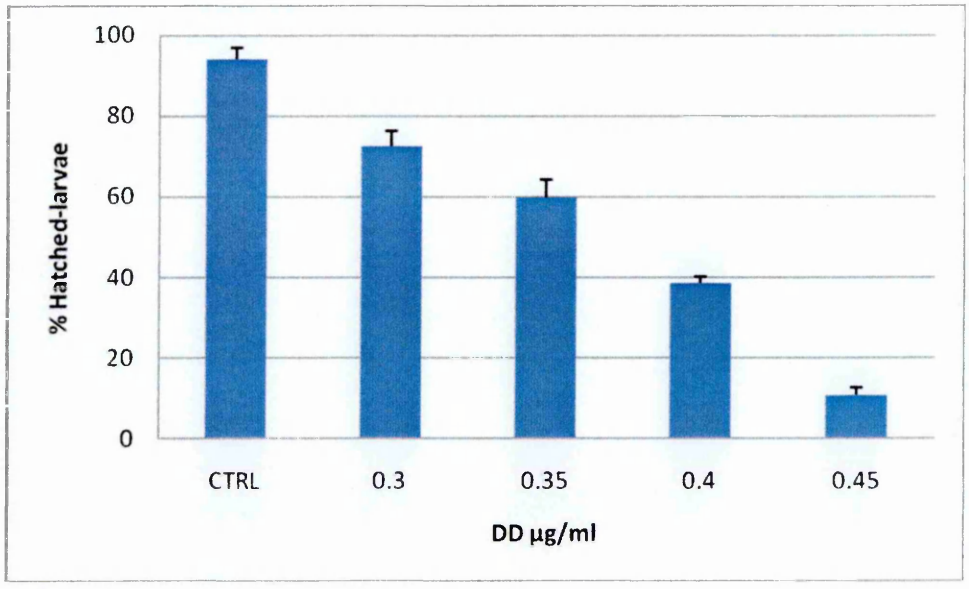

Fig. 3.3 - % hatched larvae versus D increasing concentrations after treatment on 32-cell stage embryos. Data are expressed as mean % number of hatched larvae ± standard deviation (sd). Ten experiments were considered to calculate the sd.

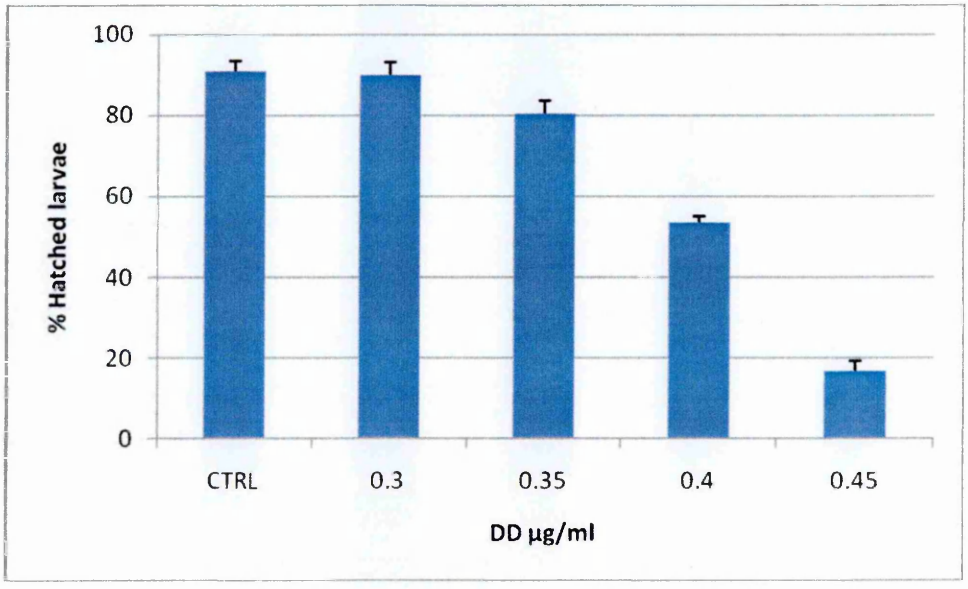

Fig. 3.4 - % hatched larvae versus DD increasing concentrations after treatment on newly fertilized eggs. Data are expressed as mean % number of hatched larvae ± standard deviation (sd). Ten experiments were considered to calculate the sd.

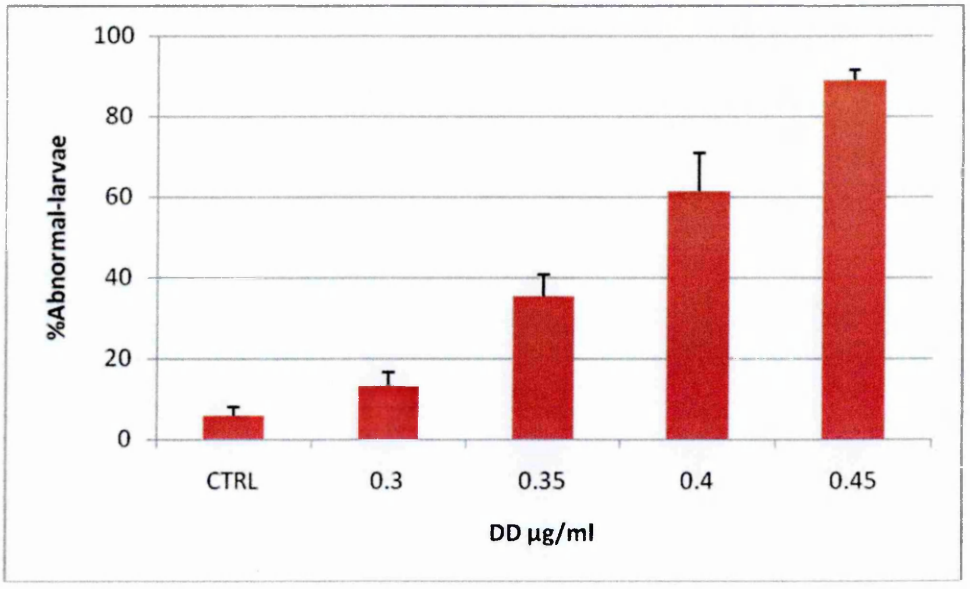

Fig. 3.5 - % abnormal larvae versus DD increasing concentrations, after treatment on 32-cell stage embryos. Data are expressed as mean % number of abnormal larvae ± standard deviation (sd). Ten experiments were considered to calculate the sd.

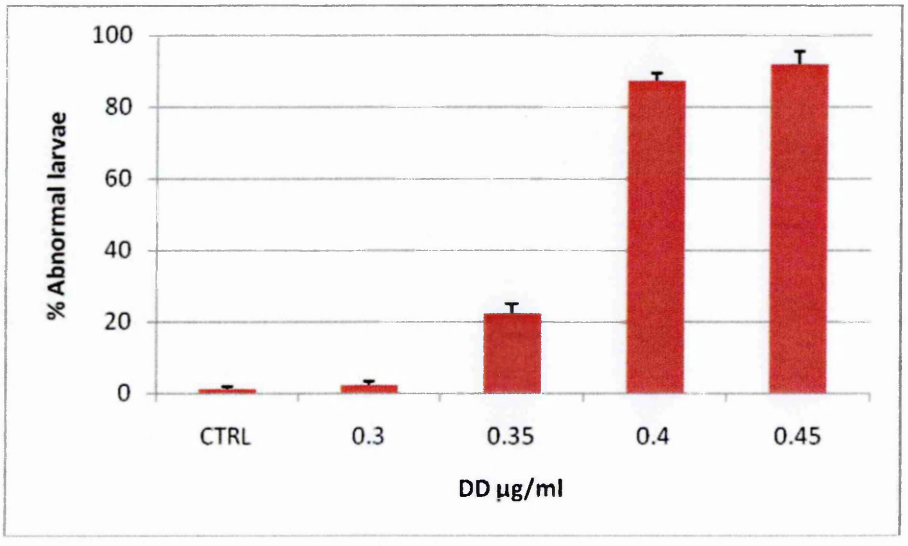

Fig. 3.6 - % abnormal larvae versus DD increasing concentrations, after treatment on newly fertilized eggs. Data are expressed as mean % number of abnormal larvae ± standard deviation (sd). Ten experiments were considered to calculate the sd.

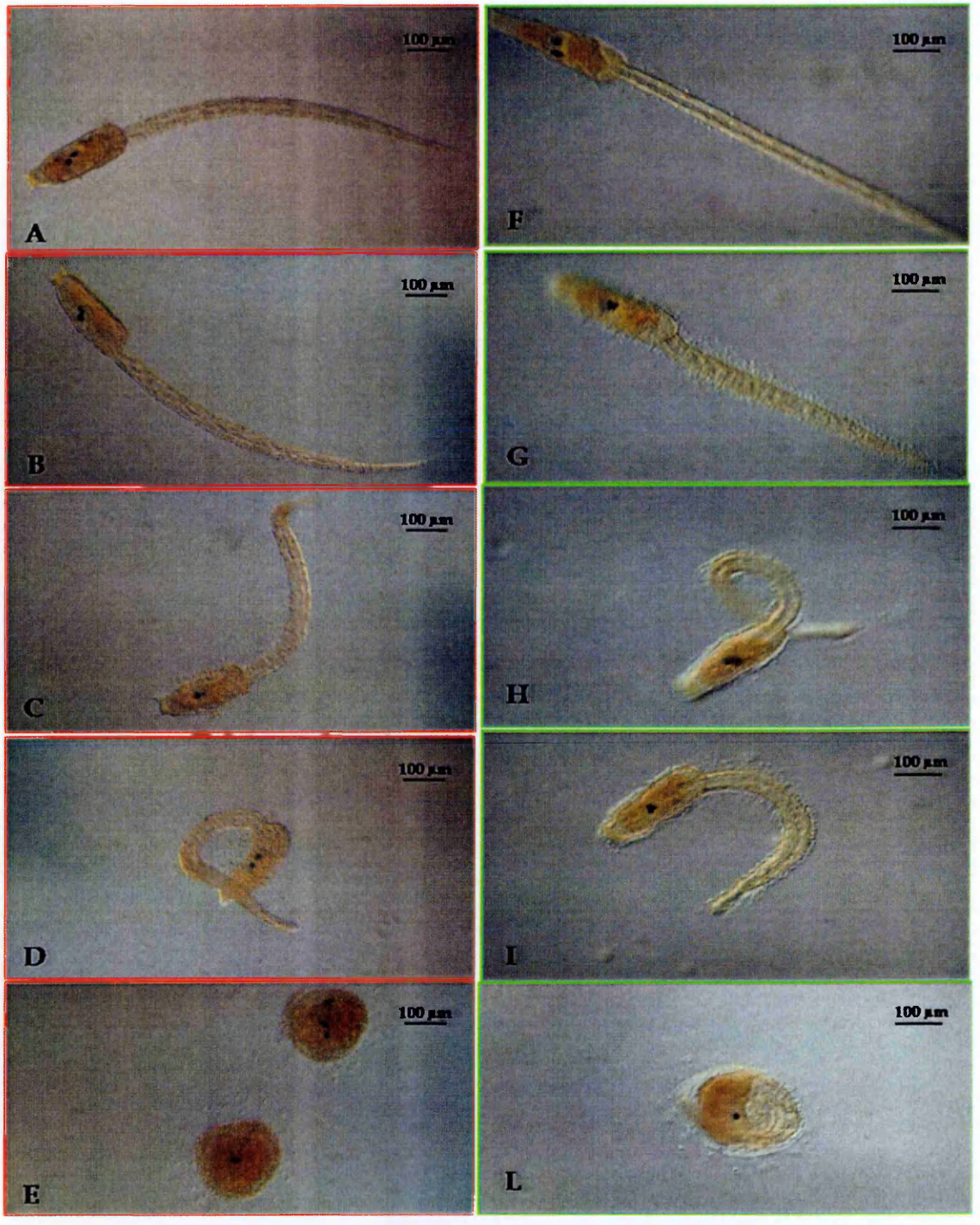

Fig. 3.7 - Aberrant phenotypes. Left panel (red) shows hatched larvae after DD treatment on fertilized eggs (A:CTRL; B:0.30µg ml^{-1}; C:0.35µg ml^{-1}; D: 0.40µg ml^{-1}; E:0.45 µg ml^{-1}). Right panel (green) shows hatched larvae after DD treatment on 32-cell stage embryos (F:CTRL; G:0.30µg ml^{-1}; H:0.35 µg ml^{-1}; I: 0.40µg ml^{-1}; L:0.45 µg ml^{-1}).

DD (µg/ml)	Treatment on fertilized eggs	Treatment on 32-cell stage embryos
—	Normal phenotype (A)	Normal phenotype (F)
0.30	Normal phenotype (B)	tails resulted shorter than the control; cells were not well intercalated and not well vacuolated (G)
0.35	tail was shorter than the control, kinked and disorganized (C)	tail was even shorter, kinked and disorganized (H)
0.40	tail was even shorter, kinked and disorganized; the trunk seemed quite normal (D)	tail was even shorter, kinked and disorganized; the trunk seemed quite normal (I)
0.45	larvae were completely disorganized and failed to hatch (E)	larvae were completely disorganized and failed to hatch (L)
0.50	no development	no development

Tab. III.4 - Description of the aberrations. Left column reports DD concentrations in µg ml^{-1}; central column reports aberrations after DD treatment on newly fertilized eggs (capital letters refer to the corresponding picture in fig 3.5). Right column reports aberrations after DD treatment on 32-cell stage embryos (capital letters refer to the corresponding picture in fig 3.5).

DD effect on swimming behavior

In both experiments malformed hatched larvae showed an abnormal swimming behavior; in fact, they could move their tail but they could not swim forward as they would normally do but could only trace circles around themselves.

Developmental delay

After DD treatment on newly fertilized eggs, a developmental delay was also observed (Fig. 3.6). This delay was visible throughout the stages of development and was dose-dependent. In fact, about 24 hpf (hours post fertilization) whereas there was 100% hatching in control embryos treated with 0.30 µg mL^{-1}, at 0.35 µg mL^{-1} the percentage of hatched larvae was only 20% and reached 100% about 30 min. after

control embryos. At 0.40 µg mL^{-1}, hatching success was 10% and reached 100% about 1 h after controls. This value drastically decreased at 0.45 µg mL^{-1} when only 1% of the embryos hatched after 24h and it took about 1.5 h to reach 100% compared to the control (Fig. 3.8). At 0.50 µg mL^{-1} none of the larvae hatched and development was blocked. The same trend was observed after treatment on 32-cell stage embryos, but in this case a slight delay was observed after treatment with 0.30 µg mL^{-1}.

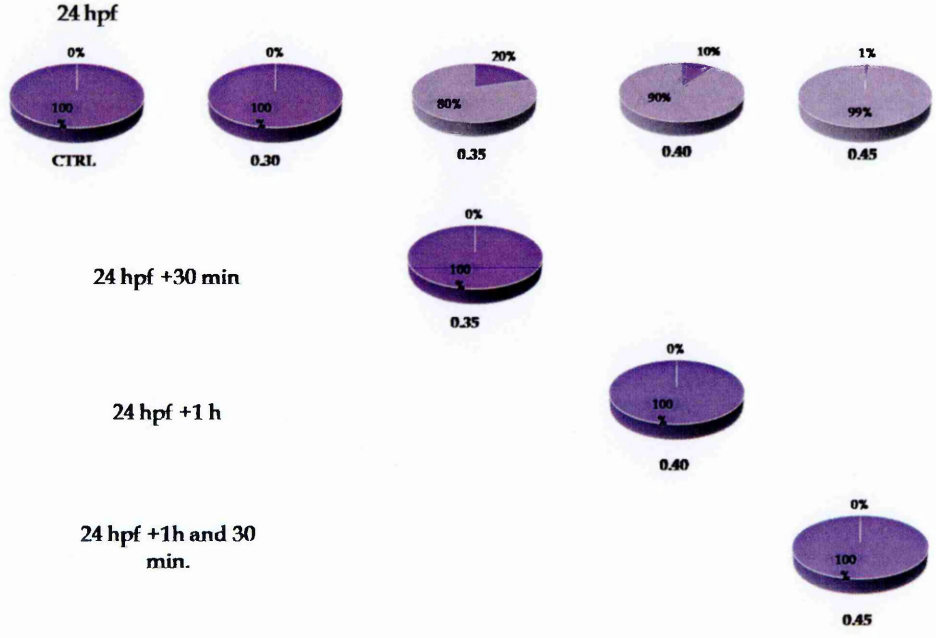

Fig. 3.8 - Developmental delay after DD treatment on fertilized eggs. % of hatched larvae are dark purple; % of no hatched larvae are light purple. This scheme shows how % of hatched larvae increases with time.

3.3.3 Recovery experiments

To understand if the effects of DD were reversible, two wash steps were introduced after treatment. Rinsing 8-cell stage embryos twice for five minutes did not

reverse the effect of DD at any of the DD concentrations used. Even if treated embryos were rinsed at the 32-cell stage, they did not recover their ability to develop normally.

3.4 Discussion

3.4.1 DD effect on *Ciona* oocytes

When virgin oocytes were treated with increasing DD solutions (0.20-0.40-0.60 µg mL^{-1}) and then fertilized with untreated sperm, a small decrease in hatching percentage was observed, but hatched larvae were normal. These results were different from the results previously described on *Ciona* by Tosti *et al* (Tosti *et al.*, 2003). After treatment of oocytes with increasing DD concentrations ranging from 0.10 to 1.5 µg mL^{-1}, they observed a decrease in first cleavage. Moreover, they observed an increase in the percentage of abnormal larvae at DD concentrations between 0.10 and 0.20 µg mL^{-1}. The difference between the two results (Tosti and our results) could be explained by the differences in the treatments. In fact, in the case of Tosti's experiments, eggs were dechorionated before treatments, whereas in the present study eggs were not dechorionated. Ascidian eggs are covered by an acellular, proteinaceous egg coat called the vitelline coat (VC) or chorion. This envelope consists of a fibrous chorion and a layer of large follicle cells attached to its outer surface. Between the chorion and the surface of the oocyte there is a perivitelline space filled with the test cells. The presence of the chorion could protect eggs from DD, thereby weakening the effect of this aldehyde.

3.4.2 DD effect on *Ciona* zygotes and embryos

Developmental delay

Data were compared from two treatments performed on 32-cell stage embryos and fertilized eggs, respectively. A developmental delay was observed after DD treatment on fertilized eggs and on 32-cell stage embryos. In both cases the delay was dose-dependent. The same delay was also observed in sea urchins; at concentrations lower than (1.32-5.26 μM-0.20-0.80 μg mL^{-1}, respectively) the concentration required to block cleavage (1 μg mL^{-1}-6.58 μM), DD retarded development (Romano *et al.*, 2010).

DD effect on hatching success

Hatching success decreased after DD treatment in a dose-dependent manner. This effect occurred after both treatments; fertilized eggs and 32-cell stage embryos. This effect was also observed in other marine organisms. For example, in the sea urchin *Paracentrotus lividus* DD exerted a very strong dose-dependent effect on hatching success. At concentrations of circa 3.0 μM (0.50 μg mL^{-1}), DD reduced hatching viability to <50%; total inhibition of hatching viability occurred at DD concentrations of 3.95 μM (0.60 μg mL^{-1}) (Romano *et al.*, 2010).

Effect of DD on larval phenotype

After treatment on 32-cell stage embryos a gradual abnormal phenotype was obtained with increasing DD concentrations; in particular, the abnormal phenotype was obtained with DD concentrations ranging from 0.30-0.45 μg mL^{-1}. After treatment on fertilized eggs larvae were normal at a DD concentration of 0.30 μg mL^{-1}. A severely abnormal phenotype was observed immediately beyond this concentration, at 0.35 μg mL^{-1}. Apparently, the effect on 32-cell stage embryos would be stronger because

abnormal larvae appear at lower DD concentrations, 0.30 μg mL^{-1} versus 0.35 μg mL^{-1} after treatment on fertilized eggs. Moreover, after treatment on fertilized eggs mild abnormal phenotypes were no longer observed. In other words, there was an abrupt passage in the appearance of abnormal phenotypes indicating a threshold DD concentration at which this phenotype appears. It seemed that, there was some process that protected the embryos until 0.30 μg mL^{-1}.

3.4.3 Reversibility of DD effect

To test whether the effect of DD was reversible, two wash steps were introduced. Results obtained indicate that DD treatment on both newly fertilized eggs and 32-cell stage embryos did not reverse the aberrant phenotype at any of the concentrations tested, even the lowest one (0.30 μg mL^{-1}). These results differ from those obtained by Tosti *et al.* (2003) who demonstrated that the effect of 1 μg mL^{-1} DD (a concentration that is much higher than the value reported in the present study) on development was completely reversible if the oocytes were rinsed 2 min after fertilization. Rinsing fertilized oocytes after 10 min did not reverse the effect of DD on development. The difference between the two experiments could be due to differences in the two treatments.

In Tosti's experiments, DD treatment was on virgin oocytes, whereas in this work, DD treatments were performed after fertilization. This could mean that the processes that occur after fertilization would be affected by DD in a more severe manner.

The irreversibility of the phenotype after treatment on newly fertilized eggs demonstrated also that the effect of DD on the maternal determinant was as important as the effect on the zygotic transcript.

3.4.4 Aberrant phenotypes

Aberrations occurred mainly on the tail of the larvae. The ascidian tadpole tail is composed of mononucleate striated muscle cells, arranged in three rows along each side of the notochord, which runs all along the tail and also extends into the caudal most part of the trunk. The notochord is covered dorsally by the neural tube, ventrally by the endodermal strand, and is surrounded by the tail muscles and the epidermis. The tunic is the most external structure of the tail (Chambon *et al.*, 2002). According to the abnormal phenotype obtained, it seemed that the most affected tail tissue was the notochord. In fact, at sub-lethal DD concentrations (0.35-0.45 $\mu g\ mL^{-1}$), tails of hatched larvae were disorganized; in particular, notochord cells were not well intercalated and vacuolated; in fact, the central lumen between the adjacent notochord cells, clearly visible in a normal tail, were lost in the abnormal phenotype. Previous studies have demonstrated that, during ascidian tail morphogenesis, notochord and muscle differentiation are crucial (Di Gregorio *et al.*, 2002). Moreover extension of the notochord is required for organization of the muscle cells. If the notochord does not extend properly in the embryos, the tails of these tadpoles are malformed and often kinked (Di Gregorio *et al.*, 2002). The same paper also indicated that signals from the notochord are required to organize both muscles and endodermal strand (Di Gregorio *et al.*, 2002).

3.4.5 Effect of DD on Ciona swimming behaviour

Essentially, morphological aberrations concerned the skeletal system (axial or appendicular); in other words, embryos/larvae organization was compromised to the point that they could no longer swim correctly; in fact, they could move their tail but they could not swim forward but only in circles. This abnormal swimming behavior has also been observed in copepods (Poulet *et al.*, 2005). Some authors found that nauplii hatched from diatom-fed females were generally deformed and expressed marked morphological asymmetry. Most deformed nauplii died after hatching, whereas those that survived displayed greatly impaired swimming behavior (Uye *et al.*, 1996); other authors (Miralto *et al.*, 1998) recorded that of about 80% of spawned eggs of the copepod *Calanus simillimus* underwent abnormal development resulting in either abortions or production of asymmetrical larvae. The severity of swimming behaviour was directly linked to an abnormal asymmetric development and asymmetrical nauplii that tended to turn in the direction opposite to the most developed swimming appendages (Poulet *et al.*, 1995). Such a change in locomotory capacity will impair feeding efficiency and escape behaviour (Titelman *et al.*, 2003).

3.2.1 Additional experiments

The effects of PUA-producing diatoms have been mostly studied on crustacean copepods by conducting feeding experiments testing the effects of diatom diets on reproduction and development of their offspring. I therefore also tried to conduct feeding experiments on *Ciona intestinals* adults to test whether a PUA-producing diatom diet would induce the same deleterious effects on *C. intestinalis* offspring as when gametes were exposed to pure PUAs (decadienal). But I obtained poor results due to a number of experimental problems. Experiments were carried out in the

following way: about twenty *Ciona* adults (ten for the treatment and ten for the control) were kept in two tanks with constantly flowing seawater. Ten animals were fed on toxic diatom known to producing PUAs, such as *Skeletonema marinoi* for 48 h. The other ten animals were fed on a non-PUA producing algae as a control (*Isochrisys galbana).* During feeding the sea water flux was interrupted. After 48 h, adults were induced to spawn, were fertilized and embryos were incubated up to hatching. No results were obtained.

Possibly the feeding experiments should have lasted longer than 48h in order to accumulate toxic compounds to affect developing oocytes, as demonstrated for some copepod species that are more resistant to these compounds. Another possible explanation for the lack of an effect is that the concentration of toxic algae was not enough for a filter feeding organism such as *C. intestinalis* which has a very high filtration rate. To answer these questions, I should have changed the experimental conditions. For example: increase the algal concentration, or the time of feeding (from two days to 1 week); add, as a control, animals treated directly with the decadienal. It would also have been interesting to change the experimental apparatus, for example by keeping the animals in closed tanks without constantly flowing seawater.

Unfortunately, it was not possible to repeat these experiments due to problems with the animal facility at the Zoological Station. Repeating these experiments under the appropriate conditions would be important so as to compare the effects of diatoms on *Ciona* and copepods, but also to simulate what happens in the field when an organism like *Ciona* comes into contact with oxylipins in the surrounding water, as during the end of a diatom bloom.

Chapter 4: Microarray analysis

4.1 Introduction

After the first experimental observation that a diatom diet induced a decrease in egg hatching success in the copepod *Temora stylifera* (Ianora and Poulet, 1993), numerous studies (reviewed by Paffenhöfer *et al.*, 2005; Pohnert, 2005; Ianora *et al.*, 2010), followed over the years, demonstrating the negative effect of diatom oxylipins on the embryonic and larval development of several marine organisms. Although the majority of these studies have been focused on the impact of these compounds (in particular of 2-trans,4-trans-decadienal) on organism physiology and though their biological activity was observed in all cases, their inhibitory mechanism still remains unknown (Adolph *et al.*, 2004). So far, despite this enormous amount of experiments showing that diatom oxylipins negatively impact invertebrate reproduction and development, information on the molecular mechanisms and the associated genes underlying the effects of the oxylipins on the development of marine organisms is lacking. There are several studies, however, that have considered changes in gene expression due to diatom oxylipins. These studies have been conducted mainly on sea urchins and copepods.

Romano *et al.* (2011) used a reverse transcription-quantitative real time polymerase chain reaction (RT-qPCR) approach to study the effect of DD treatment on development in the sea urchin, *Paracentrotus lividus*. They found that hsp70 (heat shock protein 70) expression levels in embryos from eggs treated with DD increased via nitric oxide production. These results have important implications for understanding the cellular mechanisms underlying the response of benthic organisms to aldehyde

exposure (Romano *et al.*, 2011). In the same organism, Marrone *et al.* (2012), in addition to hsp70, reported that the activity of a series of other genes are affected by decadienal; they investigated the change in the expression levels of genes implicated in various functional responses in sea urchins including stress (heat shock protein 60-56), development (SRY-sex determining region Y-box 9), hatching (hatching enzyme) and skeletogenesis (Spicule matrix protein 30-50, nectin, univin,).

Lauritano *et al.* (2011a-2011b-2012a) studied the effects of toxic diatom diets on copepod fitness and survival. They studied changes in expression level of genes which are known to have a primary role in generic stress responses (hsp40 and hsp70), defense systems (e.g. aldehyde, free fatty acid and free radical detoxification, aldh2, aldh3, aldh6, aldh7, aldh8 and aldh9, cyp4 and gst, cat-sod-gsh, respectively) or apoptosis regulation (cas, carp and iap). Just recently, in addition to the pioneering work of Lauritano *et al.* (2011a-2011b-2012a), transcriptomic tools were developed for *Calanus finmarchicus* (An EST database and a microarray were generated by Lenz *et al.*, 2013) and *Calanus helgolandicus* (ESTs libraries, Carotenuto *et al.*, 2014). Carotenuto *et al.* (2014) generated two Expressed Sequence Tags (ESTs) libraries of the copepod *C. helgolandicus* feeding on the oxylipin-producing diatom *Skeletonema marinoi* and the cryptophyte *Rhodomonas baltica* as a control, using suppression subtractive hybridization (SSH), in order to investigate differences in the transcriptome between females fed toxic and non-toxic diets and identify differentially expressed genes and biological processes targeted by this diatom. The above mentioned studies have some limitations due mainly to the organisms and the techniques used. In fact, regarding copepods the biggest disadvantage is the lack of a sequenced genome and of a genomic and post-genomic tools useful in these cases; this last is true also for sea urchin. Moreover, the (RT-qPCR) approach is suitable technique to analyze a few number of

genes and this is a limitation when you are trying to shed light on a mechanism on which little is known; in these cases a more general approach is more advantageous.

To overcome these limitations, in my work the tunicate *Ciona intestinalis* was used. *Ciona* has major advantages for studies of this nature. The life cycle includes a simple swimming tadpole larva that develops in 18 hours and consists of a small number of tissues and organs, including the epidermis, central nervous system, endoderm, mesenchyme, notochord and muscle (Satoh, 1994). Embryogenesis is simple and the lineage of embryonic cells is well documented (Conklin, 1905; Nishida and Satoh, 1983; Nishida and Satoh, 1985; Nishida, 1987), allowing visualization of any alterations in development, at the morphological level, caused by treatment of embryos with external reagents. Furthermore, *Ciona* offers a number of genomic and post-genomic tools, including the sequenced genome (Dehal *et al.*, 2002). These comprise numerous markers specific for tissue and organ formation, both for early embryogenesis-larval and juvenile stages; a cDNA collection of 17,834 independent clones arrayed in well plates; diverse chip microarrays, including a cDNA chip array. I used a microarray approach to study the effect of DD on development of *C. intestinalis*, because with this approach tens of thousands of transcript species can be detected and quantified simultaneously.

The principle of a microarray experiment is that mRNAs from a given cell line, tissue or embryos are used to generate a labelled sample, sometimes termed the 'target', which is hybridized in parallel to a large number of DNA sequences, immobilized on a solid surface in an ordered array (Schulze and Downward, 2001). The number of molecules of mRNA, coming from the transcription of a given gene, can be considered as an approximation to the level of expression of that gene. There is a

great variability related with this: some genes act on other genes without transcription; in other cases a high activity is the consequence of small mRNA concentration. In spite of this variability the broad idea can be considered valid (Sanches and de Villa, 2008) and here we considered it so. With this technology, cells or tissues or embryos can be exposed to toxicants, and then gene expression can be measured by collecting mRNA, converting mRNA to labeled cDNA, hybridizing it to the DNA array, staining it with an appropriate dye, and visualizing the hybridized genes using a fluorometer. The raw data are analyzed using bioinformatic softwares and databases (Fig.4.1). The aim is to obtain meaningful biological information such as patterns of relative induction/repression levels of gene expression, and participation in biochemical pathways (Lettieri, 2006).

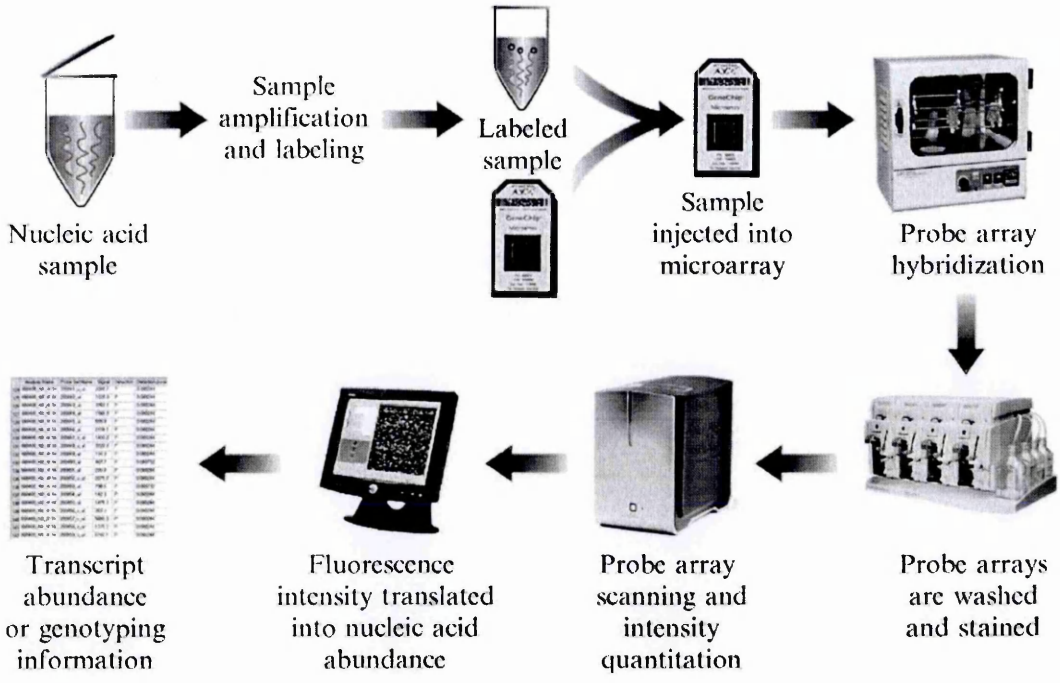

Fig. 4.1 - Flowchart of a GeneChip System microarray experiment. Once the nucleic acid sample has been obtained, target amplification and labeling result in a labeled sample. The labeled sample is then injected into the probe array and allowed to hybridize overnight in the hybridization oven. Probe array washing and staining occur on the fluidics station, which can handle four probe arrays simultaneously. The probe array is then ready to be scanned in the Affymetrix GeneChip scanner, where the fluorescence intensity of each feature is read. Data output includes an intensity measurement for each transcript (adapted from Dalma-Weiszhausz *et al.*, 2006).

4.2 Materials and Methods

4.2.1 Embryo collection

Embryos at late-tailbud stage (about 9 hour post fertilization-hpf) were collected after treatment on fertilized eggs (see Chapter 3) with the two highest sub-lethal DD concentrations tested (0.40-0.45 µg mL^{-1} as described in Chapter 3), so as to have three experimental conditions A, B and C, that represent treatment with 0.40 µg mL^{-1},0.45 µg mL^{-1} DD and the control, respectively (Table IV.1).

Condition	C	A	B
Stage (hour post fertilization hpf).	tailbud (9 hpf)	tailbud (9 hpf)	tailbud (9 hpf)
DD treat	No	Fert. eggs	Fert. eggs
DD conc.	No	0.40 µg/mL	0.45 µg/mL

Tab. IV.1 - Description of the experimental condition. Condition C is the control; Condition A represents treatment with 0.40µg mL DD, and condition B represents treatment with 0.45µg mL.

Embryos were collected in 500 µL lysis buffer of the RNAqueous-micro kit (Ambion) and frozen at -80°C until RNA extraction. Embryos were collected from three different experiments (three biological replicates). This was important for the statistical analysis of the microarray data.

4.2.2 RNA extraction and RNA quality detection

Total RNA extraction was performed using the RNAqueous-micro kit (Ambion) from previously frozen samples in lysis buffer. RNA extraction was performed following manufacturer's recommendations and eluted in 2x15 µL of pre-warmed (70°C) elution buffer. Total RNA (1 µL) was analyzed with the BioAnalyzer (Agilent Technologies) using the Eukaryote total RNA Micro Series II kit and the mRNA Smear Nano program following manufacturer's instructions (Agilent Technologies). The integrity of total RNA was estimated by RNA Integrity Number (RIN) values, calculated by an algorithm that assigns a numbering system from 1 to 10, with 1 being the most degraded and 10 being the most intact. In this way integrity is no longer determined by the ratio of the ribosomal bands, but by the entire electrophoretic trace of the RNA sample. This includes the presence or absence of degradation products.

4.2.3 Microarray Hybridization

RNA extracted was reverse transcribed and the resulting cDNA was hybridized to the *Ciona intestinalis* custom-design Affymetrix GeneChip. The total GeneChip microarray contains 30,970 distinct probe sets (each made of 16 individual probes, with all 16 probes corresponding to one transcript - Fig.4.2). Every probe set was associated to a specific annotation file which includes the nucleotide sequences of probes (retrieved from Affymetrix library file); the transcript models and annotations (downloaded from the ANISEED database, JGI version 1, KYOTOGRAIL2005, KH and ENSEMBL); the gene and its functions.

cDNA synthesis and hybridization were performed at the Genomic analysis facility of the Stazione Zoologica in Ariano Irpino, Italy.

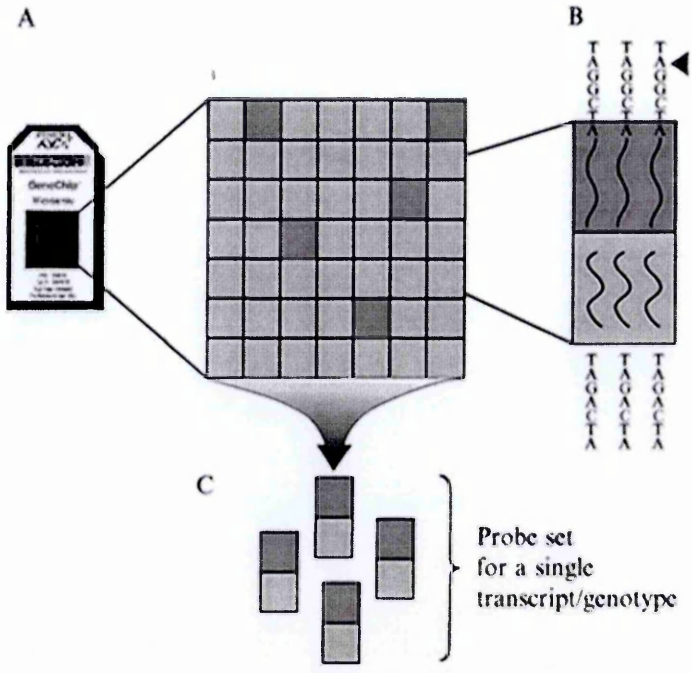

Fig. 4.2 - Dissection of a probe array. (A) Inside the probe array (left) is a piece of quartz, generally containing a synthesis area of 1.28 cm^2 and carrying more than a million different features. Each feature, in turn, is composed of millions of oligonucleotide sequences. (B) A probe example that constitutes a probe set. (C) Each probe set is made of 16 individual probes with all 16 probes corresponding to one transcript (adapted from Dalma-Weiszhausz *et al.*, 2006).

4.2.4 Microarray data analysis

A main issue in microarray studies is how to retrieve valuable information from the enormous amount of generated data. The main processes in the data analysis are: background correction, meaning that there is some amount of unspecific background noise in every scanner image which has to be removed; normalization, which adjusts the data obtained from individual arrays so that they can be compared in terms of signal intensity; summarization, which combines the multiple probe intensities associated to the same gene to a single expression value. These processes permit to obtain a single gene expression value out of raw probe intensity measurements. Before the analysis of microarray data the quality of the data obtained from each GeneChip was checked. The exact measurements used for judging data quality depends on the

microarray platform used and the types of controls present on the microarray. The Affymetrix GeneChip system includes a number of standard controls and quality measures.

Microarray data analysis were carried out with the GeneSpring GX 12.5 (Agilent Technologies, Santa Clara, CA, USA), a popular gene expression analysis software that provides powerful, accessible statistical tools for fast visualization and analysis of expression and genomic structural variation data. Raw data were imported into GeneSpring and normalized using global normalization. After the normalization the expression of each gene was reported as the ratio of the value obtained for each condition relative to the control condition. The normalized data were used to identify changes in gene expression in the two different conditions (DD treatment 0.40-0.45 μg mL^{-1}) compared to the control. A gene was identified as statistically and significantly affected if it showed increased or decreased expression according to an arbitrary cut-off of 1.5-fold change at $p<0.05$, according to the GeneSpring statistical package. Gene significance was performed by statistical analysis on the normalized data, t-test and one-way ANOVA; Fold Change analysis was performed on probe sets showing p-values below 0.05. The Fold Change is a ratio between the intensity of the signal of a probe in the treated and in the control embryos.

4.2.5 GO analysis

A typical analysis of microarray expression data produces a long list of genes (see Appendix I), which are potentially interesting in the analyzed process. In order to gain biological understanding from this type of data, it is necessary to analyze the functional annotations of all genes in this list. The GeneOntology (GO) Consortium (Ashburner *et al.* 2000) generates one of the most widely used of these classifications.

GO database provides a useful tool to annotate and analyze the functions of a large number of genes. Genes in biological databases are linked to GO terms, providing a specific type of information about a gene or protein, its molecular function, the broader biological processes it is involved in and the cellular compartment it acts in.

The GO Consortium has developed three ontologies: molecular function, biological process, and cellular component, to describe attributes of gene products or gene product groups. Briefly, molecular function describes what a gene product does at the biochemical level. Biological process describes a broad biological objective. Cellular component describes the location of a gene product, within cellular structures and within macromolecular complexes. Each principal ontology can be subdivided into sub-ontologies.

Several tools have emerged to automate this type of analysis. These programs rely on a priori classification of genes into biological functional groups. In my work I used the GeneSpring GX 12.5 software.

4.3 Results

4.3.1 RNA quality detection

In microarray analysis high quality RNA is very important. After analysis with the BioAnalyzer, the software assigns a RIN value ranging between 1-10. The best RIN values for microarray analysis have to be ≥ 8. For my RNA, I obtained RIN values ranging from 9.60 to 9.80 (Fig 4.3).

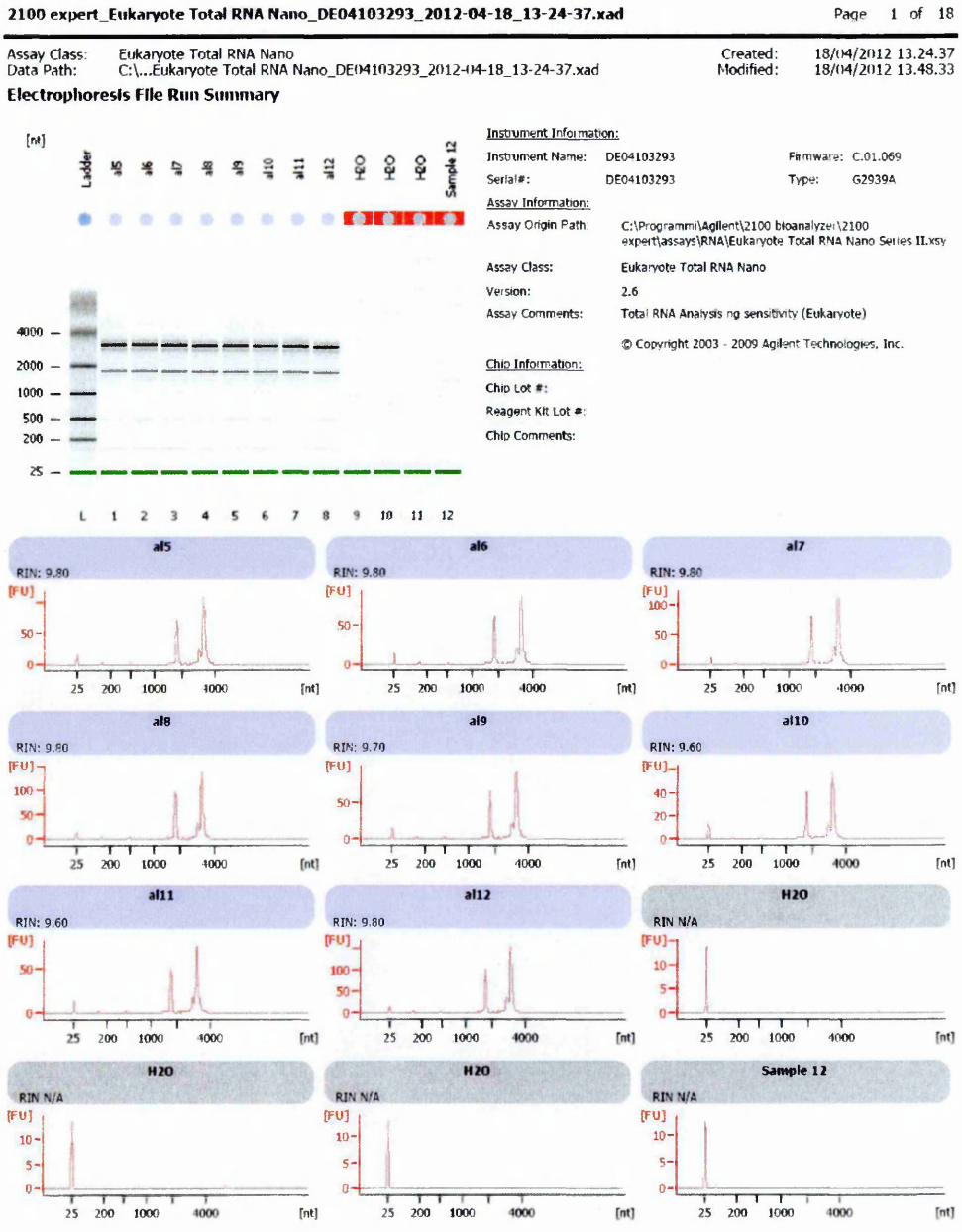

Fig. 4.3 - Summary of the electrophoresis profiles generated by the BioAnalyzer. The upper panel shows the virtual electrophoresis gel image of 8 RNA samples (lane 1-8), used in my experiments; the first lane represents the electrophoretic profiles of the ladder and the lanes named H20 the blanks. The lower panels show the electropherogram profiles summary of my RNA samples (1-8) and blanks (H_20).

4.3.2 Microarray data analysis

Genes derived from ANOVA and Fold Change analyses were plotted in a Venn diagram that shows the intersection among the three possible comparisons of the three groups.

The intersections considered were:

- A vs C (condition A versus Control);
- B vs C (condition B versus Control);
- (A vs C) vs (B vs C).

The first intersection represents the transcripts that are differentially expressed in condition A compared to the control. The second intersection the transcripts differentially expressed in condition B compared to the control. The third one represents the transcripts that change their expression after both treatments compared to the control.

I found that about 402 transcripts changed their expression after treatment with 0.40 μg mL^{-1} DD; 1146 transcripts changed after treatment with 0.45 μg mL^{-1}; 356 of which changed after both treatments (Fig. 4.4). These transcripts were up/down-regulated after DD treatment.

Fig. 4.4 - Venn-diagram. Transcripts differentially expressed in A vs. C are shown in red. Transcripts that are differentially expressed in B vs. C are shown in blue. Overlying area represents the transcripts that change after both treatments.

4.1.1 GO analysis

According to GO term, this analysis showed that the transcripts differentially expressed after both treatments (A vs C) vs (B vs C) are divided in three main Ontologies as follows:

- Molecular function 49.94%;
- Biological process 49.58%;
- Cellular component 0.48%.

Each ontology was represented in a plot (Fig 4.5) with the relative percentages.

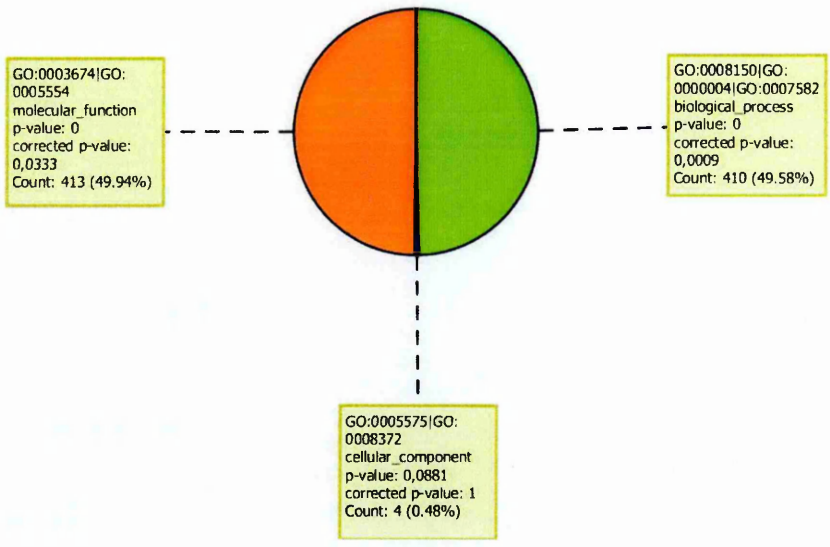

Fig 4.5 - Ontologies. Transcripts belonging to Ontology-Molecular function are represented in orange and those belonging to Ontology-Biological processes in green. Transcripts belonging to the Ontology Cellular Component are represented in blue.

Transcripts represented in the relative sub-ontologies were also checked. I found that, within the ontology Biological processes they were grouped as follows:

- Cellular process 41.26%;
- Metabolic process 30.65%;
- Localization 13.87%;
- Biological regulation 7,93%;
- Single organism process3.15%
- Establishment of localization 3.15%.
- Sub-ontologies are represented in a plot (Fig 4.6)

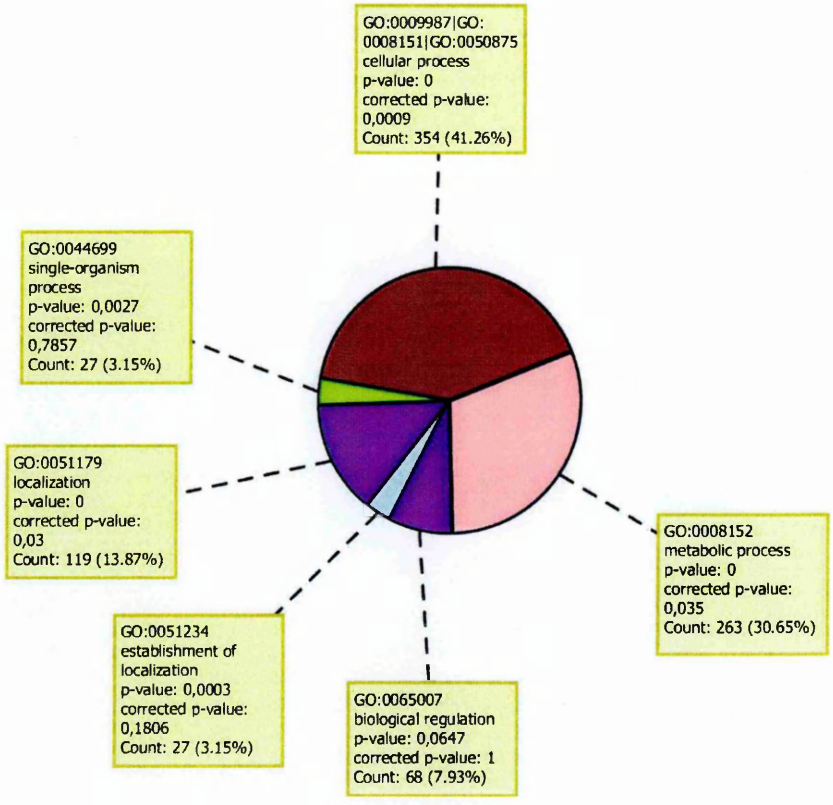

Fig. 4.6 - Biological process. Transcripts belonging to Cellular process Are represented in brown. Transcripts belonging to Metabolic process are represented in pink. Transcripts belonging to Localization and to Biological regulation are represented in purple. Single organism process are represented in green and establishment of localization in light blue.

I did this analysis for all three main Ontologies. In the case of Molecular function I found the following sub-ontologies:

- Catalytic activity 50.07%;
- Binding 36.76%;
- Transporter activity 7.17%

Figure 4.7 shows the sub-ontologies with the relative percentages.

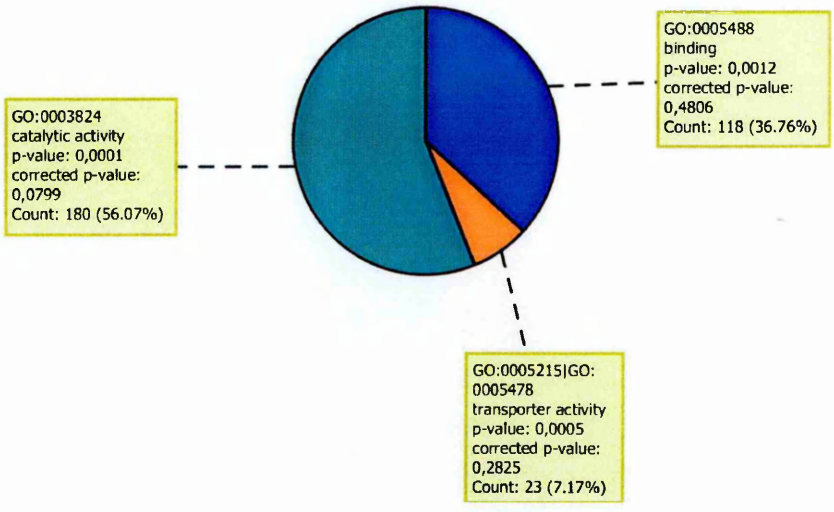

Fig. 4.7 - Molecular function. Transcripts belonging to Catalytic activity are represented in turquoise, those belonging to Binding in blue and transcripts belonging to Transporter activity in orange.

Finally the sub-ontologies of Cellular component were represented as follows (Fig. 4.8):

- Macromolecolar complex 33.33%;
- Cell 33.33%;
- Cell part 33.33%.

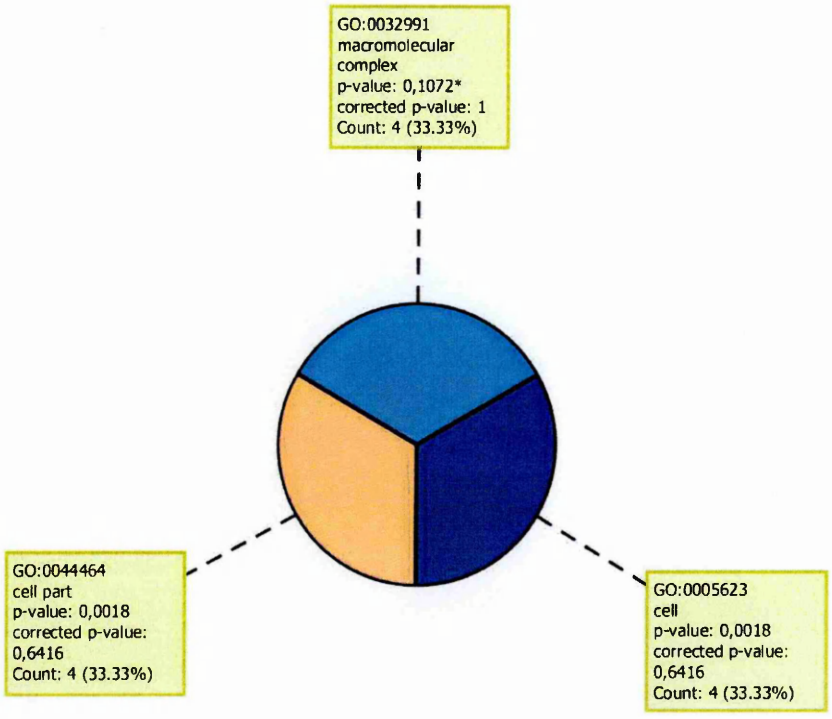

Fig. 4.8 - Cellular Component. Transcripts belonging to Macromolecular complex are represented in light blue, those belonging to Cell in dark blue and those belonging to Cell part in orange.

The next step, the boinformatic analysis, identified the cellular pathways in which the transcripts were involved. Using the same software, I found about 51 pathways (Tab IV.2).

Pathway	MatchedEntities	Pathway	MatchedEntities
XPodNet protein-protein interactions in the podocyte	19	Delta-NotchSignalingPathway	3
mRNA_processing	11	PrimaryFocalSegmentalGlomerulosclerosis	3
PluriNetWork	7	GPCRsClassARhodopsin-like	3
Purine metabolism	7	One carbon metabolism and related pathways	3
TNF-alpha NF-kB Signaling Pathway	6	GlycogenMetabolism	3
Calcium Regulation in the Cardiac Cell	4	NuclearReceptor	3
Regulation of ActinCytoskeleton	4	Alpha6-Beta4 IntegrinSignalingPathway	3
Amino Acid metabolism	4	EukaryoticTranscriptionInitiation	3
FocalAdhesion	4	Glutathionemetabolism	3
B Cell Receptor Signaling Pathway	4	Toll-like receptor signaling pathway	3
WntSignalingPathway	3	Na+/Cl- dependent neurotransmitter transporters	3
StriatedMuscleContraction	3	Nuclear receptors in lipid metabolism and toxicity	2
Retinolmetabolism	3	G13 SignalingPathway	2
Keap1-Nrf2	3	IL-5 SignalingPathway	2
Apoptosis	3	Alanine and aspartatemetabolism	2
ApoptosisModulation by HSP70	3	Tryptophanmetabolism	2
Integrin-mediated Cell Adhesion	3	Chemokinesignalingpathway	2
MAPK signalingpathway	3	Splicing factor NOVA regulated synpatic proteins	2

Tab. IV.2 - Pathway list. The "Pathway" columns describe the type of pathway according to GO. The "Matched Entities" columns represent the number of genes involved in a pathway found in the list of genes of the microarray.

For each pathway present in this list I generated a table in which the identity of the genes involved are presented, as well as information as to whether the genes are up or down regulated after DD treatment, and the extent to which they are up/down-regulated. I show the most interesting pathways in the discussion that follows.

4.4 Discussion

Given the huge amount of data resulting from microarray analysis, I decided to start from the data available in the literature. In many of the papers that I mentioned in the introduction of this chapter, the molecular analysis was done considering how DD treatment affected the expression of the genes involved in stress response mainly in copepods and sea urchins. For example, in sea urchins heat shock protein 70 was analyzed (Romano *et al.*, 2011). The authors demonstrated that sea urchin embryos treated with low DD concentration (0.25 mg mL) showed an increase in expression levels of hsp70 at the swimming blastula stage (9 hpf). However, prolonged exposure to DD (24 and 48 hpf) at this concentration led to a decrease in hsp70 expression levels compared to controls and a concomitant increase in the expression of the initiator caspase-8 after 48 hpf. The authors explained this result as due to a protective mechanism, activated by NO, and exerted through the action of heat shock protein 70. This mechanism did not work when treatment with DD was prolonged (48hr). At this point sea urchins activated an apoptosis program, as demonstrated by the activation of the initiator caspase-8. In another study (Marrone *et al.*, 2012), in addition to hsp70, the heat shock proteins 60 and 56 were analyzed. The authors demonstrated that also the expression levels of these two hsp increased 9 hpf after treatment with low DD concentrations (0.20 to 0.35 mg mL). A similar result was reported on copepods by Lauritano *et al* (2012a). The authors showed that after 48 hr. of feeding on the aldehyde-producing diatom *Skeletonema marinoi*, HSP40 and HSP70 increased in the copepod *Calanus helgolandicus* suggesting a protective chaperoning activity.

Looking at the pathways listed in Table IV.2, I searched for hsp70. I found that there was a pathway named "Apoptosis Modulation by HSP70" in which three genes associated to stress response were present (Tab IV.3).

Pathway	Genes	Regulation	Fold Change A vs C	Fold Change B vs C
Apoptosis Modulation by HSP70	Hsp70,	up	113,9	169,0
	Casp2	up	1,5	1,7
	AIF	up	1,3	1,6

Tab. IV.3 - Apoptosis Modulation by HSP70 pathway. The "genes" column indicates the name of genes involved in the pathway that was disregulated in *ciona* embryos after DD treatments. The "regulation" column indicates the type of regulation of the genes. The "Fold Change"columns indicate the FC values after treatment with 0.40 µg mL^{-1} (A vs C) and 0.45 µg mL^{-1} (B vs C), respectively.

The Fold Change values for Hsp70 was very high in both conditions (A and B). This suggests that the response to DD treatment in *Ciona* embryos (at the late tailbud stage-9hpf) was mediated principally by hsp70. These results are very similar to those obtained in sea urchins. Moreover, the presence of the Casp 2 (Caspase 2) and AIF (Apoptosis Inducing Factor) suggests that the apoptosis machinery is initiated, even if the lower FC values suggest that this process is not yet functionally active. Moreover, Lauritano *et al.* (2012a) considered other genes involved in oxidative stress response, such as glutathione synthase (GSH-S) and glutathione S transferase (GST). Also in this case the expression levels were significantly up-regulated. So, I searched for this gene and found a Glutathione metabolism pathway (Tab. IV.4).

Pathway	Genes	Regulation	Fold Change A vs C	Fold Change B vs C
Glutathione metabolism	Gclm	up	4,6	5,1
	Gstt1	up	5,2	8,4

Tab. IV.4 - Glutathione metabolism pathway. The "genes" column indicates the names of genes involved the pathway that was disregulated in *ciona* embryos after DD treatments. The "regulation" column indicates the type of regulation of the genes. The "Fold Change" columns indicate the FC values after treatment with 0.40 µg mL^{-1} (A vs C) and 0.45 µg mL^{-1} (B vs C), respectively.

The two genes γ-glutamyl-cysteine ligase modifier subunit (ci-gclm) and glutathione S transferase (Gstt1), involved in this pathway, were up-regulated. This suggests that in *Ciona* embryos (at the late tailbud stage-9hpf) a stress response is under way, at high DD concentrations (0.40-0.45 µg mL^{-1}). This response also involves a glutathione (GSH) that is considered to be an important cellular component involved in protecting cells, both as a metalchelating agent and oxygen radical scavenger.

Recently, GSH was demonstrated to mediate a stress response induced by metals in *C. intestinalis* (Franchi *et al.*, 2012). Interestingly, I noticed another GSH related/modulatedpathway, the Keap1-Nrf2 (Nrf2/antioxidant response element (ARE) signaling pathway; Tab IV.5). Activation of Nrf2 protects against neurotoxicity induced by mild oxidative insults (Pastore *et al.*, 2012).

Pathway	Genes	Regulation	Fold Change A vs C	Fold Change B vs C
Keap1-Nrf2 pathway	Keap1	Up	6,8	6,9
	Maff	Up	2,2	2,4
	Gclm	Up	4,6	5,1

Tab. IV.5 - Keap1-Nrf2 pathway. The "genes" column indicates the names of genes involved the pathway that was disregulated in *ciona* embryos after DD treatments. The "regulation" column indicates the type of regulation of the genes. The "Fold Change" columns indicate the FC values after treatment with 0.40 μg mL^{-1} (A vs C) and 0.45 μg mL^{-1} (B vs C), respectively.

All these results, taken together, suggest that *Ciona* embryos responded to the stress induced by DD in a stronger manner than sea urchins since at high DD concentrations I found that genes involved in different stress response were strongly up-regulated. Moreover, this response was mediated principally by heat shock protein 70 and by Glutathione.

Finally, I was not only interested in the stress response to these aldehydes, but also in the developmental processes that could be affected by DD treatment. These other aspects are discussed in the next chapter.

Chapter 5: Quantitative Real-time PCR analysis

5.1 Introduction

In the previous chapter I presented microarray results of gene expression levels after DD treatment on newly fertilized eggs. In this chapter I describe the results of Quantitative Real-time PCR (qPCR) analysis performed after DD treatment on newly fertilized eggs to validate microarray data, and on 32-cell stage embryos to compare gene expression levels after both treatments. In addition to stress response genes, I also considered genes involved in developmental processes and cell adhesion. In particular, I focused my attention on the following set of genes (Tab.V.1).

To select these genes, different criteria were utilized. Some of them were chosen according to their high FC value (such as Semaphorine and Pselectine); some of them were chosen according to their role in stress response (such as Gclm, Gst, keap1), or in the development (such as Hox1 and Hox12), and ,in particular, in the tail development (such as Cdx), given the aberrant phenotype obtained, that results in aberrations mainly on the tail of the hatched larvae. Some other were chosen considering multiple criteria; for example, Semaphorine and Pselectin were chosen according to their high FC values and given their role in the notochord formation. In the following paragraphs these genes will be described in more details.

Genes	Function	Category
glutamyl-cysteine ligase modifier subunit (Gclm)	Enzyme involved in Glutathione biosynthesis	Stress response
glutathione S-transferase (Gst)	Enzyme involved in the transfer of glutathione to compound to be detoxified	Stress response
inhibitor kelch-like ECH-associated protein 1 (Keap1)	Substrate adapter protein for the E3 ubiquitin ligase complex	Stress response
Homeobox1(Hox1)	Transcription factor	Development
Homeobox12(Hox12)	Transcription factor	Development
Caudal-type (Cdx)	Transcription factor	Development
Selectin P-granule membrane protein antigen CD62 (Psel)	Cell adhesion molecule (CAM)	Cell adhesion
Sema domain, immunoglobulin domain (Ig), short basic domain, secreted (Semaphorin) (Sem)	Secreted and membrane proteins that act as axonal growth cone guidance molecule	Cell adhesion

Tab. V.1 – List of the genes analyzed by qPCR. The left column indicates the names of genes analyzed for qPCR analysis. The central column indicates the function of the genes. The right column indicates the category.

5.1.1 Stress response: Gclm-Gst-Keap1

The common property of these genes is that they all code for proteins involved in protection against oxidative stress.

Gclm

Gclm gene codes for the modifier subunit of the γ-glutamyl-cysteine ligase (GCL). GCL is a heterodimeric enzyme composed of a catalytic subunit (GCLC; 73 kDa) and a modifier subunit (GCLM; 31 kDa). It catalyzes the first of the two reactions that lead to glutathione (GSH) biosynthesis. In fact, GSH synthesis from its constituent amino acids involves two sequential adenosine triphosphate (ATP)-dependent steps: first, gamma-glutamylcysteine is synthesized from L-glutamate and cysteine via the

enzyme gamma-glutamylcysteine synthetase (GCL); second, glycine is added to the C-terminal of gamma-glutamylcysteine via the enzyme glutathione synthetase (GSS).

Glutathione (GSH; γ-glutamylcysteinyl glycine) is a multifunctional metabolite endogenously synthesized with important biochemical properties. GSH serves several vital functions including 1) detoxifying electrophiles; 2) scavenging free radicals; 3) maintaining the essential thiol status of proteins; 4) providing a reservoir for cysteine; and 5) modulating critical cellular processes such as DNA synthesis, microtubular related processes, and immune function. GSH provides the most abundant redox buffer in eukaryotic cells and contributes to a key pathway of phase II detoxification (Lu *et al.*, 2009).

Genomic analyses have revealed a conserved glutathione homeostasis pathway in the invertebrate chordate *Ciona intestinalis* (Nava *et al.*, 2009).

Gst

Gst gene codes for a GSH-S transferase that catalyzes reactions of S-glutathionylation. This reaction occurs through the reversible addition of a proximal donor of glutathione to thiolate anions of cysteines in target proteins, where the modification alters molecular mass, charge, and structure/function and/or prevents degradation from sulfhydryl overoxidation or proteolysis (Lu, 2009). A major function of GSH is detoxification of xenobiotics and/or their metabolites. These compounds are electrophiles or electron-loving substances and form conjugates with GSH.

S-Glutathionylation is a mechanism of signal transduction by which cells respond effectively and reversibly to redox inputs. The glutathionylation regulates most cellular pathways. It is involved in oxidative cellular response to insult by

modulating the transcription factor Nrf2 and inducing the expression of antioxidant genes (ARE); it contributes to cell survival through nuclear translocation of NFkB and activation of survival genes, and to cell death by modulating the activity of caspase 3. It is involved in mitotic spindle formation during cell division by binding cytoskeletal proteins thus contributing to cell proliferation and differentiation (Pastore *et al.*, 2012).

Keap1

This gene codes a protein containing KELCH-1 like domains, as well as a BTB/POZ domain. Kelch-like ECH-associated protein 1 interacts with NF-E2-related factor 2 (Nrf2). The transcription factor Nrf2 (NF-E2-related factor 2) is a potent transcriptional activator and plays a central role in inducible expression of many cytoprotective genes in response to oxidative and electrophilic stresses (Nguyen *et al.*, 2009). The Keap1-Nrf2 regulatory pathway plays a central role in the protection of cells against oxidative and xenobiotic damage. Under unstressed conditions, Nrf2 is constantly ubiquitinated by the Cul3-Keap1 ubiquitin E3 ligase complex and rapidly degraded in proteasomes. Upon exposure to electrophilic and oxidative stresses, modifications of critical thiol groups on Keap1 result in dissociation of the Keap1-Nrf2 complex with translocation of Nrf2 into the nucleus, where it binds to the ARE leading to the activation of phase 2 detoxifying enzymes (Kensler *et al.*, 2007).

Keap1-Nrf2 genes are also conserved in the invertebrate chordate *Ciona intestinalis* (Nava *et al.*, 2009).

5.1.2 Developmental processes: Hox1-Hox12-Cdx

Hox genes have been noted to play a central role in the anterior-posterior patterning throughout animal phylogeny. They are characterized by the clustering

organization on a chromosome and the colinear expression during development (Garcia-Fernandez *et al.*, 2005). These observations have led to the hypothesis that the physical organization of the Hox genes on the chromosome is closely related to their role in animal development. In the ascidian *Ciona intestinalis*, previous studies have identified 9 Hox genes of distinct subgroups, suggesting the presence of a single Hox gene cluster (Dehal *et al.*, 2002; Spagnuolo *et al.*, 2003).

Hox1

Hox1 is a representative of anterior Hox class genes (Spagnuolo *et al.*, 2003). The Hox1 gene expression in the urochordate ascidian *Ciona intestinalis* was first detected at the early tailbud stage in development in the epidermis and the central nervous system (CNS) around the junction of the trunk (head of the ascidian tadpole) and the tail without clear anterior and posterior expression boundaries is expressed in the nerve cord and epidermis (Kanda *et al.*, 2013).

Hox12

Hox12 is a representative of posterior Hox class genes (Spagnuolo *et al.*, 2003). In normal larval development of the ascidian *Ciona intestinalis*, Ci-Hox12 is expressed from neurula stage onwards in posterior ectodermal cells, and at the tailbud stage in the end of the posterior nerve cord and epidermis (Ikuta *et al.*, 2004). It has been demonstrated that Ci-Hox12 plays an important role in maintaining the expression of Ci-Fgf8/17/18 at the tail tip, which in turn controls the length of the tail, but not the cell morphology, after the early tailbud stage (Ikuta, 2010). Moreover, Ci-Hox12, even after early tailbud stage, plays a role in the formation of columnar cells at the tail tip and in the formation of tapered tail end morphology through the maintenance of Ci-Wnt5 expression (Ikuta *et al.*, 2010).

Cdx

Cdx, is one of the three members of the ParaHox cluster (Ferrier *et al.*, 2002), which is an evolutionary sister group of the Hox cluster, based on their sequence similarity to the Hox cluster genes (Wada *et al.*, 2003). ParaHox genes are found mainly in endodermal tissues (Garcia-Fernandez *et al.*, 2005). The posterior ParaHox gene Cdx is expressed in caudal tissues (tail epidermis endodermal strand and nerve cord); its dominant site of expression is in the posterior endoderm. Caudal gene was demonstrated to be involved in ascidian tail formation (Katsuyama *et al.*, 1999).

5.1.3 Cell adhesion: Psel-Sem

Psel

This gene codes for a protein, P-selectin, that functions as a cell adhesion molecule (CAM) on the surfaces of activated endothelial cells. In the tunicate *Ciona intestinalis*, it is expressed, at the larval stage: in apical trunk epidermal neurons; in the notochord; in palps; in rostral trunk epidermal neurons (Aniseed source: http://aniseed-ibdm.univ-mrs.fr/~ciona/ANISEED/index.php).

Sem

Semaphorins are a class of secreted and membrane proteins that act as axonal growth cone guidance molecules. They primarily act as short-range inhibitory signals and signal through multimeric receptor complexes. In the tunicate *Ciona intestinalis*, it is expressed, at the larval stage in the central nervous system and in the notochord (Aniseed source: http://aniseed-ibdm.univ-mrs.fr/~ciona/ANISEED/index.php).

I chose these genes because they were listed among the Brachyury-downstream genes (Hotta *et al.*, 2008; Kugler *et a.*, 2008). Brachyury codes a prototypic member of

the T-box family of transcription activation factors, which are defined by a conserved, sequence-specific DNA-binding domain. It plays an essential role in notochord development in the ascidian *Ciona intestinalis*.

5.2 Materials and Methods

5.2.1 Embryo collection

Embryos at late-tailbud stage (about 9 hour post fertilization-hpf) were collected after treatment on newly fertilized eggs and on 32-cell stage embryos with three different DD concentrations 0.35-0.40-0.45 μg mL^{-1}(as described in Chapter 3) and placed in 500 μL lysis buffer of the RNAqueous-micro kit (Ambion), and frozen at -80°C until RNA extraction. Embryos were collected from three different experiments (three biological replicates). A treatment panel like this was chosen for two reasons:

1. To validate the microarray results after DD (0.40-0.45 μg mL^{-1}) treatment on newly fertilized eggs;
2. To compare results after both treatments mainly at DD concentrations of 0.35 μg mL^{-1} which is the point where the two treatments result in different behavior: normal larvae on 32-cell stage versus abnormal larvae in fertilized eggs (see results Chapter 3).

5.2.2 RNA extraction and RNA quality detection

Total RNA extraction was performed using the RNAqueous-micro kit (Ambion,) from previously frozen samples in lysis buffer. RNA extraction was

performed following manufacturer's recommendations and eluted in 2x15 µL of pre-warmed (70°C) elution buffer. Total RNA (1µL) was analyzed with the BioAnalyzer (Agilent Technologies) using the Eukaryote total RNA Micro Series II kit and the mRNA Smear Nano program following manufacturer's instructions (Agilent Technologies) (as described in Chapter 4).

5.2.3 cDNA synthesis

Single strand cDNA synthesis from total RNA was obtained by iScript™cDNA Synthsis Kit (Biorad). This kit included two tubes: first tube containing the iScript reaction mix with all components (Random hexamer and/or oligo(dT)18 primers, MgCl2 (6 mM final conc.), BSA, DTT, dNTP) necessary for each reverse transcription PCR reaction; second tube containing the iScript Reverse Transcriptase. This is a RNAse H+ modified MMLV-derived reverse transcriptase. The reaction was carried out following the manufacturer instructions. Briefly, 1 µg of total RNA was resuspended in RNase-free H_2O in a final volume of 10 µL; this volume was added to 4 µL of iScript reaction mix. Finally, 1 µL of iScript Reverse Transcriptase was added to obtain a final volume of 20 µL. The reaction mix was incubated at different temperatures for different lengths of time as follow: 5' at 25 °C, 30' at 42 °C, 5' at 85 °C.

5.2.4 Quantitative Real-time PCR (qPCR)

The reverse transcription polymerase chain reaction (RT-qPCR) is a sensitive method for the detection mRNA levels. qPCR uses fluorescent reporter dyes to combine the amplification and detection steps of the PCR reaction in a single tube format.

The assay relies on measuring the increase in fluorescent signal, which is proportional to the amount of DNA produced during each PCR cycle. Fluorescence values are recorded during every cycle and represent the amount of product amplified to that point in the amplification reaction. The more template present at the beginning of the reaction, the fewer number of cycles it takes to reach a point in which the fluorescent signal is first recorded as statistically significant above back ground levels. This point is defined as threshold cycle (Ct) and will always occur during the exponential phase of amplification. The Ct is used to calculate the initial DNA copy number, because the Ct value is inversely related to the starting amount of target. The more target there is in the starting material, the lower the Ct. This correlation between fluorescence and amount of amplified product permits accurate quantification of target molecules. Therefore, PCRs from different samples can be compared to determine which contains higher amounts of a specific sequence. This is done by setting a threshold in the linear phase of amplification and assessing how many cycles (Ct) are necessary to reach the same level of product amplification in different samples. Because of the chemistry used, when the difference in the amount of a specific sequence between two samples (a "control" and an "experimental" one) is assessed, this is given by $2^{\Delta C}t$, where 2 is the multiplier for amplification per cycle, and ΔCt is the difference in the Ct between the two samples. The dye used was Fast Sybr Green Master Mix (Applied Biosystems), which binds to double stranded DNA (dsDNA).

Moreover, a melting curve analysis of each product is needed to ensure that the fluorescent signal observed is from the desired PCR product distinguishing it from primer dimers and other small amplification artifacts, as SYBR green dye cannot distinguish between the amplicon and contamination products from mispairing or primer-dimer artifacts.

RT-PCR-specific errors in the quantification of mRNA transcripts are easily compounded by any variation in the amount of starting material between samples. This is especially relevant when the samples have been obtained from different individuals. The accepted method for minimizing these errors is to amplify, simultaneously with the target, a cellular RNA that serves as an internal reference against which other RNA values can be normalized. The ideal internal standard should be expressed at a constant level among different tissues of an organism, at all stages of development, and should be unaffected by the experimental treatment. A pair of primers for Rps27 ribosomal gene, which is therefore ubiquitary in *Ciona* embryos, has been used as a standard reference.

For each gene qPCR primers have been designed to generate products of 100-200 bp, by using online based "Primer 3, v.0.4.0" software (http://fokker.wi.mit.edu/primer3/input.html; Table V.2). Blast searches against the whole *Ciona* genome have been performed to verify primers specificity. The number of cycles needed for the standards to reach a specified Ct is used to normalize the Ct for the selected genes. To capture intra-assay variability all RT-qPCR reactions have been carried out in triplicate and the average Ct value was taken into account for further calculations.

The efficiency of each pair of primers was calculated according to standard method curves using the equation $E=10^{-1/slope}$. Five serial dilutions have been set up to determine the Ct value and the efficiency of reaction of all pairs of primers. Standard curves were generated for each oligonucleotides pair using the Ct value versus the logarithm of each dilution factor. Diluted cDNA was used as template in a reaction

containing a final concentration of 0.70 pmol μL^{-1} for each primer and 1X Fast SYBR Green master mix (total volume of 10 µL).

PCR amplifications have been performed in triplicate in a ViiA7 ABI Applied Biosystems thermal cycler, using the following thermal profile: 95°C for 20", one cycle for cDNA denaturation; 95°C for 1" and 60°C for 20", 40 cycles for amplification; 95°C for 15", 60°C for 1' and 95°C for 15", one cycle for melting curve analysis, to verify the presence of a single product. Each assay included a no-template control for each primer pair.

Real time PCR has been carried out in order to analyze expression changes between embryos (after treatment on newly fertilized eggs with 0.35-0.40-0.45 $\mu g.mL^{-1}$ DD) versus control embryos (not treated). Parallel qPCR were carried out with the same conditions to analyze expression changes between embryos (after treatment on 32-cell stage with 0.35-0.40-0.45 $\mu g\ mL^{-1}$DD) versus control embryos (not treated).

The relative expression ratio (R) of target gene is calculated based on E (Efficiency) and the Ct deviation of unknown sample versus a control, and expressed in comparison to a reference gene, using Pfaffl Method based on the equation (Pfaffl *et al.*, 2001):

$$\text{Ratio} = \frac{E\,(\text{Target})^{\Delta Ct\ \text{target(Control-Treated)}}}{E\,(\text{Reference})^{\Delta Ct\ \text{reference(Control-Treated)}}}$$

The above equation shows a mathematical model of relative expression ratio in real-time PCR. The ratio of a target gene is expressed in a sample versus a control in comparison to a reference gene. E_{target} is the real-time PCR efficiency of target gene

transcript; E_{ref} is the real-Time PCR efficiency of a reference gene transcript; ΔCt_{target} is the Ct deviation of control-sample of the target gene transcript; ΔCt_{ref} is the Ct deviation of control-sample of reference gene transcript. Data for each gene were normalized against Rps27. Changes in gene expression were considered significant only at greater than a 1.5 fold level over controls.

Oligo name	Oligo sequenze
Gclm F	5′-ATCGTCTCCCTCCCCATATC-3′
GclmR	5′-ATCCTTGCCCAATCATTCAA-3′
GstF	5′CAGCGAGAACAGGCTTTACC-3′
GstR	5′-AAAAGGTTTCAGCCAGACGA-3′
Keap1F	5′-GGACAATCTTCCCAGCCATA-3′
Keap1R	5′-TTCTTCTTCCGTGGCATTTC-3′
Hox1F	5′-CATTGCGCCTTAATGAAACC-3′
Hox1R	5′-GATGATGACGATGCGAGGTA-3′
Hox12F	5′-TGGATCATTACGGCTCACAG-3′
Hox12R	5′-TGGATGATGGTGGTGTGGTA-3′
CdxF	5′-AAGGCCGTATGAGTGGATAAG-3′
CdxR	5′-TGTCCTTAGTTCGCGTTTTG-3′
PselF	5′-ATGTGGAGATGGAAGCGAAC-3′
PselR	5′-CGAGGACCAAGAAAAGATCG-3′
SemF	5′-AAACGAAACGCTGCTACGAT-3′
SemR	5′-GCGAGCAAGAAAAAGGACAC-3′

Tab. V.2. – List of the oligonucleotides used for qPCR. The oligo names are indicated in the left column; F letter indicates the Forward oligo, R reverse oligo. The sequence (5′ →3′) of the oligo primers are indicated in the right column.

5.3 Results

5.3.1 qPCR results

qPCR analysis demonstrated that embryos (at late tailbud stage-9 hpf) after DD treatment on newly fertilized eggs showed an increased expression level of the genes

involved in stress response (Gclm-Gst-Keap1-Fig. 5.1). In particular: Gclm was already significantly (≥1.5) up-regulated at the lowest DD concentration tested (0.35 μg mL^{-1}); up-regulation increased as DD concentration increased. The same occurred also for Keap1; while Gst was significantly (≥1.5) up-regulated at DD concentrations ≥ 0.35 μg mL^{-1}.

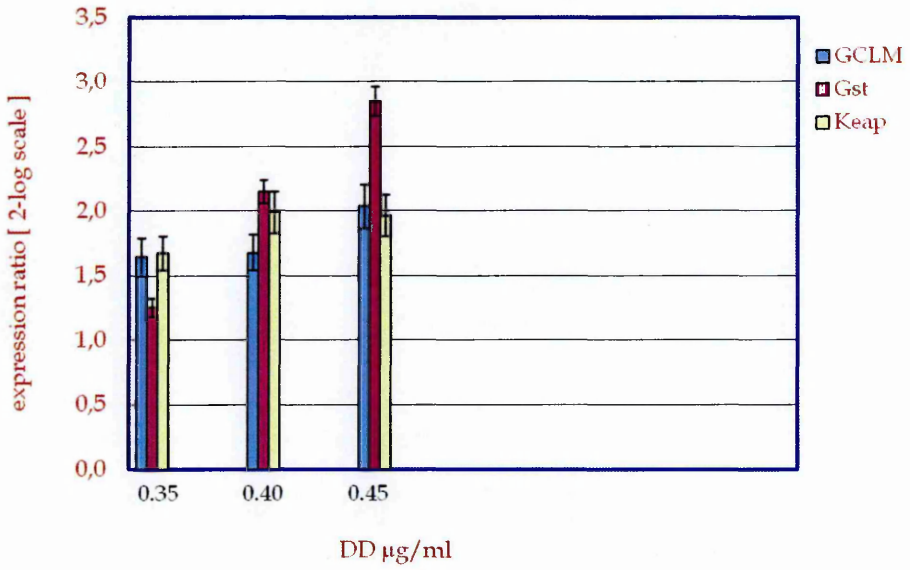

Fig. 5.1 - Regulation of stress genes. This plot represents the regulation of stress genes after DD treatment on fertilized eggs. The expression ratios (resulted from the Pfaffl equation) ± the standard deviation are indicated on the y-axis. DD concentrations are reported on x-axis and are reported as μg mL^{-1}. The legend on the right indicates the colours associated to the genes.

The expression levels of the developmental genes (Hox1-Hox12-Cdx), instead, decreased after DD treatment on newly fertilized eggs (Fig. 5.2). All the three genes were significantly (≤-1.5) down-regulated already at 0. 35 μg mL^{-1}DD. Moreover they were further down-regulated at higher DD concentrations.

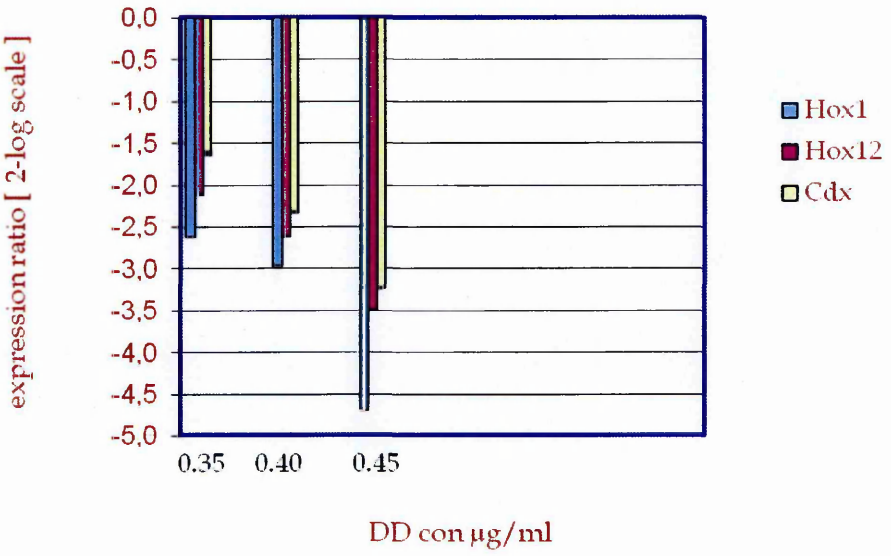

Fig. 5.2 - Regulation of developmental genes. This plot represents the regulation of developmental genes after DD treatment on fertilized eggs. The expression ratios (resulted from the Pfaffl equation) ± the standard deviation are indicated on the y-axis. DD concentrations are reported on x-axis and are reported as µg mL^{-1}. The legend on the right indicates the colours associated to the genes.

Finally, genes involved in cell adhesion decreased their expression levels after DD treatment (Fig. 5.3). In particular, Psel were significantly (≤-1.5) down-regulated already at the lowest DD concentration (0.35 µg mL^{-1}); while Sem was significantly down-regulated at 0.40 µg mL^{-1} DD. Both genes were further down-regulated as DD concentration increased.

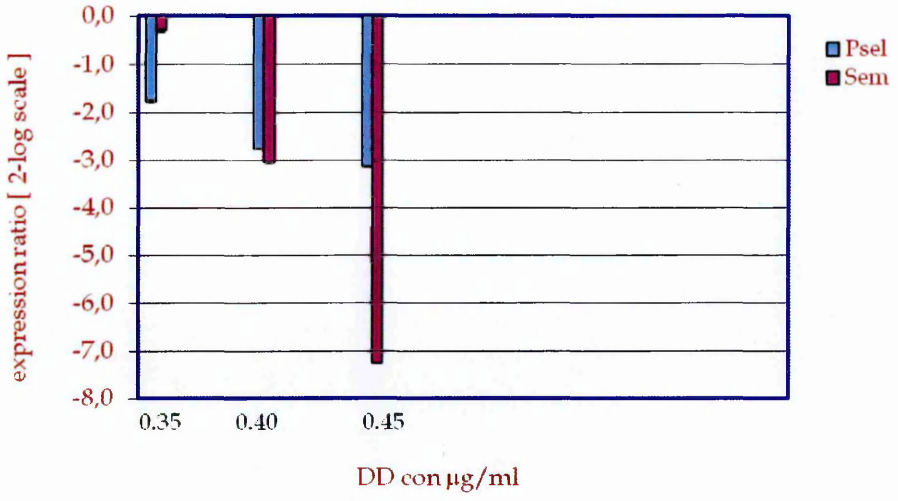

Fig. 5.3 - Regulation of cell adhesion genes. This plot represents the regulation of cell adhesion genes after DD treatment on fertilized eggs. The expression ratios (resulted from the Pfaffl equation) ± the standard deviation are indicated on the y-axis. DD concentrations are reported on x-axis and are reported as µg mL^{-1}. The legend on the right indicates the colours associated to the genes.

The results of qPCR performed on embryos after DD treatment on 32-cell stage show that genes involved in stress response were significantly up-regulated after treatment with the three DD concentrations tested, but with some differences (Fig. 5.4). In fact, while Gclm and Keap1 showed a significant up-regulation already at the lowest DD concentration, Gst was significantly up-regulated at DD concentrations higher than 0.40 µg mL^{-1}.

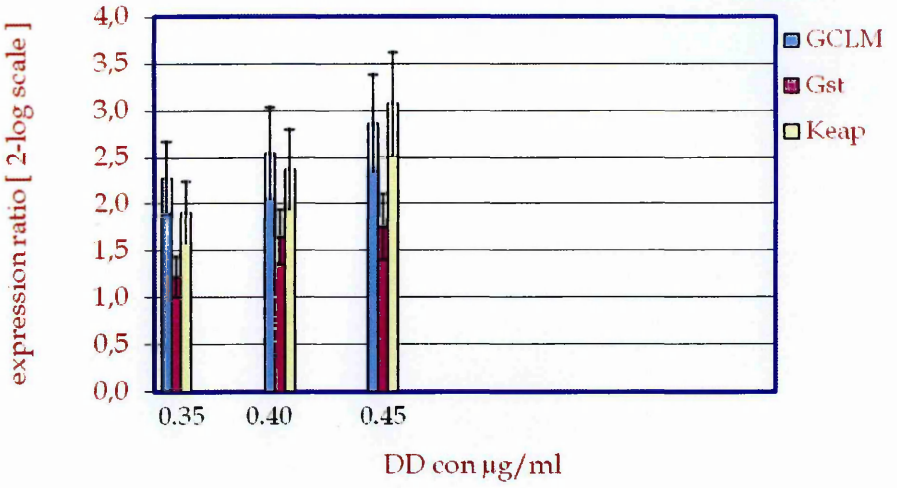

Fig. 5.4 - Regulation of stress genes. This plot represents the regulation of the stress genes genes after DD treatment on 32-cell stage embryos. The expression ratios (resulted from the Pfaffl equation) ± the standard deviation are indicated on the y-axis. DD concentrations are reported on x-axis and are reported as µg mL^{-1}. The legend on the right indicates the colours associated to the genes.

In the same condition (treatment on 32-cell stage embryos), genes involved in developmental processes were down-regulated (Fig. 5.5). All three genes (Hox1-Hox12-Cdx) showed a significant down-regulation at DD concentrations > 0.40 µg mL^{-1}.

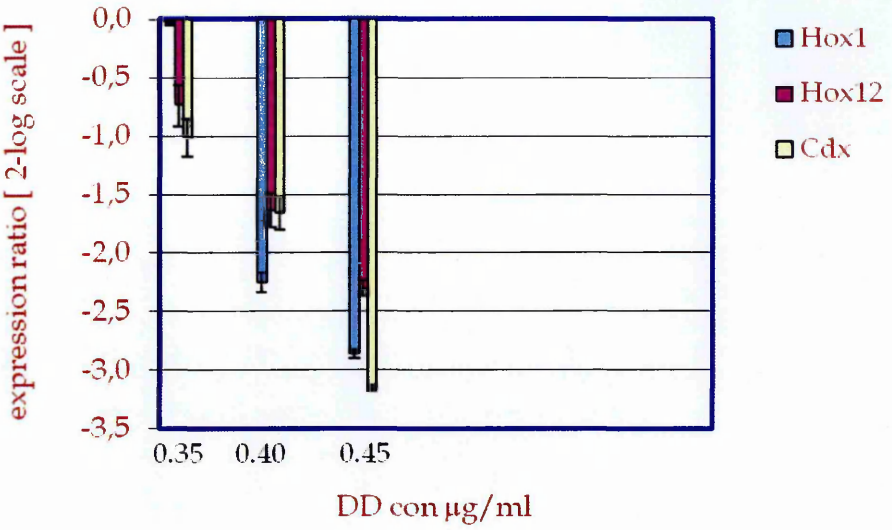

Fig. 5.5 - Regulation of developmental genes. This plot represents the regulation of developmental genes after DD treatment on 32-cell stage embryos. The expression ratios (resulted from the Pfaffl equation) ± the standard deviation are indicated on the y-axis. DD concentrations are reported on x-axis and are reported as µg mL^{-1}. The legend on the right indicates the colours associated to the genes.

Finally, both genes involved in cell adhesion shown reduced expression levels after DD treatment on 32-cell stage embryos (Fig. 5.6). In this case, Psel was significantly down-regulated already at 0.35 µg mL^{-1} DD and was further down-regulated at the higher DD concentrations; Sem, instead, was down-regulated in a more significant manner at 0.40 µg mL^{-1} DD.

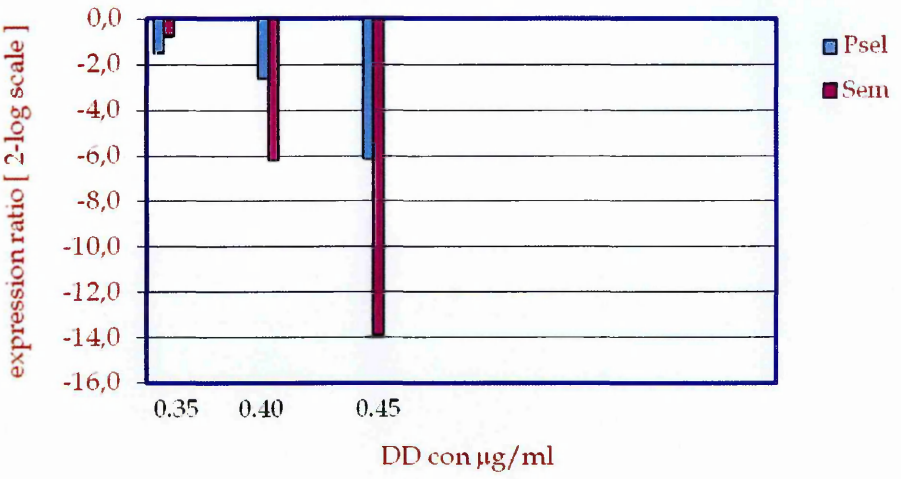

Fig. 5.6 - Regulation of cell adhesion genes. This plot represents the regulation of cell adhesion genes after DD treatment on 32-cell stage embryos. The expression ratios resulted from the Pfaffl equation) ± the standard deviation are indicated on the y-axis. DD concentrations are reported on x-axis and are reported as µg mL^{-1}. The legend on the right indicates the colours associated to the genes.

Summary of microarray results

Category	Genes	Regulation	Fold Change A vs C	Fold Change B vs C
Stress Genes	Gclm	up	4,6	5,1
	Gst	up	5,2	8,4
	Keap1	up	6,8	6,9

Tab. V.3 - Stress genes. The "genes" column indicates the names of genes involved in the pathway that was disregulated in *ciona* embryos after DD treatments on newly fertilized eggs. The "regulation" column indicates the type of regulation of the genes. The "Fold Change"columns indicate the FC values after treatment with 0.40 µg mL^{-1} (A vs C) and 0.45 µg mL^{-1} (B vs C), respectively.

Category	Genes	Regulation	Fold Change A vs C	Fold Change B vs C
Developmental genes	Hox1	down	-2.7	-5.3
	Hox12	down	-1.7	-2.6
	Cdx	down	-1.6	-2.4

Tab. V.4 - Developmental genes. The "genes" column indicates the names of genes involved in the pathway that was disregulated in *ciona* embryos after DD treatments on newly fertilized eggs. The "regulation" column indicates the type of regulation of the genes. The "Fold Change"columns indicate the FC values after treatment with 0.40 µg mL^{-1} (A vs C) and 0.45 µg mL^{-1} (B vs C), respectively.

Category	Genes	Regulation	Fold Change A vs C	Fold Change B vs C
Cell adhesion molecules	Psel	down	-7	-15
	Sem	down	-2.9	-4.6

Tab. V.5 – Cell adhesion genes. The "genes" column indicates the names of genes involved in the pathway that was disregulated in *ciona* embryos after DD treatments on newly fertilized eggs. The "regulation" column indicates the type of regulation of the genes. The "Fold Change"columns indicate the FC values after treatment with 0.40 µg mL^{-1} (A vs C) and 0.45 µg mL^{-1} (B vs C), respectively.

5.4 Discussion

qPCR results, after treatment on newly fertilized eggs, confirmed the microarray results. In fact, genes involved in stress response (Gclm-Gst_Keap1) were up-regulated both in the microarray (Tab. V.3) and with qPCR (Fig. 5.1), after treatment with both DD concentrations (0.40-0.45 µg mL^{-1}). Transcription factors involved in developmental processes (Hox1-Hox12-Cdx) were down-regulated in the microarray (Tab.V.4) and this result was confirmed by qPCR (Fig. 5.2). The same was true for the genes involved in cell adhesion (Psel-Sem), which were strongly down-

regulated in the microarray (Tab. V.5) after treatment with both DD concentrations (0.40-0.45 μg mL^{-1}), and confirmed by qPCR analysis (Fig. 5.3).

qPCR analysis was carried out also on embryos after treatment on 32-cell stage. This was done to allow a comparison between the two treatments (on fertilized eggs and on 32-cell stage embryos). All of the qPCR results after treatment on 32-cell stage embryos were consistent with those obtained after treatment on fertilized eggs. In fact, all genes tested behaved the same way after both treatments: genes up-regulated (stress genes - Fig. 5.4) in one case were up-regulated also in the other case. This was true also for those genes that were down-regulated (developmental and cell adhesion genes - Fig. 5.5-5.6). This consideration was valid in relation to the two highest DD concentrations (0.40-0.45 μg mL^{-1}).

Moreover, to perform qPCR analysis I considered a further DD concentration, lower than the others (0.35 μg mL^{-1}). Comparing the results obtained at this DD value, it was interesting to note that there were some differences after the two treatments. In particular, these differences concerned the genes that were down-regulated (Hox1-Hox12-Cdx-Psel-Sem). In the case of developmental genes, after treatment on newly fertilized eggs, all three genes (Hox1-Hox12-Cdx) showed a significantly strong down-regulation at DD concentrations of 0.35 μg mL^{-1}. Instead, after treatment on 32-cell stage embryos, at the same DD concentration none of the three genes reached the cut off value of -1.5. Even, Hox1 seemed not to be down-regulated at all. The same was true for Psel and Sem genes as well. It was interesting to observe the phenotypes detected with the two different treatments. In fact, in Chapter 3 (Fig. 3.5) I noticed that, at 0.35 μg mL^{-1} DD, abnormal larvae showed a severe tail phenotype after treatment on fertilized eggs. While at the same DD concentration after treatment on 32-cell stage

embryos, abnormal larvae showed a mild tail phenotype. This situation could reflect the difference in expression levels of developmental genes and genes involved in cell adhesion between the two conditions. In particular, this could imply that these genes were less down-regulated when the phenotype was less severely modified (32-cell stage embryos). Instead, they showed a stronger down-regulation when the phenotype was more severely modified (fertilized eggs). This could be a strong confirmation of the consistence of the results. Moreover, since all the genes that showed this behavior are expressed mainly on the tail of the larvae, it could be a confirmation that, DD could affect the processes that lead to tail formation in *Ciona intestinalis* embryos.

These differences were not found in the case of the stress genes. In fact, all three genes had the same trend after both treatments. In particular, Gclm and Keap1 were up-regulated already at 0.35 μg mL^{-1}DD. This could imply that in both cases, embryos were able to contrast the stress stimuli, represented by DD treatment. This could be in relation to the low levels (<50%) of abnormal larvae detected after both treatments (Fig.3.3-3.4, Chapter 3).

Chapter 6: General discussion

6.1. Oxidative Stress

As described in Chapter 3 and Chapter 4, DD treatment on newly fertilized eggs and on 32-cell stage embryos induced a stress response studied at the tailbud stage (i.e. the stage when microarrays were assayed). Microarray results were then confirmed by qPCR analysis. The data showed an increased expression of genes involved in stress response, in particular hsp70, Gclm, Gst and Keap1.

Hsp70 codes for a heat shock protein involved in response to heat stress. The Fold Change values, revealed by microarray analysis for this gene, (113,9 A vs C and 169,0 B vs C - Table IV-2 - Chapter 4), indicated that the gene was strongly up-regulated. This could imply that the primary response was mediated by this protein.

The other genes that were up-regulated were Gclm, Gst and Keap1. These genes are involved in glutathione (GSH) metabolism. GSH is an important metabolite that mediates, among other processes, a response to oxidative stress. Gclm codes for the modifier subunit that, together with the catalytic (Gclc), constitutes a Glutamate-cysteinlygase (Gcl-formerly γ-glutamyl-cysteinesynthase). Gcl is the enzyme that catalyzes the first of the two reactions which leads to the biosynthesis of GSH. Glutathione S-transferases (GSTs) codes for phase II metabolic enzymes that catalyze the conjugation of the reduced form of glutathione (S-glutathionilation) to xenobiotic substrates, for the purpose of detoxification, or to endogenous proteins, for regulatory purposes. Keap1 codes for a modulating factor susceptible to glutathionilation. It belongs to a Nrf2-Keap1 signaling that regulates numerous genes through Antioxidant Response Elements (AREs) that are activated by an oxidative signal.

The activity of Gcl is a major determinant of the rate of GSH synthesis. A change in Gcl activity is responsible for alteration in cell GSH in many conditions. It has been well documented, in fact, that stress conditions induced by a variety of agents are associated to an increased expression of Gcl levels (Luv *et al.*,2009). In most cases, the two Gcl subunits are simultaneously up-regulated by many inducers of oxidative stress (Lu *et al.*, 2009). There are also examples of a differential regulation of the two subunits. For example, Lu *et al* (2009) demonstrated that hormone treatments, such as insulin or hydrocortisone transcriptionally activate only the catalytic subunit in rat hepatocytes (Lu *et al.*, 2009). The transcriptional induction of only the modifier subunit has also been demonstrated. For example, treatment with thyroid hormone is reported to preferentially induce Gclm in primary cultures of rat astrocytes (Dasgupta *et al.*, 2006). Moreover, genetic alteration of the GSH synthesis gene Gclm can exacerbate the response of the lung to DEP (diesel exhaust particulate)-induced lung inflammation in mice (Weldy *et al.*, 2011).

The correlation between GSH biosynthesis has been reported also in marine organisms. Many studies have shown the induction of genes encoding for both Gcl subunits in aquatic animals exposed to environmental pollutants, such as methylmercury and quinines, which generate ROS (Krzwansky *et al.*, 2004).

In the tunicate *Ciona intestinalis*, a conservation of a GSH homeostasis pathway was pointed out by Nava *et al.* (2009). These authors reported also an increased abundance of RNA transcripts of the two genes encoding the enzyme for GSH synthesis, Gclm and Gclc, in *Ciona* adults in response to the antioxidant tert-butylhydroquinone (Nava *et al.*, 2009).

In *Ciona* other authors have demonstrated that the exposure of adult animals to metals (Cd, Cu and Zn) induces an up-regulation of both subunits of Gcl (Franchi *et al.*, 2012). Moreover, it has been shown that Cd, in particular, induces an increase in Gs gene expression levels. Gs codes for a glutathione synthase, the enzyme responsible for the second step of GSH biosynthesis.

It is interesting to note that microarray results after DD treatment on *Ciona* embryos showed a statistically significant increase in Gclm expression levels but not in Gclc. This could depend on the different response induced by different stimuli (metal vs aldehydes), or the different life stages considered (adult vs embryos). Moreover, after DD treatment, microarray results showed an up-regulation of a Gst gene. This gene has also been shown to be up-regulated in the intertidal copepod, *Tigriopus japonicus*, in response to trace metals such as arsenic, cadmium copper, and silver and hydrogen peroxide (Lee *et al.*, 2008) and to Cu and Mn (Lee *et al.*, 2007).

All these results, taken together, indicate that *C. intestinalis* may be an important animal model for comparative ecotoxicology due to its lifestyle as a filter feeder which constantly expose it to marine pollutants. It might therefore be interesting to develop a kind of "gene-panel" in this species to study stress response in order to detect which pollutants are present in a given area. The measurement of gene expression levels after exposure to a chemical can be used both to provide information about the mechanism of action of the toxicant and to form a sort of "genetic signature" for the identification of toxic products.

A microarray approach has already been used in toxicogenomic studies. For example, microarrays have been used to understand the response to endocrine modulators in zebrafish (Hoyt *et al.*, 2003). A similar approach has been used to study

gene expression profiling in response to environmental stressors in the typical plant model organism *Arabidopsis thaliana* (Seki *et al.*, 2004).

In my opinion the microarray approach has two major limitations. The first is the high cost associated with the technology itself. These costs render repeated measurements very expensive, and thus often only limited experimental data are available. The second limitation concerns the large data set that has to be analyzed. A more feasible approach to ecotoxicogenomic studies might therefore be to select and analyze only a significant set of genes (for example, the genes involved in GSH metabolism) with a cheaper technique. Despite this consideration, the microarray approach remains a good tool in cases like mine when nothing is known about the phenomenon and its molecular targets; in this case a wide-range approach is required.

For my own personal curiosity, I studied the literature on the effects of DD on human health. Trans,trans-2,4-decadienal (DD) is the most abundant genotoxic and cytotoxic compound found in oil fumes formed from heating common commercial cooking vegetable oils (such as soybean oil, sunflower oil, peanut oil). It has been demonstrated that exposure to cooking oil fumes (COF) is strongly associated with lung adenocarcinoma in non-smokers. DD has been demonstrated to induce oxidative stress, through an increase in ROS production, and a decrease in GSH/GSSG ratio (glutathione status) and as a consequence an increased cell proliferation and expression and release of pro-inflammatory cytokines TNFα and IL-1b in human bronchial epithelial cell lines, suggesting that DD may play a role in cancer promotion (Chang *et al.*, 2006). Moreover, another interesting study demonstrated that DD from oil fumes decreased cellular GSH content and activities of GSH enzymes (glutathione S-transferase and glutathione reductase) and, as a consequence, induced oxidative DNA

damage and cell injury, resulting in cell death in human lung carcinoma pulmonary type II-like epithelium cells (A-549 cell-Dung *et al.*, 2006). An apoptotic effect of DD on human colon adenocarcinoma, Caco2, cell lines was already demonstrated by Miralto *et al.* (1999).

6.2. Developmental disorders

In the previous chapter I demonstrated that DD treatments on *Ciona* embryos impaired the normal developmental program. This was confirmed by the presence of abnormalities in hatched larvae.

I performed DD treatment on two different stages: soon after fertilization and about two hours after fertilization, when embryos were at 32-cell stage (when zygotic transcription is already initiated in *Ciona* embryos). This was done to look for any potential "phenotypic" dissimilarities in the resulting larvae that could be related to different actions exerted by DD on maternal or zygotic transcription. In fact, it is well known that the earliest developmental program in animal embryos is carried out with maternally supplied information, which subsequently triggers the zygotic program. This phase has been called maternal-to-zygotic transition (MZT) (Tadros *et al.*, 2009). It is interesting to note that I obtained abnormal larvae developed from embryos treated with DD just after fertilization as well as at the 32 cell stage. In both cases the phenotypes were comparable and aberrations were evident mainly on the tail of the larvae. However, after treatment at the 32-cell stage, the abnormal phenotype appeared at a lower DD concentration ($0.3 \mu g mL^{-1}$). This could suggest that the MZT represents a

very critical step in development in which embryos could be more susceptible to a stress stimulus such as DD treatment.

As previously mentioned, fertilized eggs resulted in abnormal larvae at DD concentration starting from 0.35 μgmL^{-1}; at lower concentrations larvae appeared pretty normal. This could suggest that the fine distribution of the maternal determinants in the egg before fertilization behaves as a barrier versus external insults, such as DD treatment, at least up to certain concentrations. It is known that the fertilizable mature oocytes of *C. intestinalis* are polarized along a primary (a-v) axis defined with respect to the cortical position of a small meiotic apparatus arrested in the first metaphase of meiosis. Generally, the animal-vegetal (a-v) axis is already present in unfertilized eggs. Ascidian eggs undergo dramatic cytoplasmic and cortical reorganizations between fertilization and the beginning of the first cleavage; this process has been called ooplasmic segregation. Reorganization occurs in two major phases. Shortly after fertilization (0–5 min in *Ciona*), the first phase is actin-dependent and concentrates cortical maternal determinants for the vegetal-most fate, endoderm, and for gastrulation at the vegetal pole of the embryo (Nishida, 2005). The second phase of reorganization (25–45 min in *Ciona*) brings maternal axial determinant components along the microtubules toward the future posterior pole and is relevant to specification of the a-p axis (Nishida, 2005). On these grounds one can hypothesize that the pre-existing egg program could protect embryos from DD treatment, at least up to a certain DD concentration (0.30 $\mu g\ mL^{-1}$). Beyond this threshold the egg program could become unable to exert its protective action versus DD, thus resulting in larvae with abnormal phenotype.

Considering the aberrant phenotype obtained, my results indicate that DD is able to affect mostly, but not exclusively, the processes which leads to tail elongation. One can envisage that the effects are exerted mainly by interfering with notochord specification, based on the literature data that demonstrate that signals from the notochord are required to organize the tail tissues, such as muscles and the endodermal strand, in order to direct tail elongation (Di Gregorio *et al.*, 2002).

Ascidian eggs are typical mosaic eggs and the cell fates of muscle, endoderm and epidermis are determined by the maternal factors that are prelocalized in the eggs. These tissues differentiate autonomously without any inductive signals from the surrounding cells (Nishida, 2005). Inductive signals are instead required for differentiation of the notochord, mesenchyme and nervous system (Imai *et al.*, 2004).

Specification of the notochord requires an inductive signal from the endoderm, which has been identified as fibroblast growth factor (FGF) (Jiang and Smith, 2007). In the primary lineage this induction occurs at the 32-cell stage, and notochord precursors acquire developmental autonomy at the 64-cell stage. The secondary lineage differentiates slightly later and becomes restricted to notochord fate at the 110-cell stage. Moreover, the FGF signal is transduced by FGF receptor, Ras, MEK and MAPK (ERK1/2) in the notochord (Nishida, 2003).

A preliminary analysis of microarray results indicated that the fibroblast growth factor was down-regulated, while its receptor was up-regulated (Appendix I). Moreover, some MAPK appeared to be up-regulated. These data indicate that FGF signaling is somehow affected by DD treatment, thus suggesting a potential correlation between the alteration of the signaling governed by FGF factor and the tail aberrations resulting from DD treatments.

Obviously, these results have to be confirmed by *in vivo* experiments in order to clarify if the DD insult is mediated by these molecules.

In the ascidian, tail elongation is driven by movements of the cell: convergence extension and intercalation. Convergence and extension processes are associated to at least three molecular mechanisms: actin-based protrusive extension; actomyosin-based cortical contractility and integrin or cadherin-based cell adhesion (Munro and Odell, 2002). Interestingly, the three pathways were perturbed as revealed by microarray analysis in *Ciona* embryos treated with DD (Appendix I). This could further support the phenotypic effects of DD on notochord formation. Also in this case, the results should be confirmed by further experiments.

Among the impaired pathways, revealed by microarray analysis after DD treatments on *Ciona* fertilized eggs, there is the very interesting pathway implicated in retinol metabolism (Appendix I). It is well established that retinoic acid (RA) signaling at the gastrula stage strongly influences anterior-posterior (a-p) patterning of the neurula and later stages (Koop *et al.*, 2010). Retinoic acid (RA) is a small lipophilic molecule derived from vitamin A. RA is the biologically active derivative of vitamin A, which is oxidized in a two-step process: the first step of RA synthesis, oxidation of retinol to retinaldehyde, is catalyzed by several alcohol dehydrogenases (ADHs) and retinol dehydrogenases (RDHs). The second step of RA synthesis, oxidation of retinaldehyde to RA, is catalyzed by three retinaldehyde dehydrogenases (RALDH1, RALDH2, and RALDH3). RA serves as a ligand for two families of nuclear receptors that bind DNA and directly regulate transcription: (1) the RA receptors (RARα, RARβ, and RARγ) that bind the abundant form of RA known as all-trans-RA and (2) the retinoid X receptors (RXRα, RXRβ, and RXRγ) that bind an isomer known a9-cis-RA

(Duester *et al.*, 2008). Many cells also contain cellular retinol-binding proteins (CRBPs) and cellular retinoic acid-binding proteins (CRABPs) that bind retinol and retinoic acid respectively, inside the cell. CRBPs belong to the fatty acid-binding protein (FABP) family. They bind both all-trans-retinol and all-trans-retinaldehyde, and may function to control levels of intracellular retinol accumulation and esterification. CRABPs solubilise and protect RA in the aqueous cytosol, presenting RA to metabolizing (CYP26) enzymes, and favoring nuclear import and delivery of RA to RARs by direct protein-protein interactions. RA has been extensively studied for its effects on cell cultures, embryonic development, adult growth, regeneration and carcinogenesis in chordates. Moreover, RA signaling primarily acts via regulation of Hox transcription (in particular Hox1 and Hox3) to establish the a-p patterning of amphioxus and vertebrate embryos (Koop *et al.*, 2010). Very recently, it has been demonstrated that *Ciona intestinalis* has a nerve cord enhancer in the second intron of Ci-Hox1, containing a putative retinoic acid response element (RARE), with retinoic acid (RA) playing a major role in activating this enhancer (Kanda *et al.*, 2013). It is interesting to note that in the pathway of retinol metabolism three genes are present: Rlbp1(Cellular retinaldehyde-binding protein 1); Aldh1a2 (Retinal dehydrogenase 2); Crabp2 (Cellular Retinoic Acid Binding Protein 2). The two binding proteins were down-regulated by DD treatment, while the dehydrogenase was up-regulated (Appendix I). Possibly the dysregulation of these genes involved in retinoic acid metabolism could be implicated in the failure of a correct body plan specification in *Ciona* embryos treated with DD. Here too, further *in vivo* experiments will be instrumental to clarify the role of this molecule in mediating DD effect.

6.3. Conclusion and future perspectives

In synthesis, my work has revealed the following major findings:

1. DD affects *Ciona* hatching success in a dose-dependent manner;
2. DD causes a delay in hatching;
3. DD impairs *Ciona* development, affecting maternal as well as zygotic transcription. The zygotic transcription seems to be affected in a more severe manner, while the maternal developmental program could protect the embryos from this insult;
4. DD induces aberrations mainly on the tail in hatched larvae. Probably this would be due to a "dysregulation" of signaling pathways which lead to a correct tail elongation. Probably, all this is due to failure of notochord specification;
5. DD induces a strong stress response in *Ciona* embryos mediated mainly by Hsp70 and GSH.

All the results obtained have to be confirmed. This could be done through experiments of transgenesis inducing a perturbation of the signaling pathways that seems to be affected by DD and comparing the resulting phenotypes. It would be interesting also to study the expression levels of the genes of interest at earlier or later developmental stages to better understand when these genes start to be dysregulated.

Moreover, further studies of the genes involved in stress response could pave the way for finding general biomarkers to detect exposure to pollutants. This could have important implications on defining the chemical defensome or stress surveillance system that organisms activate against environmental chemicals represented by

microbial products, heavy metals, phytotoxins and other natural compounds, present in the marine environmental, as already described for sea urchins by Marrone *et al.* (2012). Chemical defense genes may be especially important for early embryos, which must cope with the environment during sensitive stages of differentiation and development.

My results may have important implications for understanding the cellular mechanisms underlying the responses of benthic organisms to aldehyde exposure. Tunicates such as *Ciona intestinalis* may come into contact with diatom DD or other PUAs in the field at the end of a bloom, with the mass sinking of diatoms to the sediment. Since they are strong filter feeders, grazing mainly on phytoplankton cells including diatoms, they may accumulate PUAs through feeding or be exposed to high local concentrations of these compounds that may affect growth performance. This is of considerable ecological relevance considering the importance of diatom blooms in nutrient-rich aquatic environments.

Appendix I: microarray supplementary data

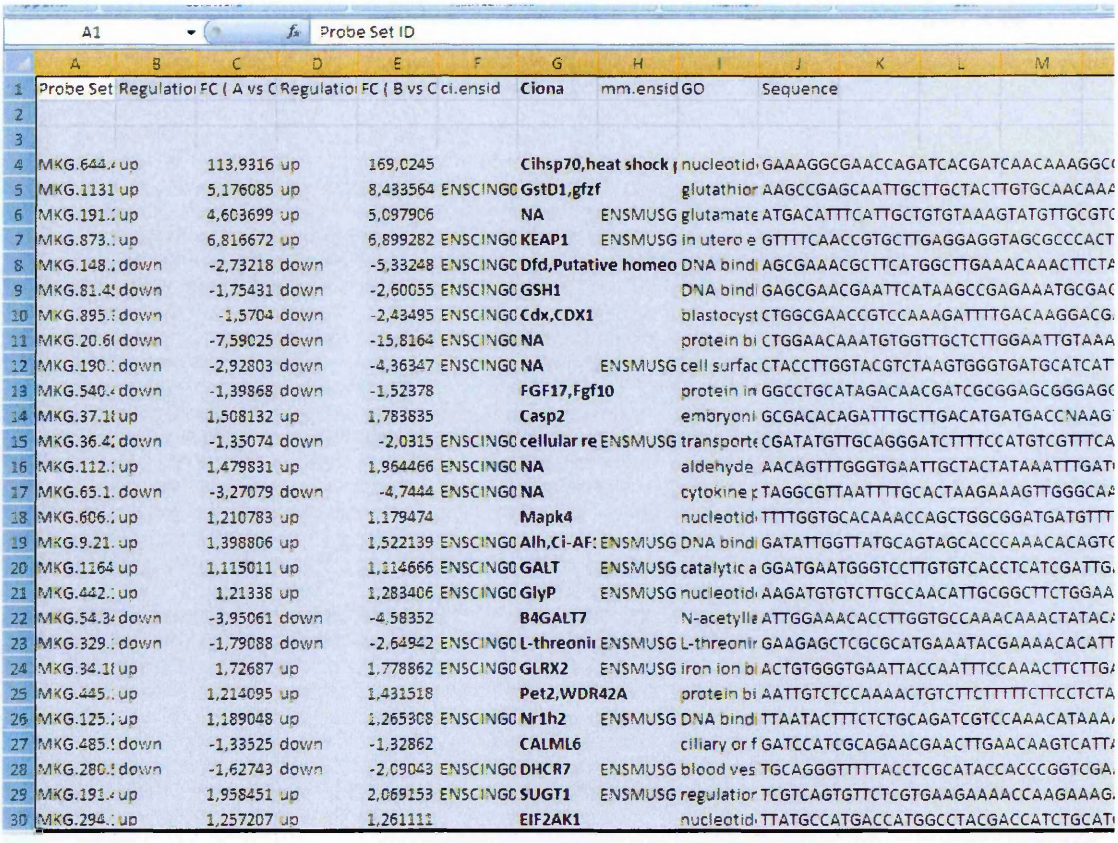

	A	B	C	D	E	F	G	H	I	J	K	L	M
1	Probe Set	Regulatio	FC (A vs C	Regulatio	FC (B vs C	ci.ensid	Ciona	mm.ensid	GO	Sequence			
2													
3													
4	MKG.644.4	up	113,9316	up	169,0245		Cihsp70,heat shock p		nucleotid	GAAAGGCGAACCAGATCACGATCAACAAAGGC			
5	MKG.1131	up	5,176085	up	8,433564	ENSCING0	GstD1,gfzf		glutathior	AAGCCGAGCAATTGCTTGCTACTTGTGCAACAAA			
6	MKG.191.1	up	4,603699	up	5,097906		NA	ENSMUSG	glutamate	ATGACATTTCATTGCTGTGTAAAGTATGTTGCGTC			
7	MKG.873.1	up	6,816672	up	6,899282	ENSCING0	KEAP1	ENSMUSG	in utero e	GTTTTCAACCGTGCTTGAGGAGGTAGCGCCCACT			
8	MKG.148.1	down	-2,73218	down	-5,33248	ENSCING0	Dfd,Putative homeo		DNA bindi	AGCGAAACGCTTCATGGCTTGAAACAAACTTCTA			
9	MKG.81.4	down	-1,75431	down	-2,60055	ENSCING0	GSH1		DNA bindi	GAGCGAACGAATTCATAAGCCGAGAAATGCGAC			
10	MKG.895.1	down	-1,5704	down	-2,43495	ENSCING0	Cdx,CDX1		blastocyst	CTGGCGAACCGTCCAAAGATTTTGACAAGGACG			
11	MKG.20.6	down	-7,59025	down	-15,8164	ENSCING0	NA		protein bi	CTGGAACAAATGTGGTTGCTCTTGGAATTGTAAA			
12	MKG.190.1	down	-2,92803	down	-4,36347	ENSCING0	NA	ENSMUSG	cell surfac	CTACCTTGGTACGTCTAAGTGGGTGATGCATCAT			
13	MKG.540.1	down	-1,39868	down	-1,52378		FGF17,Fgf10		protein in	GGCCTGCATAGACAACGATCGCGGAGCGGGAGC			
14	MKG.37.1	up	1,508132	up	1,783835		Casp2		embryoni	GCGACACAGATTTGCTTGACATGATGACCNAAG			
15	MKG.36.4	down	-1,35074	down	-2,0315	ENSCING0	cellular re	ENSMUSG	transporte	CGATATGTTGCAGGGATCTTTTCCATGTCGTTTCA			
16	MKG.112.1	up	1,479831	up	1,964466	ENSCING0	NA		aldehyde	AACAGTTTGGGTGAATTGCTACTATAAATTTGAT			
17	MKG.65.1	down	-3,27079	down	-4,7444	ENSCING0	NA		cytokine p	TAGGCGTTAATTTTGCACTAAGAAAGTTGGGCAA			
18	MKG.606.1	up	1,210783	up	1,179474		Mapk4		nucleotid	TTTTGGTGCACAAACCAGCTGGCGGATGATGTTT			
19	MKG.9.21	up	1,398806	up	1,522139	ENSCING0	Alh,Ci-AF:	ENSMUSG	DNA bindi	GATATTGGTTATGCAGTAGCACCCAAACACAGTC			
20	MKG.1164	up	1,115011	up	1,114666	ENSCING0	GALT	ENSMUSG	catalytic a	GGATGAATGGGTCCTTGTGTCACCTCATCGATTG			
21	MKG.442.1	up	1,21338	up	1,283406	ENSCING0	GlyP	ENSMUSG	nucleotid	AAGATGTGTCTTGCCAACATTGCGGCTTCTGGAA			
22	MKG.54.3	down	-3,95061	down	-4,58352		B4GALT7		N-acetylla	ATTGGAAACACCTTGGTGCCAAACAAACTATAC			
23	MKG.329.1	down	-1,79088	down	-2,64942	ENSCING0	L-threonir	ENSMUSG	L-threonir	GAAGAGCTCGCGCATGAAATACGAAAACACATT			
24	MKG.34.1	up	1,72687	up	1,778862	ENSCING0	GLRX2	ENSMUSG	iron ion bi	ACTGTGGGTGAATTACCAATTTCCAAACTTCTTG			
25	MKG.445.1	up	1,214095	up	1,431518		Pet2,WDR42A		protein bi	AATTGTCTCCAAAACTGTCTTCTTTTTCTTCCTCTA			
26	MKG.125.1	up	1,189048	up	1,265308	ENSCING0	Nr1h2	ENSMUSG	DNA bindi	TTAATACTTTCTCTGCAGATCGTCCAAACATAAA			
27	MKG.485.1	down	-1,33525	down	-1,32862		CALML6		ciliary or f	GATCCATCGCAGAACGAACTTGAACAAGTCATT			
28	MKG.280.1	down	-1,62743	down	-2,09043	ENSCING0	DHCR7	ENSMUSG	blood ves	TGCAGGGTTTTTACCTCGCATACCACCCGGTCGA			
29	MKG.191.4	up	1,958451	up	2,069153	ENSCING0	SUGT1	ENSMUSG	regulatior	TCGTCAGTGTTCTCGTGAAGAAAACCAAGAAAG			
30	MKG.294.1	up	1,257207	up	1,261111		EIF2AK1		nucleotid	TTATGCCATGACCATGGCCTACGACCATCTGCAT			

Fig. I.1 – Description of the microarray results. This image represents a file excel view resulted from microarray statistical analysis. Each column describes information about the transcripts. A: number of the probe; B: type of regulation in condition A vs C; C: Fold Change value in condition A vs C; D: type of regulation in Condition B vs C; E: Fold Change value in condition B vs C; F: ensemble ID; G: name of the gene in *Ciona intestinalis*; H: ensemble ID in mouse; I: the GO term; J: the sequence of the probe.

Pathway	Matched Entities	Pathway	Matched Entities
XPodNet protein-protein interactions in the podocyte	19	Delta-Notch Signaling Pathway	3
mRNA_processing	11	Primary Focal Segmental Glomerulosclerosis	3
PluriNetWork	7	GPCRs ClassA Rhodopsin-like	3
Purine metabolism	7	One carbon metabolism and related pathways	3
TNF-alpha NF-kB Signaling Pathway	6	Glycogen Metabolism	3
Calcium Regulation in the Cardiac Cell	4	Nuclear Receptor	3
Regulation of Actin Cytoskeleton	4	Alpha6-Beta4 Integrin Signaling Pathway	3
Amino Acid metabolism	4	Eukaryotic Transcription Initiation	3
Focal Adhesion	4	Glutathione metabolism	3
B Cell Receptor Signaling Pathway	4	Toll-like receptor signaling pathway	3
Wnt Signaling Pathway	3	Na+/Cl- dependent neurotransmitter transporters	3
Striated Muscle Contraction	3	Nuclear receptors in lipid metabolism and toxicity	2
Retinol metabolism	3	G13 Signaling Pathway	2
Keap1-Nrf2	3	IL-5 Signaling Pathway	2
Apoptosis	3	Alanine and aspartate metabolism	2
Apoptosis Modulation by HSP70	3	Tryptophan metabolism	2
Integrin-mediated Cell Adhesion	3	Chemokine signaling pathway	2
MAPK signaling pathway	3	Splicing factor NOVA regulated synpatic proteins	2

Tab. I.1 - Pathway list. The "Pathway" columns describe the type of pathway according to GO. The "Matched Entities" columns represent the number of genes involved in a pathway found in the list of genes of the microarray.

The following tables indicate the more interesting pathways "disregulated" by DD treatment. Each table is organized as follow: the "genes" column indicates the names of genes involved in the pathway that was disregulated in *ciona* embryos after DD treatments. The "regulation" column indicates the type of regulation of the genes. The "Fold Change"columns indicate the FC values after treatment with 0.40 µg mL^{-1} (A vs C) and 0.45 µg mL^{-1} (B vs C), respectively.

Pathway	Genes	Regulation	Fold Change A vs C	Fold Change B vs C
Apoptosis Modulation by HSP70	Fbln2	down	-1,6	-1,6
	Arpc2	down	-1,1	-1,3
	Thra	down	-1,6	-1,8
	Sfn	down	-1,1	-1,2
	Ap2a2	down	-1,7	-1,4
	Agrn	down	-1,3	-1,3
	Coq6	up	1,3	1,3
	Nrp1	down	-1,9	-3,2
	Isl1	down	-1,3	-1,3
	CSNK2A1	down	-1,2	-1,4
	Fras1	down	-3,2	-2,3
	Vim	down	-1,7	-3,1
	Ripk1	up	1,1	1,3
	Rac1	down	-2,4	-2,6
	Col4a3	down	-1,1	-1,1
	Mcf2l	down	-1,9	-3,5
	Hif1an	down	-1,5	-2,9
	Kirrel	down	-1,7	-1,6
	Ccnd2	down	-1,3	-1,4

Tab. I.2 - Apoptosis Modulation by HSP70 Pathway.

Pathway	Genes	Regulation	Fold Change A vs C	Fold Change B vs C
mRNA processing	4930429A22Rik	Up	1,5	1,6
	Hnrpk	Down	-1,4	-1,3
	Snrpb2	Down	-1,4	-1,4
	Snrpa1	Down	-1,3	-1,4
	Prpf8	Up	1,2	1,2
	Snrpb	down/up	-1,6	1,7
	Srrm1	Down	-5,3	-7,2
	1700009P03Rik	Down	-1,2	-1,2
	1700025B16Rik	Up	1,3	1,3
	Sart3	Up	1,3	1,2
	Exosc4	Up	1,4	1,5
	Supt5h	Up	1,2	1,4
	Polr2a	Down	-1,3	-1,5
	Rnmt	Up	1,5	2,0
	Bclaf1	Down	-2,1	-2,2
	Col4a3	Down	-1,1	-1,1

Tab. I.3 - mRNA processing Pathway.

Pathway	Genes	Regulation	Fold Change A vs C	Fold Change B vs C
PluriNetWork	Smarcad1	Down	-1,4	-1,4
	Hells	Up	1,2	1,4
	Setdb1	Down	-1,3	-1,6
	Cdx2	Down	-1,6	-2,4
	Bmpr2	Down	-5,0	-5,1
	Kat5	Up	1,5	1,7
	Lyar	Down	-1,4	-1,6
	Pim3	Down	-3,0	-3,6
	Gsk3b	Down	-1,3	-1,3
	Ctnnb1	Up	1,3	1,4
	Lif	Down	-1,2	-1,2
	Cubn	Up	1,2	1,0

Tab. I.4 - PluriNetWork Pathway.

Pathway	Genes	Regulation	Fold Change A vs C	Fold Change B vs C
Focal Adhesion	Ccnd2	Down	-1,3	-1,4
	Mapk6	Up	1,2	1,2
	Col6a2			
	Rac1	Down	-2,4	-2,6
	Actg1	Down	-1,2	-1,3
	Egfr	Up	1,3	1,3
	Lama2	Up	1,3	
	Gsk3b	Down	-1,3	-1,3
	Flt1	Up	1,4	1,6

Tab. I.5 - Focal Adhesion Pathway.

Pathway	Genes	Regulation	Fold Change A vs C	Fold Change B vs C
Chemokine signaling pathway	Adcy3	Down	-1,1	-1,1
	Nfkbia	Up	1,3	1,2
	Gsk3b	Down	-1,3	-1,3
	Rac1	Down	-2,4	-2,6
	Gng10	Down	-1,8	-2,1

Tab. I.6 - Chemokine signaling Pathway.

Pathway	Genes	Regulation	Fold Change A vs C	Fold Change B vs C
Cell cycle	Gsk3b	Down	-1,3	-1,3
	Chek2	Up	1,2	1,3
	Ccnd2	Down	-1,3	-1,4

Tab. I.7 - Cell cycle Pathway.

Pathway	Genes	Regulation	Fold Change A vs C	Fold Change B vs C
Retinol metabolism	Rlbp1	Down	-1,4	-2,0
	Aldh1a2	Up	1,5	2,0
	Crabp2	Down	-3,3	-4,7

Tab. I.8 - Retinol metabolism Pathway.

Pathway	Genes	Regulation	Fold Change A vs C	Fold Change B vs C
Regulation of Actin Cytoskeleton	Pik3c2b	Up	1,4	1,5
	Egfr	Up	1,3	1,3
	Actg1	Down	-1,2	-1,3
	Mapk6	Up	1,2	1,2
	Fgf18	Down	-1,4	-1,5
	Limk1	Up	1,2	1,3
	Rac1	Down	-2,4	-2,6
	Mos	Up	1,2	1,4

Tab. I.9 - Regulation of Actin Cytoskeleton Pathway.

Pathway	Genes	Regulation	Fold Change A vs C	Fold Change B vs C
TNF-alpha NF-kB Signaling Pathway	Smarcc2	Down	-2,6	-3,5
	Hsp90ab1	Up	1,2	1,5
	Ripk1	Up	1,1	1,3
	Hsp90aa1	Up	1,6	1,7
	CSNK2A1	Down	-1,2	-1,4
	Cul1	Up	1,3	1,4
	Trpc4ap	Up	1,3	1,6
	Casp2	Up	1,5	1,8
	Ikbkap	Up	1,3	1,6
	Bcl3	Down	-2,7	-3,0
	Nfkbia	Up	1,3	1,2
	Gsk3b	Down	-1,3	-1,3
	Polr1a	Down	-1,1	-1,2
	Ikbke	Up	1,4	1,5

Tab. I.10 - TNF-alpha NF-kB Signaling Pathway.

Pathway	Genes	Regulation	Fold Change A vs C	Fold Change B vs C
Alpha6-Beta4 Integrin Signaling Pathway	Rac1	Down	-2,4	-2,6
	Rpsa	Down	-1,2	-1,4
	Vim	Down	-1,7	-3,1
	Sfn	Down	-1,1	-1,2
	Egfr	Up	1,3	1,3
	Lama2	Up	1,3	1,6

Tab. I.11 - Alpha6-Beta4 Integrin Signaling Pathway.

Pathway	Genes	Regulation	Fold Change A vs C	Fold Change B vs C
Integrin-mediated cell adhesion	Rac1	Down	-2,4	-2,6
	Mapk6	Up	1,2	1,2
	Rho	Down	-1,7	-1,9

Tab. I.12 - Integrin-mediated cell adhesion Pathway.

Pathway	Genes	Regulation	Fold Change A vs C	Fold Change B vs C
Delta Notch Signaling Pathway	Gsk3b	Down	-1,3	-1,3
	Mfng	Down	-1,6	-1,8
	Egfr	Up	1,3	1,3
	Nfkbia	Up	1,3	1,2
	Cul1	Up	1,3	1,4

Tab. I.13 - Delta Notch Signaling Pathway.

Pathway	Genes	Regulation	Fold Change A vs C	Fold Change B vs C
Wnt Signaling Pathway	Cul1	Up	1,3	1,4
	CSNK2A1	Down	-1,2	-1,4
	Gsk3b	Down	-1,3	-1,3
	Rac1	Down	-2,4	-2,6
	Ctnnb1	Up	1,3	1,4

Tab. I.14 - Wnt Signaling Pathway.

Pathway	Genes	Regulation	Fold Change A vs C	Fold Change B vs C
MAPK signaling pathway	Egfr	Up	1,3	1,3
	Mos	Up	1,2	1,2
	Hspa1a	Up	113,9	169,0
	Rac1	Down	-2,4	-2,6
	Mapk6	Up	1,2	1,2
	Casp2	Up	1,5	1,8

Tab. I.15 - MAPK signaling Pathway.

References

Adolph S, Poulet SA, and Pohnert G. 2003 Synthesis and biological activity of α,β,γ,δ-unsaturated aldehydes from diatoms. *Tetrahedron.* **59**:3003–3008.

Adolph S, Bach S, Blondel M, *et al.* 2004. Cytotoxicity of diatom-derived oxylipins in organisms belonging to different phyla. *The Journal of Experimental Biology.* **207**:2935-2946.

Andreou A, Brodhun F, and Feussner I. 2009. Biosynthesis of oxylipins in non-mammals. *Progress in Lipid Research.* **48**:148-170.

Ashburner M, Ball CA, Blake JA, *et al.* 2000. Gene Ontology: tool for the unification of biology. *Nature Genetics.* **25(1)**:25–29.

Balestra C; Alonso-Sáez L; Gasol JM, *et al.* 2011. Group-specific effects on coastal bacterioplankton of polyunsaturated aldehydes produced by diatoms. *Aquatic Microbial Ecology.* **63**:123–131.

Ban S, Burns C, Castel J, *et al.* 1997. The paradox of diatom-copepod interaction. *Marine Ecology Progress Series.* **157**: 287-293.

Bellas J, Beiras R, and Vázquez E. 2003. A standardisation of Ciona intestinalis (Chordata, Ascidiacea) embryo-larval bioassay for ecotoxicological studies. *Water Research.* **37**:4613–4622.

Bellas J, Beiras R, Marinõ-Balsa JC, *et al.* 2005. Toxicity of organic compounds to marine invertebrate embryos and larvae: a comparison between the sea urchin embryogenesis bioassay and alternative test species. *Ecotoxicology.* **14**:337–353.

Bierkens JGEA. 2000. Applications and pitfalls of stress-proteins in biomonitoring. *Toxicology.* **153**:61–72.

Blée E. 2002. Impact of phyto-oxylipins in plant defence. *Trends Plant Science.* **7**: 315-321.

Brodhun F and Feussner I. 2011. Oxylipins in fungi. *FEBS Journal.* **278**:1047-1063.

Caldwell GS, Lewis C, Olive PJW, *et al.* 2005. Exposure to 2, 4-decadienal negatively impacts upon marine invertebrate larval fitness. *Marine Environmental Research.* **59**:405–417.

Caldwell GS. 2009. The influence of bioactive oxylipins from marine diatoms on invertebrate reproduction and development. *Marine Drugs.* **7**:367–400.

Carotenuto Y, Ianora A, Buttino I, *et al.* 2002. Is postembryonic development in the copepod Temora stylifera negatively affected by diatom diets? *Journal of Experimental Marine Biology Ecology.* **276**:49- 66.

Carotenuto Y, Wichard T, Pohnert G, *et al.* 2005. Life-history responses of *Daphnia pulicaria* to diets containing freshwater diatoms: Effects of nutritional quality versus polyunsaturated aldehydes. *Limnolology and Oceanography.* **50(2)**:2005, 449–454.

Carotenuto Y, Dattolo E, Lauritano C, *et al.* 2014. Insights into the transcriptome of the marine copepod *Calanus helgolandicus* feeding on the oxylipin-producing diatom *Skeletonema marinoi. Harmful Algae* **31**:153–162.

Casotti R, Mazza S, Brunet C, *et al.* 2005. Growth autoinhibition and genotoxicity of the diatom aldehyde 2-trans-4-trans decadienal on *Thalassiosira weissflogii* (*Bacillariophyceae*). *Journal of Phycology.* **41**:7-20.

Chambon JP, Soule J, Pomies P, *et al.* 2002. Tail regression in Ciona intestinalis (Prochordate) involves a Caspase-dependent apoptosis event associated with ERK activation. *Development.* **129**: 3105-3114.

Chang L W, Lo W S, and Lin P. 2005. Trans, Trans-2,4-Decadienal, a product found in cooking oil fumes, induces cell proliferation and cytokine production due to reactive oxygen species in human bronchial epithelial cells. *Toxicological Sciences.* **87**:337–343.

Conklin EG. 1905a. Mosaic development in ascidian egg. *Journal of Experimental Zoology.* **2**:145-223.

Conklin EG. 1905b. Organ-forming substances in the eggs of ascidians. *The Biological Bulletin.* **8**:205-30.

Conklin EG. 1905c. The organization and cell-lineage of the ascidian egg. *Journal of the Academy of Natural Sciences.* **13**:1-119.

Dalma-Weiszhausz D, Warrington J, Tanimoto EY, *et al.* 2006. The Affymetrix GeneChip® Platform: An Overview. *Methods in Enzymology.* **410**:3-28.

Dasgupta A, Das S, Sarkar PK. 2006. Thyroid hormone promotes glutathione synthesis in astrocytes by up regulation of glutamate cysteine ligase through differential stimulation of its catalytic and modulator subunit mRNAs. *Free Radical Biology & Medicine.* **42**: 617–626.

Dehal P, Satou Y, Campbell RK, *et al.* 2002. The draft genome of Ciona intestinalis: insights into chordate and vertebrate origins. *Science.* **298**:2157-2167.

Dickinson DA and Forman HJ. 2002. Cellular glutathione and thiols metabolism. *Biochemical Pharmacology*. **64**:1019-1026.

Dörthe D, Katschinski M. 2004. On Heat and Cells and Proteins. *Physiology*. **19**:11-15.

Dröege W. 2002. Free radicals in the physiological control of cell function. *Physiological Review*. **82**:47–95.

Duester G. 2008. Retinoic acid synthesis and signaling during early organogenesis. *Cell*. **134**:921-931.

Di Gregorio A, Harland RM, Levine M, *et al.* 2002. Tail morphogenesis in the ascidian, *Ciona intestinalis*, requires cooperation between notochord and muscle. *Developmental Biology*. **244**:385–395.

d'Ippolito G, Romano G, Iadicicco O, *et al.* 2002a. New birth-control aldehydes from the marine diatom *Skeletonema costatum*: characterization and biogenesis. *Tetrahedron Letters*. **43**:6133-6136.

d'Ippolito G, Iadicicco O, Romano G, *et al.* 2002b. Detection of short chainaldehydes in marine organisms: the diatom *Thalassiossira rotula*. *Tetrahedron Letters*. **43**:6137-6140.

Dung CH, Wu SC, and Yen GC. 2006. Genotoxicity and oxidative stress of the mutagenic compounds formed in fumes of heated soybean oil, sunflower oil and lard. *Toxicology in Vitro*. **20**:439–447.

Dutz, J, Koski, M, Jónasdóttir SH. 2008. Copepod reproduction is unaffected by diatom aldehydes or lipid composition. *Limnology and Oceanography*. **53**:225–235.

Falkowski PG, Kats ME, Knoll AH, *et al.* 2004. The evolution of modern eukaryotic phytoplankton. *Science*. **305**:354-360.

Ferrier DEK and. Holland PWH. 2002. *Ciona intestinalis* ParaHox genes: evolution of Hox/ParaHox cluster integrity, developmental mode, and temporal colinearity. *Molecular Phylogenetics and Evolution*. **24**:412–417.

Fleige S, Walf V, Huch S, *et al.* 2006. Comparison of relative mRNA quantification models and the impact of RNA integrity in quantitative real-time RT-PCR. *Biotechnology Letters*. **28**:1601–1613.

Fontana A, d'Ippolito G, Cutignano A, *et al.* 2007. A metabolic mechanism for the detrimental effect of marine diatoms on zooplankton grazers. *ChemBiochem*. **8**:1810–1818.

Franchi N, Ferro D, Ballarin L, *et al.* 2012. Transcription of genes involved in glutathione biosynthesis in the solitary tunicate *Ciona intestinalis* exposed to metals. *Aquatic Toxicology* **114- 115**:14- 22.

Fujii J, Ito J, Zhang. X, *et al.* 2011. Unveiling the roles of the glutathione redox system *in vivo* by analyzing genetically modified mice. *Journal of Clinical Biochemistry and Nutrition.* **49**: 70–78.

Funk CD. 2001Prostaglandins and Leukotrienes: Advances in Eicosanoid Biology. *Science.* **294**:1871-75.

Garcia-Fernàndez J. 2005. The genesis and evolution of Homeobox gene clusters. *Nature Reviews/Genetics.* **6**:881-892.

Guschina IA, and Harwood JL. 2006. Lipids and lipid metabolism in eukaryotic algae. *Progress in Lipid Research.* **45**:160-186.

Hansen E, Even Y and Geneviève AM. 2004. The α,β,γ,∂-unsaturated aldehyde 2-trans-4 trans-Decadienal disturbs DNA replication and mitotic events in early sea urchin embryos. *Toxicological Science.* **81**: 190–197.

Holland LZ, Laudet V, and Schubert M. 2004. The chordate amphioxus: an emerging model organism for developmental biology. *Cellular and Molecular Life Sciences.* **61**:2290-308.

Hotta K, Mitsuhara K, Takahashi H *et al.* 2007. A web-based interactive developmental table for the ascidian *Ciona intestinalis*, including 3D real-image embryo reconstructions: I. from fertilized egg to hatching larva. *Developmental Dynamics.* **236**:1790–1805.

Hotta K, Takahashi H, Satoh N, *et al.* 2008. Brachyury-downstream gene sets in a chordate, *Ciona intestinalis*: integrating notochord specification, morphogenesis and chordate evolution. *Evolution and Development.* **10**:37–51.

Hoyt P R, Doktycz M J, Beattie K L, *et al.* 2003. DNA microarrays detect 4-Nonylphenol-induced alterations in gene expression during zebrafish early development. *Ecotoxicology.* **12**:469-474.

Hudson C and Yasuo H. 2008. Similarity and diversity in mechanisms of muscle fate induction between ascidian species. *Biology of the Cell.* **100**:265-77.

Ianora A, Poulet S, and Miralto A. 2003. The effects of diatoms on copepod reproduction: a review. *Phycologia.* **42**:351–363.

Ianora A, Miralto A, Poulet SA, *et al.* 2004. Aldehyde suppression of copepod recruitment in blooms of a ubiquitous planktonic diatom. *Nature.* **429**:403-407.

Ianora A, Boersma M, Casotti R, Fontana, *et al.* 2006. New trends in Marine Chemical Ecology. *Estuaries and Coasts.* **29**:531-551.

Ianora A and Miralto A. 2010. Toxigenic effects of diatoms on grazers, phytoplankton and other microbes: a review. *Ecotoxicology.* **19**:493–511.

Ikuta T, Satoh N and Saiga H. 2010. Limited functions of Hox genes in the larval development of the ascidian *Ciona intestinalis. Development.* **137**:1505-1513.

Imai K S, Hino K, Yagi K, *et al.* 2004. Gene expression profiles of transcription factors and signaling molecules in the ascidian embryo: towards a comprehensive understanding of gene networks. *Development.* **131**:4047-4058.

Jiang D, Munro E M and Smith WC. 2005. Ascidian prickle regulates both mediolateral and anterior-posterior cell polarity of notochord cells. *Current Biology.* **15**:79–85.

Jiang D and Smith WC. 2007. Ascidian notochord morphogenesis. *Developmental Dynamics.* **236(7)**: 1748–1757.

Jüttner F. 2001. Liberation of 5,8,11,14,17-eicosapentaenoic acid and other polyunsaturated fatty acids from lipids as a grazer defense reaction in epilithic diatom biofilms. *Journal of Phycology.* **37**:744–755.

Kanda M, Ikeda T and Fujiwara S. 2013. Identification of a retinoic acid-responsive neural enhancer in the *Ciona intestinalis* Hox1 gene. *Development Growth and Differentiation.* **55**: 260–269.

Katsuyama Y, Sato Y, Wada S, *et al.* 1999. Ascidian tail formation requires caudal function. *Developmental Biology.* **213**: 257–268.

Katz MJ. 1983. Comparative anatomy of the tunicate tadpole, *Ciona intestinalis. The Biological Bulletin.* **164**:1-27.

Kensler TW, Wakabayashi N, and Biswal S. 2007. Cell survival responses to environmental stresses via the Keap1-Nrf2-ARE pathway. *Annual. Review of Pharmacology and Toxicology.* **47**:89–116.

Kim GJ, Yamada A and Nishida H. 2000. An FGF signal from endoderm and localized factors in the posterior-vegetal egg cytoplasm pattern the mesodermal tissues in the ascidian embryo. *Development.* 127:2853-2862.

Köhler HR, Sandu C, Scheil V, *et al.* 2007. Monitoring pollution in river Mures, Romania, Part III: biochemical effect markers in fish and integrative reflection. *Environmental Monitoring and Assessment.* **127**:47–54.

Koop D, Holland ND, Sémon M, *et al.* 2010. Retinoic acid signaling targets Hox genes during the amphioxus gastrula stage: Insights into early anterior-posterior patterning of the chordate body plan. *Developmental Biology.* **338**:98–106.

Kozlowsky-Suzuki B, Koski, M, Hallberg E, *et al.* 2009. Glutathione transferase activity and oocyte development in copepods exposed to toxic phytoplankton. *Harmful Algae.* 8:395-406.

Krenek S, Schlege M, and Berendonk TU. 2013. Convergent evolution of heat-inducibility during sub-functionalization of the Hsp70 gene family. *BMC Evolutionary Biology.* **13**:1-15.

Kugler JE, Passamaneck YJ, Feldman TG, *et al.* 2008. Evolutionary conservation of vertebrate notochord genes in the ascidian *Ciona intestinalis. Genesis.* **46**:697–710.

Kühn H, Walther M, and Kuban RJ. 2002. Mammalian arachidonate 15- LOXs. Structure, function, and biological implications. *Prostaglandins and Other Lipid Mediators.* **68–69**:263–290.

Krzywanski DM, Dickinson DA, Iles KE, *et al.* 2004. Variable regulation of glutamate cysteine ligase subunit proteins affects glutathione biosynthesis in response to oxidative stress. *Archives of Biochemistry and Biophysics.* **423**:116–125.

Kumano G and Nishida H. 2007. Ascidian embryonic development: an emerging model system for the study of cell fate specification in chordates. *Developmental Dynamics* **236**:1732–1747.

Lauritano C, Borra M, Carotenuto Y, *et al.* 2011a. Molecular evidence of the toxic effects of diatom diets on gene expression patterns in copepods. *PLoS One.* **6(10)**: e26850.

Lauritano C, Borra M, Carotenuto Y, *et al.* 2011b. First molecular evidence of diatom effects in the copepod *Calanus helgolandicus. Journal of Experimental Marine Biology and Ecology.* **404**: 79–86.

Lauritano C, Carotenuto Y, Miralto A. 2012a Copepod population-specific response to a toxic diatom diet. *PLoS One.* **7(10)**: e47262.

Lauritano C, Procaccini G, Ianora A. 2012b. Gene expression patterns and stress response in marine copepods. *Marine Environmental Research.* **76**: 22–31.

Lee KW, Raisuddin S, Rheec JS, *et al.* 2008. Expression of glutathione S-transferase (GST) genes in the marine copepod *Tigriopus japonicus* exposed to trace metals. *Aquatic Toxicology.* **89**:158–166.

Lee YM, Lee KW, Park H, *et al.* 2007. Sequence, biochemical characteristics and expression of a novel Sigma-class of glutathione S-transferase from the intertidal copepod, *Tigriopus japonicus* with a possible role in antioxidant defense. *Chemosphere.* **69**: 893–902.

Leflaive J and Ten-Hage L. 2009. Chemical interactions in diatoms: role of polyunsaturated aldehydes and precursors. *New Phytologist.* **184**: 794–805.

Legendre L. 1990. The significance of microalgal blooms for fisheries and for the export of particulate organic carbon in oceans. *Journal of Plankton Research.* **12**: 681-699.

Lenz PH, Unal E, Hassett RP, *et al. 2012.* Functional genomics resources for the North Atlantic copepod, Calanus finmarchicus: EST database and physiological microarray. *Comparative Biochemistry and Physiology, Part D.* **7**:10–123.

Lemaire P. 2009. Unfolding a chordate developmental program, one cell at a time: Invariant cell lineages, short-range inductions and evolutionary plasticity in ascidians. *Developmental Biology.* **332**:48–60.

Lettieri T. 2006. Recent applications of DNA microarray technology to toxicology and ecotoxicology. *Environmental Health Perspectives.* **1**:4-9.

Lindquist S. 1988. The Heat-Shock proteins. *Annual Review of Genetics.* **22**:631-77.

Lu S C. 2009. Regulation of glutathione synthesis. *Molecular Aspects of Medicine.* **30**:42–59.

Marikawa Y, Yoshida S, and Satoh, N. 1994. Development of egg fragments of the ascidian *Ciona savignyi*: the cytoplasmic factors responsible for muscle differentiation are separated into a specific fragment. *Developmental Biology.* **162**:134-42.

Marrone V, Piscopo M, Romano G, *et al.* 2012. Defensome against toxic diatom aldehydes in the sea urchin *Paracentrotus lividus.* PLoSone **7(2)**:e31750.

Matsuoka T, Ikeda T, Fujimaki *et al.* 2013. Transcriptome dynamics in early embryos of the ascidian, Ciona intestinalis. *Developmental Biology.* **384**:375–385.

McCall MN, Murakami PN, Lukk M, *et al.* 2011. Assessing affymetrix Gene Chip microarray quality. *BMC Bioinformatics.* **12**:137-147.

Minokawa T, Yagi K, Makabe KW, *et al.* 2001. Binary specification of nerve cord and notochord cell fates in ascidian embryos. *Development.* **128**:2007-2017.

Miralto A, Barone G, Romano G, *et al.* 1999. The insidious effect of diatoms on copepod reproduction. *Letters to Nature.* **402**:173-176.

Miralto A, Ianora A, Guglielmo L, *et al.* 1998. Egg production and hatching success in the peri-Antarctic copepod *Calanus simillimus*. *Journal of. Plankton Research.* **20**:2369-2378.

Montanari C, Sado Kamdem SL, Serrazanetti DI. 2013. Oxylipins generation in Lactobacillus helveticus in relation to unsaturated fatty acid supplementation. *Journal of Applied Microbiology.* **115**: 1388-1401.

Montillet JL, Agnel JP, Ponchet M, *et al.* 2002 Lipoxygenase-mediated production of fatty acid hydroperoxides is a specific signature of the hypersensitive reaction in plants. *Plant Physiology and Biochemistry.* **40**: 633-639.

Morris JP, Thatje S, and Hauton C. 2013. The use of stress-70 proteins in physiology: a re-appraisal. *Molecular Ecology.* **22**: 1494–1502.

Munro E and Odell G. 2002. Morphogenetic pattern formation during ascidian notochord formation is regulative and highly robust. *Development.* **129**:1-12.

Munro E, Robin F and Lemaire P. 2006. Cellular morphogenesis in ascidians: how to shape a simple tadpole. *Current Opinion in Genetics & Development.* **16**:399–405.

Nakashima K, Yamada L, Satou Y, *et al.* 2004. The evolutionary origin of animal cellulose synthase. *Development Genes and Evolution.* **214**:81-8.

Nakatani Y, Moody R and Smith W C. 1999. Mutations affecting tail and notochord development in the ascidian *Ciona savignyi*. *Development.* **126**:3293-3301.

Nava GM, Lee DY, Ospina JH, *et al.* 2009. Genomic analyses reveal a conserved glutathione homeostasis pathway in the invertebrate chordate *Ciona intestinalis*. *Physiological Genomics.* **39**: 83–194.

Neumann NF and Galvezb F. 2002. DNA microarrays and toxicogenomics: applications for ecotoxicology? *Biotechnology Advances.* **20**: 391–419.

Nguyen T, Nioi P, and Pickett CB. 2009. The Nrf2-antioxidant response element signaling pathway and its activation by oxidative stress. *The Journal of Biological Chemistry.* **284**:13291–13295.

Nishida H, Satoh N. 1983. Cell lineage analysis in ascidian embryos by intracellular injection of a tracer enzyme: I. Up to the eight-cell stage. *Developmental Biology.* **99(2)**:382–394.

Nishida H, Satoh N. 1985. Cell lineage analysis in ascidian embryos by intracellular injection of a tracer enzyme: II. The 16- and 32-cell stages. *Developmental Biology.* **110(2)**:440–454.

Nishida H. 1987. Cell lineage analysis in ascidian embryos by intracellular injection of a tracer enzyme. III. up to the tissue restricted stage. *Developmental Biology.* **121**:526-541.

Nishida H. 1997. Cell fate specification by localized cytoplasmic determinants and cell interactions in ascidian embryos. *International Review of Cytology.* **176**:245-306.

Nishida H. 2003. Spatio-temporal pattern of MAP kinase activation in embryos of the ascidian *Halocynthia roretzi. Development Growth and Differentiation.* **45**:27–37.

Nishida H. 2005. Specification of Embryonic Axis and Mosaic Development in Ascidians. *Developmental Dynamics.* **233**:1177–1193.

Noverr MC, Erb-Downward JR, and Huffnagle GB. 2003. Production of Eicosanoids and Other Oxylipins by Pathogenic Eukaryotic Microbes. *Clinical Microbiology Reviews.* **16**:517–533.

O'Donnell VB, Maskrey B, and Taylor GW. 2009. Eicosanoids: generation and detection in mammalian cells. *Methods in Molecular Biology.* **462**: 5-23.

Paffenhöfer GA, Ianora A, Miralto A, *et al.* 2005. Colloquium on diatom–copepod interactions. *Marine Ecology Progress Series.* **286**:293–305.

Pastore A and Piemonte F. 2012. S-Glutathionylation signaling in cell biology: Progress and prospects. *European Journal of Pharmaceutical Sciences.* **46**:279–292.

Pfaffl MW. 2001. A new mathematical model for relative quantification in real-time RT–PCR. *Nucleic Acid Research.* **29(9)**:2002-7.

Pohnert G. 2000. Wound-activated chemical defence in unicellular planktonic algae. *Angewandte Chemie International Edition.* **39**:4352–4354.

Pohnert G. 2002. Phospholipase A2 activity triggers the wound-activated chemical defense in the diatom *Thalassiosira rotula. Plant Physiology.* **129**:103-111.

Pohnert G. 2005. Diatom/Copepod Interactions in Plankton: The Indirect Chemical Defense of Unicellular Algae. *ChemBioChem.* **6**:946– 959.

Poulet SA, Ianora A, Miralto A, *et al.* 1994. Do diatoms arrest embryonic development in copepods? *Marine Ecology Progress Series.* **111**:79-97.

Poulet SA, Laabir M, Ianora A, *et al.* 1995. Reproducive response of *Calanus helgolandicus.* 1. Abnormal embryonic and naupliar development. *Marine Ecology Progress Series.* **129**:85–95.

Prodon F, Dru P, Roegiers F, *et al.* 2005. Polarity of the ascidian egg cortex and relocalization of cER and mRNAs in the early embryo. *Journal of Cell Science.* **118(11)**: 2393:2404.

Prodon F, Chenevert J and Sardet C. 2006. Establishment of animal-vegetal polarity during maturation in ascidian oocytes. *Developmental Biology.* **290**:297-311.

Pyza E, Mak P, Kramarz P, *et al.* 1997. Heat shock proteins (HSP70) as biomarkers in ecotoxicological studies. *Ecotoxicology and Environmental Safety.* **38**:244–251.

Ribalet F, Berges JA, Ianora A, *et al.* 2007. Growth inhibition of cultured marine phytoplankton by algal-derived polyunsaturated aldehydes. *Aquatic Toxicology.* **85**:219–227.

Ribalet F, Intertaglia L, Lebaron P, *et al.* 2008. Differential effect of three polyunsaturated aldehydes on marine bacterial isolates. *Aquatic Toxicology.* **86**:249–255.

Ritossa F. 1962. A new puffing pattern induced by temperature shock and DNP in *Drosophila. Experientia.* **18**:571–573.

Romano G, Russo GL, Buttino I, *et al.* 2003. A marine diatom-derived aldehyde induces apoptosis in copepod and sea urchin embryos. *The Journal of Experimental Biology.* **206**:3487-3494.

Romano G, Miralto A and Ianora A. Teratogenic effects of diatom metabolites on sea urchin *Paracentrotus lividus* embryos. Mar Drugs. 2010, 30: 950-67.

Romano G, Costantini M, Buttino I, *et al.* 2011. Nitric oxide mediates the stress response induced by diatom aldehydes in the sea urchin *Paracentrotus lividus. PLoS one.* **6(10)**: e25980.

Sardet C, Dru P, Prodon F. 2005. Maternal determinants and mRNAs in the cortex of ascidian oocytes, zygotes and embryos. *Biol. Cell.* **97**:35–49.

Sardet C, Paix A, Prodon F, *et al.* 2007. From Oocyte to 16-Cell Stage: Cytoplasmic and Cortical Reorganizations that pattern the Ascidian embryo. *Developmental Dynamics.* **236**:1716–1731.

Sarkadi B, Homolya L, Szakacs G, *et al.* 2006. Human multidrug resistance ABCB and ABCG transporters: participation in a chemoimmunity defense system. *Physiological Reviews.* **86**:1179-1236.

Satoh N. 1994. Developmental biology of the ascidians. New York: Cambridge University Press.

Satoh N. 2001. Ascidian embryos as a model system to analyze expression and function of developmental genes. *Differentiation.* **68**:1-12.

Satoh N. 2003. The ascidian tadpole larva: comparative molecular development and genomics. *Nature Reviews Genetics.* **4**:285-295.

Satou Y, Takatori N, Yamada L, *et al.* 2001. Gene expression profiles in *Ciona intestinalis* tailbud embryos. *Development.* **128**:2893-904.

Satou Y, Yamada L, Mochizuki Y, *et al.* 2002. A cDNA Resource from the Basal Chordate *Ciona intestinalis. Genesis.* **33**:153–154.

Schlesinger MJ, Ashburner M, and Tissieres A: 1982. Heat shock, from bacteria to man. *Cold Spring Harbour: Cold Spring Harbour Laboratory Press.*

Schulze A and Downward J. 2001. Navigating gene expression using microarrays – a technology review. *Nature Cell Biology.* **3**:E190-E195.

Seki M, Satou M, Sakurai T, *et al.* 2004. RIKEN Arabidopsis full-length (RAFL) cDNA and its applications for expression profling under abiotic stress conditions. *Journal of Experimental Botany.* **55**:213-223.

Spagnuolo A, Ristoratore F, Di Gregorio A, *et al.* 2003. Unusual number and genomic organization of Hox genes in the tunicate *Ciona intestinalis. Gene.* **309**:71–79.

Tadros W and Lipshitz HD. 2009. The maternal-to-zygotic transition: a play in two acts. *Development.* **136**:3033-3042.

Titelman J and Kiørboe T. 2003. Motility of copepod naulpii and implications for food encounter. *Marine. Ecology. Progress. Series.* **247**:123–135.

Tosti E, Romano G, Buttino I, *et al.* 2003. Bioactive aldehydes from diatoms block fertilization currents in ascidian oocytes. *Molecular Reproduction and Development.* **66**: 72-80.

Uye S.I. 1996. Induction of reproductive failure in the planktonic copepod *Calanus pacificus* by diatoms. *Marine. Ecology. Progress. Series.* **133**: 89–97.

Vardi A, Formiggini F, Casotti R, *et al.* 2006. A stress surveillance system based on calcium and nitric oxide in marine diatoms. *PLoS Biology.* **4**:411–419.

Vidoudez C and Pohnert G. 2008. Growth phase-specific release of polyunsaturated aldehydes by the diatom *Skeletonema marinoi. Journal of Plankton Research.* **30**:1305–1313.

Vidoudez C, Casotti R, Bastianini M, *et al.* 2011. Quantification of dissolved and particulate polyunsaturated aldehydes in the Adriatic Sea. *Marine Drugs.* **9**:500–513.

Vollenweider S, Weber H, Stolz S, *et al.* 2000. Fatty acid ketodienes and fatty acid ketotrienes: Michael addition acceptors that accumulate in wounded and diseased *Arabidopsis* leaves. *The Plant Journal.* **24**:467–476.

Wada S, Tokuoka M, Shoguchi E, *et al. 2003.* A genomewide survey of developmentally relevant genes in *Ciona intestinalis.* II. Genes for homeobox transcription factors. *Development Genes and Evolution.* **213**:222–234.

Weldy CS, White CC, Wilkerson HW, *et al.* 2011. Heterozygosity in the glutathione synthesis gene Gclm increases sensitivity to diesel exhaust particulate induced lung inflammation in mice. *Inhalation Toxicology.* **23**:724–735.

Wepener V, van Vuren JHJ, Chatiza FP, *et al.* 2005. Active biomonitoring in freshwater environments: early warning signals from biomarkers in assessing biological effects of diffuse sources of pollutants. *Physics and Chemistry of the Earth.* **30**:751–761.

Wichard T, Poulet SA, Halsband-Lenk C, *et al.* 2005 Survey of the chemical defense potential of diatoms: screening of fifty-one species for α,β,γ,δ-unsaturated aldehydes. *Journal of Chemical Ecology.* **31**:949–958.

Winterbourn CC. 2008. Reconciling the chemistry and biology of reactive oxygen species. *Nature Chemical Biology.* **4(5)**:278-286.

Yoshimi T, Minowa K, Karouna-Renier NK, *et al.* 2002. Activation of a stress-induced gene by insecticides in the midge, *Chironomus yoshimatsui. Journal of Biochemical and Molecular Toxicology.* **16**:10–17.

Questo lavoro di tesi è il risultato di un intenso e appassionato impegno intellettuale, ma è anche e ,soprattutto, il frutto di una faticosa crescita professionale e personale. Molte sono le persone che mi hanno accompagnato lungo questo percorso e le ringrazio tutte con grande affetto. Desidero rivolgere, però, dei ringraziamenti particolari a coloro che rimarranno per sempre nel mio cuore.

Il mio primo ringraziamento va ad Adrianna per la quale nutro dei sinceri sentimenti di affetto e stima. La ringrazio perché mi ha insegnato molto, in particolare ad avere il coraggio di esprimere sempre le mie idee e a non avere paura di guardare lontano. La seconda persona che voglio ringraziare è Margherita, il mio porto sicuro. Con il suo affetto e il senso di protezione che mi ha sempre trasmesso, ha contribuito anch'essa al superamento di quelle piccole paure che hanno sempre frenato il mio lavoro. Ringrazio Nietta, la mia guida scientifica. Dopo un non semplice inizio, il nostro rapporto è cresciuto in stima e affetto reciproci. Mena, Laura e Mara. Mena e Laura, sempre molto affettuose e disponibili ad ascoltare e a dispensare preziosi consigli; Mara che considero una sorella maggiore, le chiacchiere con lei sono state sempre di grande conforto. Ringrazio Rosaria, Leo ed Elena, l'affetto dei quali è stato fondamentale per superare i momenti di sconforto che si sono susseguiti in questi anni. Rosaria, piccola dolce amica. Confesso che senza i suoi richiami alla realtà, senza le nostre reciproche confessioni, senza la sua "semplice" presenza questo percorso di crescita non sarebbe stato possibile. Leo, il Prof. Il suo affetto e la sua simpatia hanno alleggerito molte "nottate" in laboratori. Elena, forte e fragile Elena, sempre pronta a darti conforto e aiuto in ogni occasione. Rivolgo dei ringraziamenti affettuosi a tutti i ragazzi che si sono succeduti in laboratorio. In particolare, Antonio, Caterina ed Anna che con la loro dolcezza e simpatia hanno conquistato un posto speciale nel mio cuore.

Un ringraziamento speciale va alla mia famiglia. I miei genitori che con grandi sacrifici mi hanno regalato la possibilità di studiare fino a raggiungere questo importante traguardo. Gennaro e Antonia, due sicurezze nella mia vita. Senza bisogno di tante parole so che potremo contare sempre gli uni sugli altri. Diego, amico e compagno di una vita. Il suo amore incondizionato, la sua allegria, la sua forza, la sua enorme pazienza, il suo ostinato ottimismo hanno reso la mia vita ricca di emozioni; grazie ,amore mio, per tutto questo e per avermi donato le gioie più grandi, i nostri figli.

Ringrazio Lello Russo, colui che ha mi ha insegnato ad ascoltare la rondine della mia anima.

Desidero, infine, ringraziare tutti coloro che non hanno creduto in me. Il loro disprezzo, la loro mancanza di fiducia e la loro durezza mi hanno dato una grande spinta ad andare avanti.